UNIVERSITY OF MESSINA

Department Of Biomedical, Dental, Morphological And Functional Imaging Sciences
MEDS-10/B

Translational Molecular Medicine and Surgery
Cycle XXXVIII

Impact of AZD5582 and hetIL-15 on HIV Latency Prevention During Early ART in SIV-Infected Rhesus macaques

---

Doctoral dissertation of
Cristina Micali, MD PhD Fellow

Supervisor
Emmanuele Venanzi Rullo, MD PhD
University of Messina

Co-Supervisor
Guido Silvestri, MD
Emory University

PhD Program Coordinator
Antonio Toscano, MD PhD
University of Messina

AA 2024/2025

Acknowledgment of Host Institution

The experimental work forming the core of this project was conducted at the Emory National Primate Research Center (Atlanta, USA) under the supervision of Doctor Guido Silvestri, in the laboratories of Doctors Guido Silvestri and Mirko Paiardini. This collaboration was essential, as Rhesus macaque (RMs) research is not possible in Italy. The choice of conducting the present study at Emory was driven by the exceptional expertise of Doctors Silvestri and Paiardini in *in vivo* studies on SIV/SHIV infected RMs, which offered unparalleled guidance and mentorship. I am also deeply grateful to all the staff and collaborators, in particular to my lab tutor, Doctor Maura Statzu, for their support, guidance, training and access to the specialized facilities that made this research possible.

Table of contents

Abstract

HIV infection persists despite suppressive antiretroviral therapy (ART) due to a latent reservoir of memory $CD4^+$ T cells harboring replication-competent virus. One of the many strategies explored for HIV/SIV eradication is based on the "shock & kill" paradigm, which postulates that the reservoir can be reduced or even eliminated by interventions that combine the reactivation of virus production in latently-infected cells (i.e., "shock", as induced by latency-reversing agents, LRA) with the immune-mediated killing of these cells (i.e., "kill", as mediated by cytotoxic T lymphocytes, NK cells, antibody-dependent cellular cytotoxicity and other mechanisms). In this study, we evaluated the SMAC mimetic AZD5582, which induces viral reactivation (shock), in combination with heterodimeric interleukin-15 (hetIL-15), which activates and expands cytotoxic T and NK cells (kill), as a strategy to prevent reservoir establishment during early SIV infection and ART.

Thirty-five rhesus macaques were infected with barcoded SIVmac239M and initiated on ART two weeks post-infection. Animals received hetIL-15 alone, AZD5582 alone, the combination of both, or ART only, and were monitored longitudinally for 45 weeks. Plasma viral loads were measured for the duration of the study. Reservoir size was assessed in PBMCs and lymph nodes (LNs) by intact proviral DNA assay, and immune cell phenotypes were characterized by flow cytometry.

Treatment with AZD5582, alone or in combination with hetIL-15, resulted in slower decline of plasma viremia after ART initiation. Levels of peripheral and LNs $CD4^+$ T cell intact proviral SIV DNA declined in all the groups over the treatment course. The frequency of $CD4^+$ T cells harboring proviral DNA tended to be lower in the animals receiving the SMAC mimetic, alone or in combination with hetIL-15. These results suggest that AZD5582, alone or with hetIL-15, transiently perturbs viral reservoir formation when administered at ART initiation during acute SIV infection, thus suggesting a disruptive effect on the reservoir establishment and providing a rationale for further evaluation as a component of HIV cure strategies.

1. Introduction

During the summer of 1981, the Centers for Disease Control and Prevention (CDC) in the United States (U.S.) reported several cases of Kaposi's sarcoma and *Pneumocystis jirovecii* pneumonia among homosexual men in California and New York City [1-2].
The global medical and scientific community was first confronted with a devastating syndrome that would later be called Acquired Immunodeficiency Syndrome (AIDS) in 1982, characterized by a progressive and profound impairment of cell-mediated immunity, responsible for making patients highly susceptible to opportunistic infections and malignancies not typically seen in otherwise healthy individuals [3-7]. This marked a turning point in medicine, as clinicians recognized that an entirely new and deadly disease entity was emerging.
Soon afterward, researchers began isolating the causative agent from lymphocytes obtained both from people affected by AIDS and from apparently healthy individuals who had been exposed to the virus. Initially, this pathogen was designated as human T-cell leukemia/lymphotropic virus type (HTLV)-III, given its similarity to other known retroviruses at the time, but it was eventually renamed the Human Immunodeficiency Virus (HIV) once its unique effects on immune system became clearer [8-9].
The first compelling evidence that AIDS might be caused by a retrovirus came in 1983, when Françoise Barré-Sinoussi and colleagues at the Pasteur Institute in Paris identified a virus in cultures derived from the lymph node of a man with persistent lymphadenopathy syndrome (LAS). These cultures contained an enzyme with reverse transcriptase activity, a hallmark of retroviruses [10]. Because lymph node swelling was a common feature in patients with LAS, typically associated with known human herpesviruses such as Epstein–Barr virus (EBV) or cytomegalovirus (CMV), many physicians initially suspected that these familiar viruses were the underlying cause of AIDS [11]. However, the characteristics of the new retrovirus closely resembled those of HTLV, which led many researchers to tentatively classify it within that group of human retroviruses [10-11].
Almost simultaneously, Montagnier and collaborators published their landmark paper “Isolation of a T-Lymphotropic Retrovirus from a Patient at Risk of Acquired Immune Deficiency Syndrome (AIDS)”, where they introduced the name lymphadenopathy-associated virus (LAV) as the cause of AIDS [12]. Not long after, in April 1984, Robert Gallo and colleagues at the U.S. National Institutes of Health (NIH) independently isolated the same virus, then designated HTLV-III, from peripheral blood mononuclear cells (PBMCs) of 48 patients, both adults and children, with AIDS [13]. This work firmly established the causal relationship between the retrovirus and the syndrome [14-15].

It is now well established that HIV belongs to the family *Retroviridae*, subfamily *Orthoretrovirinae*, genus *Lentivirus*, and is the causative agent of AIDS [16].

Phylogenetic and epidemiological analyses have revealed that HIV originated through multiple independent zoonotic transmission events from Simian Immunodeficiency Viruses (SIVs) into humans between approximately 1920 and 1940 [17-18]. More specifically, HIV-1, which is the more pathogenic and pandemic form, is derived from SIV_{cpz} strains infecting Central African chimpanzees, whereas HIV-2, a less transmissible and less pathogenic form, emerged from SIV_{smm} strains infecting sooty mangabey monkeys in West Africa [19]. Some evidence also suggests that gorillas (SIV_{gor}) played a role in certain transmission lineages [20].

Although both HIV-1 and HIV-2 share fundamental genomic organization, replication pathways, and routes of transmission, they diverge in important clinical and epidemiological aspects [21]. HIV-1 has spread worldwide and is responsible for most AIDS cases, whereas HIV-2 remains largely restricted to West Africa, the Gulf of Guinea, and certain pockets in India, South America, and the Caribbean [16, 22]. HIV-2 generally exhibits reduced transmissibility and slower disease progression compared to HIV-1, with AIDS typically developing at higher $CD4^+$ T cell counts [21]. Moreover, HIV-2 infection is characterized by more polyfunctional T cell responses and greater interleukin(IL)-2 production, which are thought to contribute to its attenuated pathogenicity [21]. Despite these differences, both viruses converge clinically in their eventual capacity to erode immune function, leading to opportunistic infections and AIDS-defining illnesses.

Since 1981, and over the past four decades, the development and implementation of highly effective treatment strategies for HIV infection have been a major global priority. This effort has faced numerous challenges, including drug toxicities, inconsistent adherence to complex multi-dose regimens, the emergence of drug resistance, uncertainties regarding the optimal timing for treatment initiation, drug–drug interactions (DDIs), and limited access to care among key populations [23-27].

In the early years of the AIDS epidemic, life expectancy for people living with HIV (PLWH) was typically limited to 1–2 years following the clinical manifestation of the syndrome [28-30]. With the advent and availability of modern antiretroviral therapy (ART), however, prognosis has improved dramatically. Current estimates indicate that PLWH who acquire the infection in their twenties and initiate sustained ART can expect to live an additional ~55 years, with life expectancy frequently extending into the early 70s and approaching that of the general population [31-32].

Thanks to the efforts of the Joint United Nations Programme on HIV/AIDS (UNAIDS), the U.S. President's Emergency Plan for AIDS Relief (PEPFAR), and the Global Fund to Fight AIDS, Tuberculosis and Malaria, 31.6 million PLWH (77% of all PLWH globally) were receiving lifesaving ART by the end of 2024, and AIDS-related deaths have declined by about 50% since 2005 [33].

Despite this remarkable progress and the global push to achieve the UNAIDS 95–95–95 targets by 2030, the global burden of HIV remains substantial.

Since the beginning of the pandemic, an estimated 91.4 million [73.4–116.4 million] people have been infected with HIV, and 44.1 million [37.6–53.4 million] have died from AIDS-related illnesses. In 2024 alone, 40.8 million [37.0–45.6 million] people were living with HIV worldwide, including 1.3 million [1.0–1.7 million] newly infected individuals, and only 31.6 million [27.8–32.9 million] were accessing ART. That same year, 630,000 [490,000–820,000] people died from AIDS-related illnesses [33].

Although it is essential to optimize treatment regimens and strengthen strategies for early diagnosis, ART access, adherence, and long-term retention in care, HIV infection is now widely regarded as a manageable chronic disease [34]. ART has progressively improved in terms of effectiveness, genetic barrier, and safety, successfully preventing both AIDS progression and viral transmission (Undetectable equals untransmissible, U=U) in individuals who maintain an undetectable viral load [35-37].
However, ART alone is incapable of eradicating HIV, as it cannot eliminate the latent reservoir of resting, infected cells from which the virus rapidly recrudesces once treatment is interrupted [38-40].
This therapeutic limitation highlights a deeper question: what is it about HIV's unique structure and life cycle that makes the virus so resilient, allowing it to persist for decades despite constant pharmacologic pressure?

1.1 Virion structure

HIV is an enveloped RNA virus with a roughly spherical morphology, belonging to the genus *Lentivirus* within the *Retroviridae* family. The mature virion measures about 100–120 nm in diameter and is surrounded by a lipid bilayer derived from the host cell membrane, into which the viral envelope glycoproteins are inserted (Fig. 1). These consist of trimeric complexes of the surface glycoprotein gp120 non-covalently associated with the transmembrane protein gp41, which together mediate attachment to host receptors and subsequent membrane fusion [41]. The synthesis of this structure involves the previous genesis of a polyprotein precursor (gp160) which is cleaved by the host cell proteases (furin) into the various subunits (gp120 and gp41), which will then remain non-covalently associated [11]. Above the surface of the viral membrane, it is also possible to observe the presence of 72 protrusions commonly called knobs or spikes, which are made up of trimers of the envelope glycoproteins [42]. These proteins are transported on the cell surface, where part of the central and N-terminal portion of gp41 are also expressed on the outside of the virion [43].
The matrix portion or in the inner part of the membrane is constituted by the protein p17 core, also called matrix protein, fundamental for the integrity of the virion and therefore for its structure [11]. The viral capsid, composed of hexameric and pentameric assemblies of the p24 protein, encloses two copies of the single-stranded positive-sense

ribonucleic acid (RNA) molecules along with essential viral enzymes: the viral RNA-dependent DNA polymerase Pol, also called reverse transcriptase (RT), integrase (IN), and protease (PR). Also contained within the capsid are accessory proteins that assist in replication and immune evasion.

This highly organized virion architecture is central to HIV's pathogenic capacity, facilitating efficient entry, integration into the host genome, and persistence despite host immune defenses and ART [44-45].

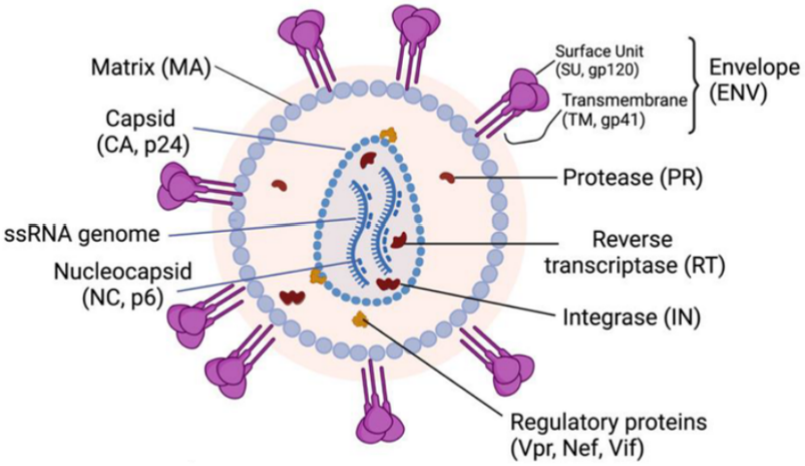

Fig. 1 HIV-1 structural organization. The virion schematic highlights the host-derived lipid envelope (ENV) with gp120/gp41 glycoproteins, the matrix (MA) layer, the conical p24 capsid (CA), and the RNA genome packaged with reverse transcriptase (RT), integrase (IN), and protease (PR). Adapted from Proulx et al. 2022 [46].

1.2 Genome structure

The integrated HIV-1 proviral DNA is approximately 9.7 kb in length and preserves the canonical retroviral arrangement of *gag*, *pol*, and *env* genes, flanked on both ends by long terminal repeats (LTRs) (Fig. 2). The provirus is inserted into the host genome, where the LTRs serve multiple regulatory functions, including transcriptional control, RNA processing, and packaging, while also providing the sites of integration.

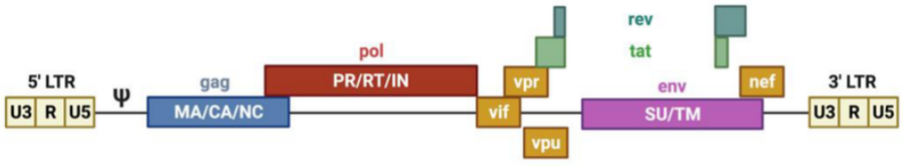

Fig. 2 Genomic organization of HIV-1 [46].

At the 5' end, the *gag* gene encodes the matrix and core structural proteins, followed by the *pol* gene, which partially overlaps *gag* and encodes the viral enzymes PR, RT, and IN. Downstream, the *env* gene encodes the surface glycoproteins required for viral

entry. Additional open reading frames encode accessory proteins critical for replication and immune evasion. Among these, *vif* overlaps with part of *pol* and extends further downstream, while *vpr* lies immediately downstream of *vif*. The *tat* and *rev* genes are organized into two exons each, with their first exons positioned between *vpr* and *env*, and their second exons residing within the *env* gene, joined by splicing. The *vpu* gene overlaps the 5′ region of *env*, whereas *nef* is positioned downstream of *env* and partially overlaps the terminal LTR. Transcription of the integrated provirus is carried out by host RNA polymerase II (RNA Pol II), initiating at the 5′ LTR. The full-length unspliced transcript serves both as genomic RNA and as mRNA for Gag and Gag-Pol precursors. Alternative splicing generates single-spliced mRNAs encoding Env, Vif, Vpr, and Vpu, as well as multiply spliced transcripts producing Tat, Rev, and Nef. Translation of these precursors is followed by proteolytic processing: Gag and Gag-Pol are cleaved by the viral protease, whereas the Env precursor undergoes cleavage by host cell proteases [47].

The *gag* gene product is a 55-kDa polyprotein that is processed into the matrix protein p17, the capsid protein p24, the nucleocapsid protein p7, and smaller peptides including p6, p2, and p1. These proteins play central roles in viral assembly, infectivity, and interaction with host factors. The matrix protein p17 directs assembly at the plasma membrane through N-terminal myristylation and contributes to nuclear import of viral deoxyribonucleic acid (DNA), facilitating infection of non-dividing cells such as macrophages, while extracellular p17 can modulate immune responses by binding IL-8 receptors. The capsid protein p24 forms the conical core and interacts with host cyclophilins, whereas the nucleocapsid p7 organizes the viral genome through zinc-finger–mediated RNA binding. The p6 domain supports viral budding and recruits Vpr into virions. Host restriction factors such as TRIM5α can recognize the viral capsid, block uncoating, and thereby interfere with replication [47].
The *pol* gene encodes three essential enzymes: PR, RT, and IN. These are produced via a ribosomal frameshift from the same transcript as Gag, resulting in lower copy numbers of Pol proteins compared to Gag [48]. PR functions as a homodimer, autocleaving from the Gag-Pol precursor and processing viral polyproteins. RT converts the viral RNA genome into DNA while its RNase H domain degrades RNA within RNA–DNA hybrids. The heterodimeric RT consists of p66 and p51 subunits, with the Tyr-Met-Asp-Asp motif providing catalytic activity. Its intrinsically low fidelity generates frequent mutations, driving viral diversity and immune escape. IN inserts the newly synthesized double-stranded DNA into host chromatin, establishing the proviral state [49].

The env gene encodes the glycoprotein gp160, cleaved into gp120 and gp41 by host proteases. Gp120 mediates binding to CD4 and chemokine coreceptors C-C chemokine receptor type 5 (CCR5) or C-X-C chemokine receptor type 4 (CXCR4), while gp41 anchors the complex in the membrane and drives fusion. Variable regions of gp120, particularly

V3, influence tropism and coreceptor usage, while conserved domains maintain essential receptor-binding functions [50]. Binding of gp120 to CD4 exposes conserved regions that interact with chemokine receptors, triggering conformational changes in gp41. The fusion peptide of gp41 is inserted into the host membrane, and the six-helix bundle formation drives membrane fusion [51].

Beyond the structural and enzymatic proteins, HIV encodes several accessory proteins that modulate replication and immune evasion [52]. Trans-activator of transcription (Tat) is essential for efficient transcriptional elongation through interaction with the trans-activation response (TAR) element, while regulator of expression of virion proteins (Rev) mediates nuclear export of unspliced and singly spliced RNAs via the Rev response element (RRE). Virion infectivity factor (Vif) counteracts the cytidine deaminase APOBEC3G, which otherwise induces lethal hypermutation. Negative factor (Nef) downregulates CD4 and major histocompatibility complex (MHC) class I, promoting immune evasion and high viral loads. Viral protein R (Vpr) enhances nuclear import of the pre-integration complex (PIC) and alters cell cycle progression, whereas Viral protein U (Vpu) promotes CD4 degradation and antagonizes tetherin, which restricts budding [47].

The LTRs at both ends of the provirus are composed of U3, R, and U5 regions and are essential for regulation of viral gene expression. U3 contains promoter and enhancer elements, including specificity protein 1 (SP1) and nuclear factor kappa-light-chain-enhancer of activated B-cells (NF-κB) binding sites, which couple viral transcription to host activation signals [53-54]. The R region includes the transcription initiation site and the TAR element required for Tat-mediated transactivation, while U5 harbors the tRNA primer-binding site necessary for reverse transcription. Together, these elements integrate viral replication with host cellular physiology, enabling HIV to persist in both resting and activated cells [47].

1.3 HIV replication cycle

The HIV replication cycle (schematically shown in Fig. 3) can be summarized in five fundamental steps:

1) Binding, entry, uncoating
2) Reverse transcription
3) Provirus integration
4) Virus proteins synthesis and assembly
5) Budding

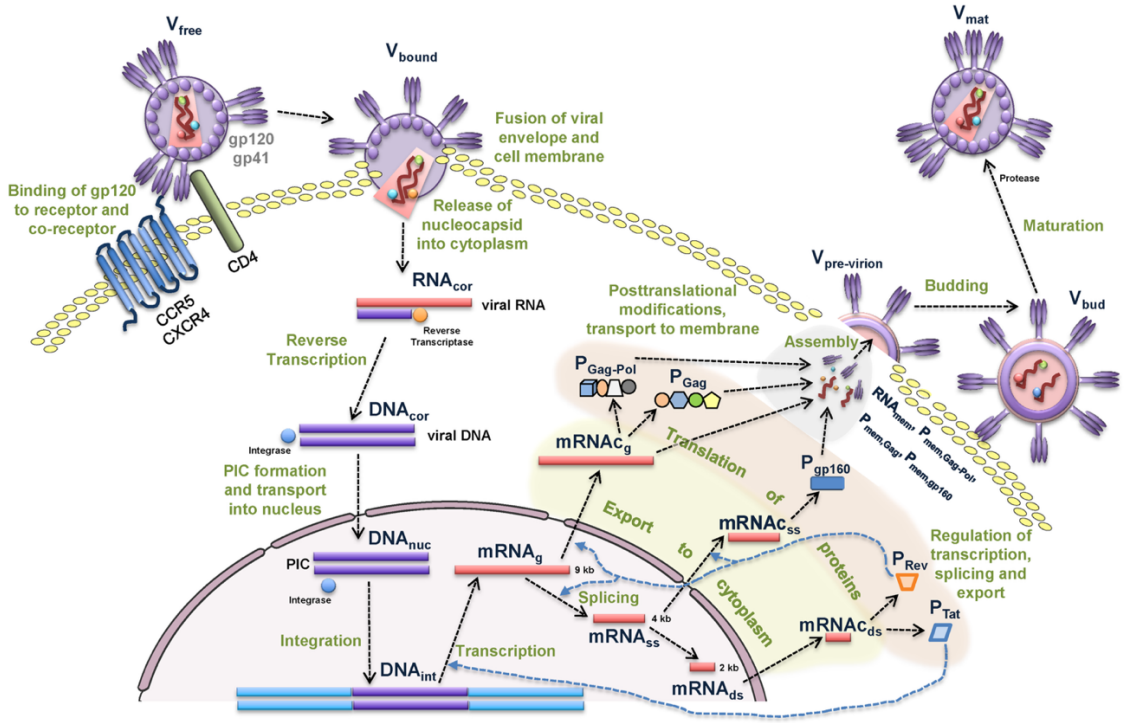

Fig. 3 Schematic representation of the HIV-1 replication cycle. The process begins with viral entry mediated by the binding of gp120 to the CD4 receptor and CCR5/CXCR4 co-receptors, followed by gp41-driven fusion of the viral and host membranes and release of the nucleocapsid into the cytoplasm. Viral RNA is reverse transcribed into complementary DNA, which is transported to the nucleus and integrated into the host genome by integrase. Integrated proviral DNA serves as a template for transcription of viral RNAs, which undergo splicing and are exported to the cytoplasm. Viral mRNAs direct the synthesis of structural proteins (Gag, Gag-Pol, Env) and regulatory proteins (Tat, Rev), as well as accessory proteins. Post-translational modifications and transport guide Env proteins to the plasma membrane, where viral assembly occurs. Immature virions bud from the host cell and undergo protease-mediated maturation to become infectious particles. Adapted from Shcherbatova et al. 2020 [71].

HIV-1 infection begins when the viral envelope glycoprotein gp120 engages the CD4 receptor on susceptible cells, including T lymphocytes, macrophages, and microglia [55-56]. Binding of gp120 to CD4 induces conformational changes that allow interaction with a chemokine coreceptor, most commonly CCR5 or CXCR4, on the surface of susceptible cells, which determines viral tropism [57-61]. CCR5 is the principal coreceptor for macrophage-tropic primary isolates, whereas CXCR4 is used by T cell–line–adapted strains, and dual-tropic variants can employ both [57-61]. Genetic studies have shown that individuals homozygous for a 32-bp deletion in CCR5 ($CCR5^{\Delta 32}$) are highly resistant to infection, while heterozygotes are susceptible but often experience delayed progression to AIDS [62-64]. The “Berlin patient”, who underwent stem cell transplantation from a $CCR5^{\Delta 32}$ homozygous donor, has remained virus-free, illustrating the potential for targeting CCR5 in curative strategies [65]. Structural studies revealed that CD4 binds gp120 via a recessed pocket that accommodates phenylalanine-43, and subsequent conformational changes expose binding sites for CCR5 or CXCR4. Additional interactions with glycosaminoglycans may also modulate gp120–coreceptor binding [66-

[67]. Engagement of the chemokine receptor triggers refolding of gp41, exposing its fusion peptide, which inserts into the host membrane and promotes fusion through six-helix bundle formation [68]. This event releases the viral capsid into the cytoplasm, where uncoating occurs in a tightly regulated process involving host factors such as cyclophilin A [69]. Accessory proteins, including Vif and Nef, further support successful disassembly [52]. The resulting PIC undergoes reverse transcription, initiated by a tRNA primer at the 5′ LTR [70], and is subsequently imported into the nucleus through signals encoded in Gag, Vpr, and IN.

Reverse transcription begins in the cytoplasm of the infected cell, initiated by annealing of a host cellular tRNA primer (specifically $tRNA^{Lys3}$ in HIV-1) to the primer binding site (PBS), an 18-nucleotide complementary sequence located near the 5′ end of the viral RNA genome [72]. DNA synthesis starts at this PBS and extends through the U5 and R regions of the 5′ LTRs, generating a short minus-strand strong-stop DNA. This newly synthesized fragment is then transferred to the 3′ end of the genomic RNA, where its R sequence anneals to the complementary R region of the 3′ LTR, allowing elongation of the minus-strand DNA [70]. During elongation, the viral ribonuclease H domain of RT degrades the RNA template, except for two purine-rich tracts (polypurine tracts, PPTs) that are resistant to degradation and subsequently serve as primers for plus-strand synthesis [70, 72]. Plus-strand DNA synthesis is initiated at the 3′-proximal PPT and extends through the U3, R, and U5 regions, reconstituting a full-length PBS at the 5′ end of the nascent DNA. Removal of the tRNA and PPT primers by RNase H activity exposes complementary PBS sequences, enabling the second strand transfer, after which elongation continues until a complete linear double-stranded DNA is produced, characterized by identical LTRs at both ends [72]. Because reverse transcription occurs in the cytoplasm, the availability of nucleotide precursors can be limiting, particularly in nondividing cells such as macrophages and dendritic cells (DCs). The cellular restriction factor sterile alpha motif and HD-domain–containing protein 1 (SAMHD1) depletes intracellular pools of deoxynucleoside triphosphates by hydrolyzing them, thereby inhibiting efficient reverse transcription [73]. SAMHD1 is antagonized by viral protein x (Vpx), a viral accessory protein encoded by HIV-2 and some SIVs, which recruits SAMHD1 for proteasomal degradation; however, HIV-1 lacks Vpx, contributing to its reduced ability to establish productive infection in DCs, macrophages, and quiescent T cells [73-75]. The completed double-stranded viral DNA remains associated with viral and host proteins in the PIC, which includes IN, the matrix protein p17, and Vpr, among others, ensuring protection and guidance of the nascent genome toward the nucleus [72]. To traverse the nuclear pore, the PIC interacts with nucleoporins such as Nup358 and with transport factors including transportin-3 (TNPO3), which together facilitate active nuclear import [76-77]. This nuclear import capacity distinguishes HIV-1 from many

other retroviruses, enabling efficient infection of nondividing cells and establishing a reservoir in long-lived myeloid populations [78-80].

Structural studies, including those employing the prototype foamy virus as a model, have further demonstrated that IN assembles as a tetramer, coordinating two catalytic sites via divalent metal ions to align the viral DNA ends for precise insertion into the host genome [81-82].

Once inside the cell host nucleus, integration is catalyzed by IN through a two-step process: 3' end processing and strand transfer (Fig. 4). During 3' end processing, two nucleotides are cleaved from each viral DNA terminus, exposing 3' hydroxyl groups essential for strand transfer. In the subsequent reaction, these hydroxyl groups attack phosphodiester bonds in the host DNA, covalently linking viral and host sequences through transesterification [83-84]. Integration induces local DNA bending, creating distortions that facilitate insertion while minimizing deleterious mutations. Host DNA repair enzymes, including Ku, ligase IV, and XRCC4, complete the repair of gaps and ensure genomic integrity [85-86]. This establishment of proviral infections allows the expression of viral accessory and structural proteins, which must assemble within the target cell to form functional progeny virions capable of initiating a new round of infection [87].

HIV does not integrate randomly: genome-wide mapping studies revealed a strong preference for transcriptionally active regions [89-90]. This specificity is largely mediated by lens epithelium-derived growth factor (LEDGF)/p75, a host factor that tethers IN to nucleosomes in euchromatic regions, favoring integration in gene-rich, actively transcribed DNA [91-93].

Other host proteins, including barrier-to-autointegration factor (BAF) and high-mobility group proteins (HMGA/HMGB), stabilize the PIC and prevent self-integration of viral DNA, further ensuring precise integration and viral genome integrity [94].

Integration of a DNA copy of the viral genome into the host cell chromosome is the hallmark of retroviral replication, distinguishing retroviruses from other viral families and enabling lifelong persistence in infected individuals [95-96]. Following integration, the provirus becomes a permanent part of the host genome. Its transcriptional fate is determined by chromatin context, epigenetic modifications, and transcription factor availability. Integration into transcriptionally permissive regions generally leads to productive viral gene expression, whereas integration into heterochromatic or transcriptionally silent regions can result in latent infection [95-96].

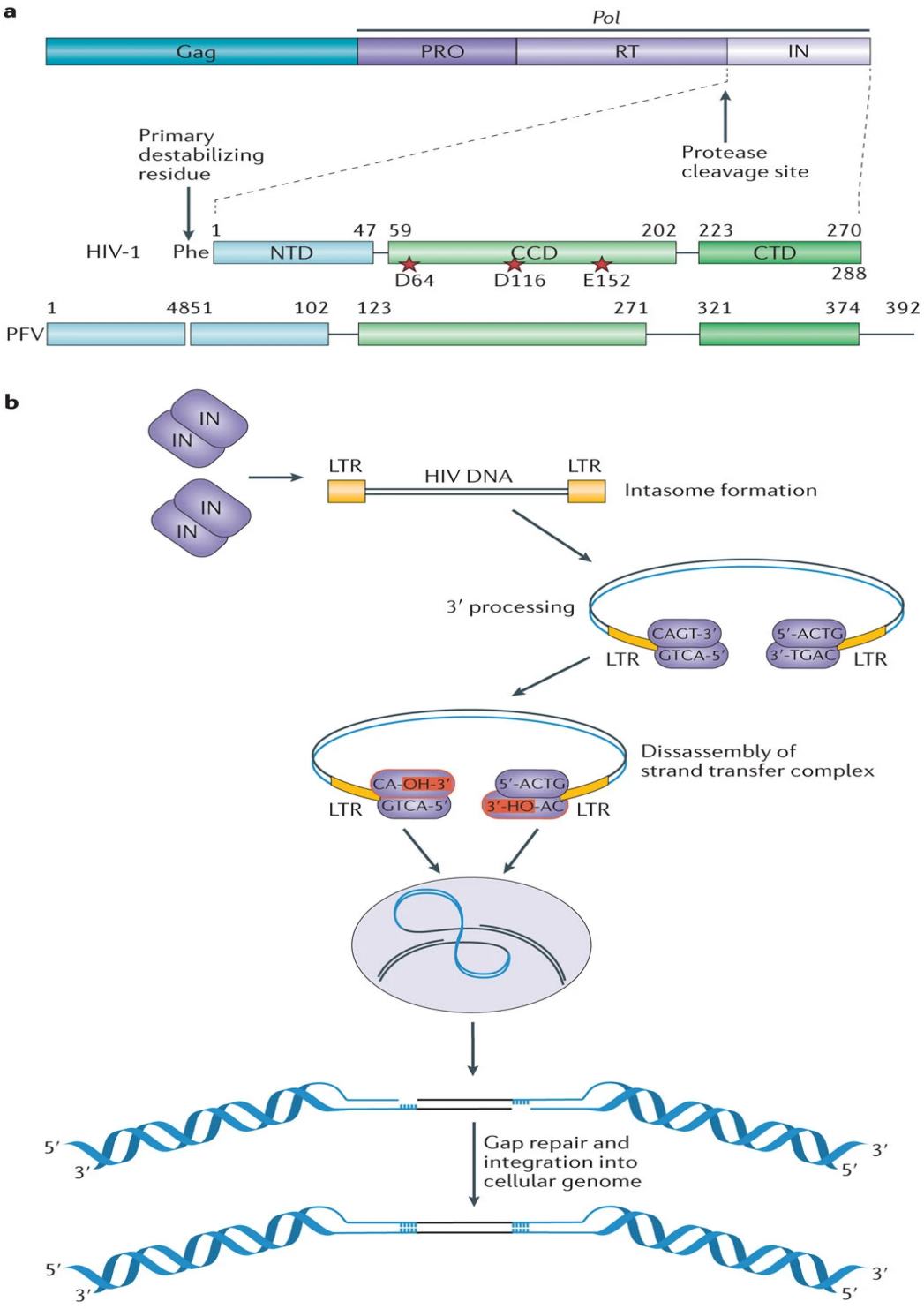

Fig. 4 HIV-1 integration mechanisms. Integrase (IN) multimerizes at the ends of the viral long-terminal repeats (LTRs) and cleaves two nucleotides from each 3′ end of the viral DNA during 3′ processing, generating recessed, chemically reactive hydroxyl groups. Following nuclear import of the pre-integration complex (PIC), IN binds to target DNA and catalyzes strand transfer. After disassembly of the strand transfer complex, the resulting DNA recombination intermediate is likely repaired by host enzymes, resulting in the provirus being stably integrated into cellular chromatin. Adapted from Lusic et al. 2017 [88].

The expression of new viral RNA genomes and proteins is tightly regulated by both viral and cellular factors. Viral production requires activation of proviral transcription from the 5′ LTR, which functions as a promoter and enhancer, and is influenced by external cues such as coinfection, inflammatory cytokines, and cellular activation [97]. A key role is played by cellular transcription factors, particularly NF-κB, which binds to motifs within the LTRs and promotes transcriptional activation [98]. HIV-1 transcription is initiated by host RNA Pol II at the U3-R junction of the LTRs, generating a full-length primary transcript that is capped, polyadenylated, spliced, and exported from the nucleus [72]. Viral gene expression is temporally regulated by differential splicing and by the actions of early viral proteins. Initially, infected cells produce 2-Kb doubly spliced mRNAs encoding regulatory proteins such as Tat, Rev, and Nef [99-101]. Tat amplifies viral transcription by binding to the TAR element at the 5′ end of nascent transcripts, dramatically enhancing elongation efficiency and driving robust RNA and protein synthesis [101]. Rev regulates RNA processing by binding to the RRE within incompletely spliced RNAs, forming multimers that facilitate nuclear export of unspliced and singly spliced transcripts, thereby enabling a switch from early gene expression to late gene expression [101]. As Rev accumulates, late transcripts encoding structural and enzymatic proteins, including Gag, Pol, and Env, as well as accessory proteins Vif, Vpu, and Vpr, are exported and translated, along with full-length genomic RNA [101]. Viral RNA packaging is dependent on a cis-acting packaging signal (Ψ) located near the 5′ end of the genome; in its absence, particles assemble but lack genomic RNA [72]. Packaging is mediated by the nucleocapsid protein (p7), which contains two zinc-finger motifs that specifically recognize Ψ and stabilize RNA incorporation. Assembly occurs predominantly at the plasma membrane, where the matrix protein p17 targets Gag to lipid raft microdomains rich in cholesterol, sphingolipids, and glycolipids [102]. The cytoplasmic tail of gp41 interacts with p17, ensuring that viral envelope proteins are incorporated into budding particles [72]. Virions bud from the host cell membrane, acquiring their envelope along with incorporated host proteins, and are released into the extracellular milieu [45, 103]. Their maturation is then driven by the viral PR, which cleaves the Gag and Gag-Pol polyproteins into their functional subunits, including matrix, capsid, nucleocapsid, RT, IN, and PR itself. These cleavage events are essential for structural and functional maturation of the virion, rendering it infectious [103].
The rapid turnover of virus and target cells, combined with error-prone reverse transcription, fuels continuous genetic diversification, immune escape, and drug resistance [104].

HIV exhibits extraordinary genetic variability, which represents one of its most important resources for persistence and a major obstacle to immune clearance, pharmacological treatment, and vaccine development [105]. The rate of mutation is estimated at approximately two to three per genome per replication cycle [44, 106],

making HIV one of the most rapidly evolving pathogens known. This variability arises from three principal mechanisms. First, RT enzyme operates in an error-prone manner, introducing on average one substitution per genome per replication round. These errors include point mutations, deletions, and insertions, which remain uncorrected due to the absence of proofreading activity in RT [106]. Second, the sheer scale of viral replication amplifies this effect: an estimated $10^{9}{}^{9}$ virions are produced daily in an infected individual, continuously generating new variants [105]. Third, recombination between two or more HIV genomes within a single host cell adds another layer of diversity, creating novel viral genotypes with distinct phenotypic properties [105-106]. Together, these processes fuel the virus's adaptability, facilitating immune escape, drug resistance, and the establishment of long-term infection.

1.4 Pathogenesis and diagnosis of HIV

HIV-1 production and T cell turnover are highly dynamic processes, with billions of virions generated and approximately one billion T cells lost and replaced each day [107-108]. This extraordinary turnover explains the rapid emergence of viral variants and the progressive depletion of $CD4^+$ T cells. Virus replication occurs in multiple compartments, each with distinct turnover rates, and even during clinical latency, ongoing infection sustains a state of immune hyperactivation [109]. $CD4^+$ recovery under ART reflects both redistribution of memory cells and gradual repopulation with newly produced naïve T (T_N) cells [110].

Early mathematical models described infection as a simple balance between viral replication and immune depletion, but these have since been replaced by more complex explanations involving indirect viral effects, immune activation, and apoptosis. Notably, $CD8^+$ T cells, although uninfected, also undergo rapid turnover, with their later depletion attributed to gp120–CXCR4 interactions [111-112]. Disease progression is further shaped by viral escape from immune control and, in some cases, by the emergence of CXCR4-using variants, though AIDS often develops in their absence [113]. Across all models, two principles remain central: a quantitative link exists between viral replication and T cell loss, and both processes are compartmentalized [107].

Beyond direct cytopathic effects, HIV also exerts profound bystander damage. PBMCs from PLWH display impaired proliferation even though only a small fraction of T cells is infected [114-116]. Additional mechanisms include defective hematopoiesis and thymopoiesis, cytokine-driven apoptosis of uninfected cells - mediated by tumor necrosis factor alpha (TNF-α), interferon alpha (IFN-α), and transforming growth factor beta (TGF-β) - and hyperactivation-induced apoptosis triggered by extracellular Tat. These indirect pathways amplify immune dysfunction and accelerate progression [47].

The remarkable variability of HIV further complicates pathogenesis. Phylogenetic analyses divide HIV-1 into groups M, N, and O, with group M responsible for the global

pandemic and comprising multiple subtypes (A–K) and circulating recombinant forms (CRFs) [117]. Zoonotic transmission from Pan troglodytes chimpanzees occurred on at least three occasions, one of which in southeastern Cameroon gave rise to group M [18, 118]. Historical reconstructions trace its introduction into the U.S. in the 1960s, from where clade B spread across Western countries, while clade C became predominant in sub-Saharan Africa and India [119]. Although once thought to arise from a single founder virus, deep sequencing now shows that up to one-third of infections begin with multiple genetically distinct transmitted/founder viruses [120-121]. Mutations, especially within gp120, drive immune escape, tropism shifts, and ART resistance. At the population level, viral phylogenetics enables reconstruction of transmission networks and epidemic spread [122].

HIV is transmitted through exposure to infected fluids: blood, genital secretions, anal secretions, breast milk, and transplacental transfer. Transmission occurs via unprotected sex, needle sharing, or vertical passage during gestation (22–30%), delivery (55–65%), or breastfeeding (12–20%), with higher overall rates in developing countries [123-124].

Clinically, in absence of ART, HIV progresses through acute infection, chronic infection, and AIDS [105]. Acute infection begins in local lymphoid tissue, followed by systemic dissemination and establishment of reservoirs in macrophages, DC, and memory $CD4^+$ T (T_M) cells [122]. Within 2–4 weeks, viremia peaks at 10^6–10^7 copies/mL, followed by a decline to the viral set point, a predictor of long-term disease course [125]. This stage is often accompanied by flu-like symptoms and detectable viral RNA, though preceded by an eclipse phase when virus remains undetectable [122, 126]. $CD8^+$ T cell responses reduce viremia but do not eliminate infection, establishing the chronic phase characterized by persistent, lower-level replication and gradual $CD4^+$ loss. With ART, PLWH can remain in this phase for decades, and those with undetectable viral loads have effectively no risk of sexual transmission [127]. Without treatment, however, chronic immune activation, lymphoid tissue destruction, and progressive $CD4^+$ depletion drive immunodeficiency [105, 122].

AIDS represents the terminal stage, diagnosed when $CD4^+$ counts fall below 200 cells/mm^3. People at this stage are highly susceptible to opportunistic infections, including Pneumocystis jirovecii pneumonia, candidiasis, CMV disease, cryptococcosis, and toxoplasmosis, as well as AIDS-defining cancers such as Kaposi's sarcoma and lymphomas [128]. Neurological complications, including HIV-associated encephalopathy, further contribute to severe disability and increased mortality [105].

Viral replication induces both humoral and cellular immune responses, with viral proteins processed and displayed on the surface of infected cells. Cellular immunity represents the earliest detectable host response [129-131], although this has not yet been

incorporated into routine diagnostic practice. In contrast, humoral responses remain central to HIV detection. Antibody production generally follows a burst of replication in which viral RNA and p24 antigen are detectable before seroconversion [132]. As with most infections, IgM is the first antibody class to appear, followed by IgG [133-134].

The diagnostic "window period" refers to the interval between infection and the time when laboratory tests can first detect the virus: initially lasting about two months, the window period was shortened to less than four weeks with improved enzyme-linked immunosorbent assays (ELISA).

The detection of p24 antigen and viral RNA before antibodies appear further reduces this interval, and reverse transcriptase activity has also been evaluated as an early diagnostic marker [135-136]. However, individual variability in viremia and antibody kinetics makes precise estimation of the window period difficult [137]. On average, third-generation antibody tests detect infection after about 22 days, fourth-generation antigen–antibody assays at about 16 days, and nucleic acid testing (NAT) shortens this by an additional 4–6 days [138-139]. Although seropositivity is usually lifelong, important exceptions exist. In advanced disease, antibody levels may decline despite high viral RNA, making serologic diagnosis difficult. Rare cases of HIV infection without detectable antibodies have been reported, generally associated with rapid disease progression [140-145]. Early initiation of ART can also delay or suppress antibody development [146-149]. In such cases, diagnosis depends on careful clinical history and the use of combined antigen–antibody or NAT testing.

ELISA was the first Food and Drug Administration (FDA)-approved HIV screening test and remains highly sensitive. Early assays used cell lysates as antigen, but these were progressively replaced by recombinant proteins and synthetic peptides, which improved specificity [150-152]. Third-generation "sandwich" ELISAs detect both IgM and IgG, improving early diagnosis. These assays were subsequently adapted into rapid formats and combined with p24 antigen detection to create fourth-generation tests [153-155].

Rapid tests, typically based on lateral or capillary flow, provide results within 30 minutes, increasing result return rates in settings such as maternity wards, sexual transmitted diseases (STD) clinics, and emergency departments. They are highly sensitive across HIV subtypes, but may lag behind ELISA by several days in detecting seroconversion, and their sensitivity for p24 antigen remains limited. Sequential use of independent rapid tests can improve diagnostic accuracy [156-159].

Saliva and urine have also been validated for HIV testing. Saliva contains transudated IgG at concentrations suitable for ELISA and Western blot. These methods are less invasive, but false negatives may occur in ART-treated people [160], and false positives increase near kit expiration [161-162].

The detection of p24 antigen adds an additional diagnostic window. p24 ELISA identifies infection before seroconversion, with a sensitivity of 5–20 pg/mL (approximately

40,000–200,000 virions) [163]. Antigen detection is transient during acute infection and reappears in advanced disease, where it is a poor prognostic marker. Heating or acid treatment of plasma improves sensitivity by dissociating immune complexes. Amplified assays have lowered detection thresholds to about 0.5 pg/mL, equivalent to 4,000 virions. These advances culminated in fourth-generation antigen–antibody assays, which simultaneously detect p24 antigen and antibodies to HIV-1 (gp41) and HIV-2 (gp36). This combined approach shortens the diagnostic window and allows a single test to confirm infection, distinguish HIV-1 from HIV-2, and provide some information about infection stage. Supplemental lateral-flow assays are often added for differentiation, and these combined methods have largely replaced Western blot in modern diagnostic algorithms [47].

Although rare, false-negative results occur in very early infection, in rare seronegative cases, in immunocompromised patients, or due to technical assay limitations [164-165]. False positives are more common, especially in low-prevalence populations, and may arise from technical errors, autoimmune disease, recent vaccination, multiparity, or cross-reactivity with infections such as syphilis, malaria, or leprosy [166-169].

To overcome these problems and further shorten the diagnostic window, NAT is widely used. NAT detects viral RNA at extremely low levels, with FDA-approved assays such as Aptima achieving a limit of detection of 13 copies/mL [138]. NAT identifies infection up to 12 days earlier than ELISA and its use in blood screening has reduced transfusion risk to approximately 1 in 2 million donations. Techniques include Polymerase Chain Reaction (PCR), Nucleic Acid Sequence-Based Amplification (NASBA), branched DNA (bDNA), and transcription-mediated amplification (TMA). Limitations include higher cost, technical complexity, susceptibility to false results, and reduced sensitivity for certain subtypes [47].

Several supplemental assays are used for confirmation. The HIV-1/2 differentiation ELISA, such as the FDA-approved MultiSpot assay, discriminates between HIV-1 and HIV-2 and confirms reactive screening results. Western blot, long considered the gold standard with specificity above 99%, is now largely obsolete. Immunofluorescence assays detect HIV antibodies via characteristic fluorescence patterns and remain highly specific but are rarely used outside resource-limited settings. Radioimmunoprecipitation assays (RIPA), which detect radiolabeled antigen–antibody complexes, were once employed to resolve indeterminate Western blot results but are now primarily of historical interest. Virus isolation in culture is technically possible but insensitive and restricted to research contexts [47].

In modern practice, diagnostic algorithms have shifted toward highly sensitive and specific stepwise protocols. The CDC recommends initial screening with a fourth-generation antigen–antibody assay. Reactive samples are then tested with an HIV-1/2 differentiation assay. If the results are discordant, HIV-1 NAT is performed. When uncertainty persists, repeat testing is advised to allow immune responses to mature.

This algorithm shortens diagnostic delays, identifies early infection, reduces false results, and facilitates immediate linkage to care [47].

1.5 ART efficacy and limitations

As of August 2025, the U.S. FDA has approved a comprehensive array of antiretroviral medications to combat HIV infection that includes over 20 individual antiretroviral agents (Table 1) and 20 fixed-dose combination (FDC) formulations (Table 2), encompassing nine distinct drug classes.

Each class is designed to block specific stages of the HIV life cycle by targeting key viral enzymes or processes.

Generic Name (Other names and abbreviations)	FDA Approval Date
Nucleoside Reverse Transcriptase Inhibitors (NRTIs)	
Abacavir, (abacavir sulfate, ABC)	1998
Emtricitabine (FTC)	2003
Lamivudine (3TC)	1995
Tenofovir Disoproxil Fumarate (TDF)	2001
Tenofovir Alafenamide (TAF)	2016
Zidovudine (azidothymidine, AZT, ZDV)	1987
Non-Nucleoside Reverse Transcriptase Inhibitors (NNRTIs)	
Doravirine (DOR)	2018
Efavirenz (EFV)	1998
Etravirine (ETR)	2008
Nevirapine (NVP)	1996
Rilpivirine (Rilpivirine hydrochloride, RPV)	2011
Protease Inhibitors (PIs)	
Atazanavir (Atazanavir sulfate, ATV)	2003
Darunavir (Darunavir ethanolate, DRV)	2006
Fosamprenavir (fosamprenavir calcium, FOS-APV, FPV)	2003
Ritonavir (RTV)	1996
Tipranavir (TPV)	2005
Integrase Strand Transfer Inhibitors (INSTIs)	
Cabotegravir (cabotegravir sodium, CAB)	2021
Dolutegravir (Dolutegravir sodium, DTG)	2013
Raltegravir (Raltegravir potassium, RAL)	2007
Fusion Inhibitors	

Enfuvirtide (T-20)	2003
CCR5 Antagonists	
Maraviroc (MVC)	2007
Attachment Inhibitors	
Fostemsavir (Fostemsavir tromethamine, FTR),	2020
Post-Attachment Inhibitors	
Ibalizumab-uiyk (IBA, Hu5A8, TMB-355, TNX-355)	2018
Capsid Inhibitors	
Lenacapavir (LEN, GS-6207, GS-HIV, GS-CA2, GS-CA1)	2022
Pharmacokinetic Enhancers	
Cobicistat (COBI, c)	2014

Table 1. FDA approved ARV drugs as 2025. Adapted from U.S. FDA, 2025 [170].

Attachment inhibitors bind directly to the viral gp120 protein, preventing the virus from engaging the CD4 receptor, while post-attachment inhibitors bind to CD4 itself, blocking subsequent conformational changes required for entry [170].

Entry inhibitors prevent HIV from attaching to or fusing with host $CD4^+$ cells. Fusion inhibitors, such as enfuvirtide, block the conformational changes in the viral gp41 protein required for membrane fusion, while CCR5 antagonists, such as MVC, bind to the CCR5 co-receptor on host cells, preventing viral entry [170-171]. By interfering with the earliest stages of infection, these drugs reduce the number of cells that become infected, lowering overall viral replication and spread.

Capsid inhibitors, such as LEN, target the viral capsid, a protein shell that encases the viral genome and essential enzymes. By destabilizing capsid assembly or preventing proper capsid function, these drugs disrupt multiple stages of the viral life cycle, including nuclear import, reverse transcription, and assembly of new virions [170].

Once inside the cell, NRTIs and NNRTIs act on the viral RT, preventing the conversion of viral RNA into cDNA [170-172]. NRTIs are analogs of natural nucleotides that become incorporated into the nascent viral DNA, resulting in chain termination and prevention of further DNA synthesis [171].

NNRTIs, in contrast, bind directly to a hydrophobic pocket in the RT enzyme, inducing conformational changes that inhibit its polymerase activity without incorporation into the viral DNA [172]. INSTIs block the IN enzyme, preventing integration of viral cDNA into the host genome by binding to the active site of IN [170, 172-173].

PIs act later in the viral life cycle, during assembly and maturation, by inhibiting viral PR [103, 171, 174]. HIV PR cleaves the Gag and Gag-Pol polyproteins into functional structural proteins and enzymes, including matrix, capsid, nucleocapsid, RT, and IN,

during virion maturation [103, 174]. Inhibition of this enzyme prevents the proper cleavage of these polyproteins, resulting in the formation of immature, non-infectious viral particles [171].

Generic Name (Other names and abbreviations)	FDA Approval Date
Fixed Dose Combination (FDC) Drugs	
Abacavir/Lamivudine (ABC/3TC)	2004
Abacavir/Dolutegravir/Lamivudine (ABC/DTG/ 3TC)	2014
Abacavir/Lamivudine/Zidovudine (ABC/3TC/ZDV)	2000
Atazanavir/cobicistat (ATV/COBI, ATV/c)	2015
Bictegravir/Emtricitabine/Tenofovir Alafenamide (BIC/FTC/TAF)	2018
Cabotegravir/Rilpivirine (CAB/RPV)	2021
Darunavir/cobicistat (DRV/COBI, DRV/c)	2015
Darunavir/cobicistat/Emtricitabine/Tenofovir Alafenamide (DRV/COBI/FTC/TAF, DRV/c/FTC/TAF)	2018
Dolutegravir/Lamivudine (DTG/3TC)	2019
Dolutegravir/Rilpivirine (DTG/RPV)	2017
Doravirine/Lamivudine/Tenofovir Disoproxil Fumarate (DOR/3TC/TDF)	2018
Efavirenz/Emtricitabine/Tenofovir Disoproxil Fumarate (EFV/FTC/TDF)	2006
Elvitegravir/cobicistat/Emtricitabine/Tenofovir Alafenamide (EVG/COBI/FTC/TAF, EVG/c/FTC/TAF)	2015
Emtricitabine/Rilpivirine/Tenofovir Alafenamide (FTC/RPV/TAF)	2006
Emtricitabine/Rilpivirine/Tenofovir Disoproxil Fumarate (FTC/RPV/TDF)	2011
Emtricitabine/Tenofovir Alafenamide (FTC/TAF)	2016
Emtricitabine/Tenofovir Disoproxil Fumarate (FTC/TDF)	2004
Lamivudine/Tenofovir Disoproxil Fumarate (3TC/TDF)	2018
Lamivudine/Zidovudine (3TC/ZDV)	1997
Lopinavir/ritonavir (LPV/r, LPV/RTV)	2000

Table 2. FDA approved Fixed Dose Combination (FDC) drugs as 2025. Adapted from U.S. FDA, 2025 [170].

Pharmacokinetic enhancers, such as RTV and COBI do not have direct antiviral activity but inhibit the metabolism of other antiretrovirals, increasing their plasma concentrations and prolonging effective drug levels [170]. They are commonly used in combination regimens to boost the efficacy of PIs or other classes, improving overall viral suppression.

In the last decades, FDC tablets and long-acting (LA) formulations have simplified treatment regimens, improved adherence and reduced the risk of resistance [170, 175].

Specifically, LA injectable formulations, such as CAB/RPV or LEN, maintain therapeutic drug levels over weeks or months, offering alternatives for patients who have difficulty with daily oral therapy [170].

Despite the remarkable efficacy of ART in suppressing viral replication and improving immune function, several limitations remain. Safety concerns arise from manageable yet potentially toxic adverse effects, including metabolic disturbances, renal and bone toxicity, and cardiovascular risks [176]. Adherence remains critical for maintaining viral suppression, even with single-tablet regimens (STR), as missed doses can lead to resistance [177]. DDIs, particularly in aging populations with polypharmacy, may complicate treatment. Furthermore, ART does not eradicate the infection: latent viral reservoirs persist, and viral replication resumes rapidly if therapy is interrupted, highlighting the need for strategies targeting viral persistence [178-181].

1.6 The obstacles to the cure

The main obstacles to HIV eradication are represented by the establishment, the persistence/expansion and the invisibility of the HIV reservoir [182], mostly represented by resting memory $CD4^+$ T cells ($CD4^+$ T_{RM}), harboring intact, integrated proviral DNA that remains transcriptionally silent, producing little or no RNA or viral proteins. However, upon appropriate cellular activation, it can be reawakened, giving rise to infectious virions [183]

Several mechanisms have been proposed to explain the establishment of latency (Fig. 5). During early stages of infection, before plasma viremia becomes detectable, HIV enters $CD4^+$ T cells, reverse-transcribes its RNA into DNA, and integrates it into the host genome. Some of these infected cells then transition into a resting state, establishing latency. In this form, they evade immune clearance and cytotoxic effects, remain unaffected by ART, and persist long-term [183].

However, it has recently been hypothesized that HIV may infect activated $CD4^+$ T cells, which subsequently revert to a quiescent G0 memory state, or it may directly infect resting $CD4^+$ T cells [184-185]. In support of these mechanisms, selective viral proteins such as Tat and Nef have been detected in T_{RM} [186], where they can modulate cell activation and facilitate viral integration [187-188]. Moreover, although resting $CD4^+$ T cells are relatively resistant to HIV compared to activated T cells, mild stimulation by chemokines such as CC ligand 19 (CCL19) and CC ligand 21 (CCL21) or cytokines like IL-4 and and IL-7 can enhance their susceptibility to infection without inducing overt activation [189-191].

HIV latency within resting $CD4^+$ T cells is remarkably stable, with integrated viral DNA showing minimal decay over time and an estimated half-life of ~25 years [192].

Resting CD4⁺ T cells comprise several subpopulations in which viral DNA has been detected in PLWH, including T_N, central memory (T_{CM}), transitional memory (T_{TM}), effector memory (T_{EM}), and stem cell memory (T_{SCM}) cells [193-196].

Among these, T_{SCM} stand out for their long lifespan, self-renewal capacity, and ability to differentiate into other memory subsets [197]. Also, their expression of the HIV co-receptors CCR5 and CXCR4 makes them highly susceptible to infection [198], and their persistence renders them one of the most durable viral reservoirs [199].

Although infected at lower frequencies, T_N can still be reactivated to produce infectious virus at levels similar to T_M cells, making them a relevant reservoir for viral rebound after treatment interruption [200-202].

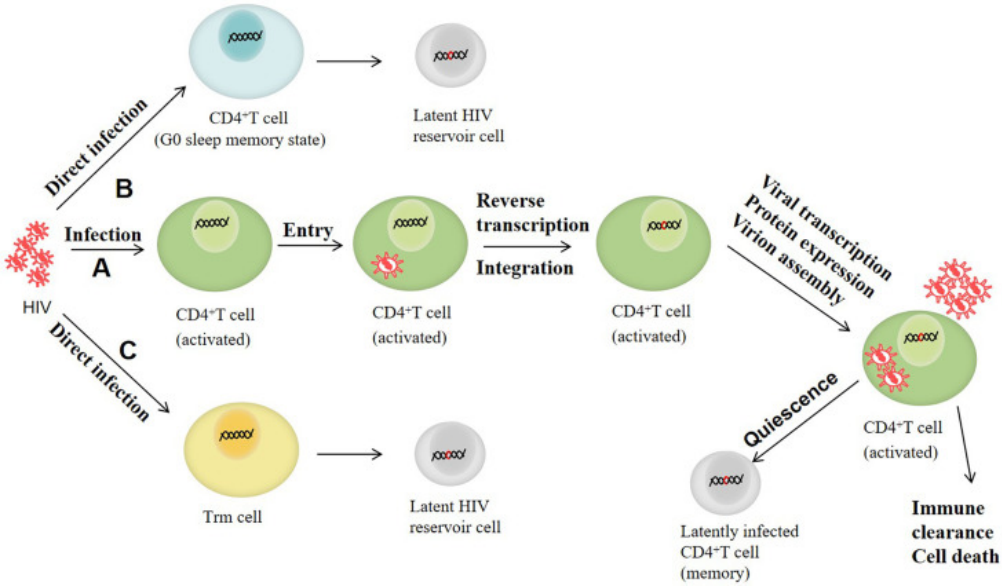

Fig. 5 Possible mechanisms of latent HIV reservoir formation. (A) HIV infects CD4⁺ T cells; viral RNA is reverse-transcribed and integrated into the host genome, and some cells become resting, forming latent HIV-infected cells. (B) HIV infects CD4⁺ T cells that revert to a dormant G0 memory state, enabling latency. (C) HIV directly infects CD4⁺ T_{rm}, establishing the latent reservoir. Adapted from Chen et al., 2022 [183]

Despite CD4⁺ T_M cells remain the primary recognized reservoir of latent HIV [203-205], the speed and frequency of viral rebound after ART interruption often exceed what can be attributed solely to CD4⁺ T cell proliferation [206]. This discrepancy suggested the contribution of additional cellular reservoirs to HIV persistence and a potential role in HIV-related comorbidities [207-209].

Several studies supported this hypothesis, showing that circulating monocytes and long-lived tissue-resident macrophages from the brain, urethra, gut, liver, lungs and spleen, and other myeloid cells can harbor reactivatable HIV, contributing to viral rebound following analytical treatment interruption (ATI) due to their longevity and immune privilege [210-212]. HIV DNA has been detected in circulating monocytes as they migrate from the bone marrow to tissues, where they rapidly differentiate into various types of tissue-resident macrophages [213]. Macrophages themselves are considered early

targets of HIV due to the expression of CD4, CCR5, and CXCR4 receptors and co-receptors on their surfaces [214]. Multiple studies suggest that macrophages play a key role in the establishment and persistence of the viral reservoir, owing to their long lifespan, relative resistance to HIV-induced apoptosis, and widespread presence across tissues [215].

In the SIV infected Rhesus macaque (RM) model, a quantitative virus outgrowth assay (QVOA) used to measure latent infection in myeloid cells revealed that mononuclear macrophages harboring latent virus were present in blood, bronchoalveolar lavage fluid, lung, spleen, and brain [216-217]. Furthermore, virus produced by these macrophages was shown to infect activated $CD4^+$ T cells, indicating that latently infected macrophages can contribute to viral rebound after ATI [216-217].

DCs also contribute to HIV persistence, functioning as both facilitators of viral spread and reservoirs of latent infection [218]. As professional antigen-presenting cells (APCs), DCs capture HIV through surface receptors such as DC-SIGN and Siglec-1, enabling them to transmit the virus to $CD4^+$ T cells through the formation of infectious or virologic synapses [219]. Beyond this role in viral spread, DCs can also harbor latent HIV-1, serving as a cellular reservoir that persists despite ART.

Interactions between DCs and T cells have been shown to reactivate latent virus, suggesting that DCs contribute not only to the maintenance of viral reservoirs but also to potential viral rebound after ATI. Moreover, HIV-1 infection can induce a tolerogenic state in DCs, impairing their capacity to mount effective antiviral immune responses and further supporting viral persistence [218].

Hematopoietic progenitor cells (HPCs) $CD34^+$ express CD4, CCR5, and CXCR4 HIV receptors and co-receptors, making them susceptible to both active and latent infection [220-221]. In ART-treated PLWH with undetectable plasma viral load (pVL), HIV genome was found in $CD34^+$ HPCs, with frequencies ranging from 3–40 genomes per 10,000 cells, indicating that these progenitor cells can serve as a long-term reservoir and contribute to residual HIV despite therapy [221]. Different HIV subtypes have been shown to infect HPCs in vivo and in vitro [222], and viral gene expression can be induced in latent HPCs through cytokine treatment or stimulation of differentiation pathways, such as with Granulocyte-Macrophage Colony-Stimulating Factor (GM-CSF) and TNF-α [220, 223].

An additional reservoir is present within the central nervous system (CNS) and it is represented by astrocytes and microglia. Astrocytes are the most abundant cell type in CNS and play a vital role in maintaining CNS homeostasis and regulating blood flow in response to injury and diseases [224]. Though infrequently infected, astrocytes can maintain latent HIV DNA and transmit viruses upon reactivation via cell-to-cell mechanisms [225].

Finally, non-immune cells such as renal tubular and hepatic epithelial cells have also been shown to harbor integrated HIV DNA and release infectious particles, highlighting the broad cellular landscape of latent reservoirs [226-227].

Beyond the cellular level, the anatomical context in which these reservoirs reside plays a critical role, as tissues provide both sanctuary sites and microenvironments that regulate viral persistence (Fig. 6).

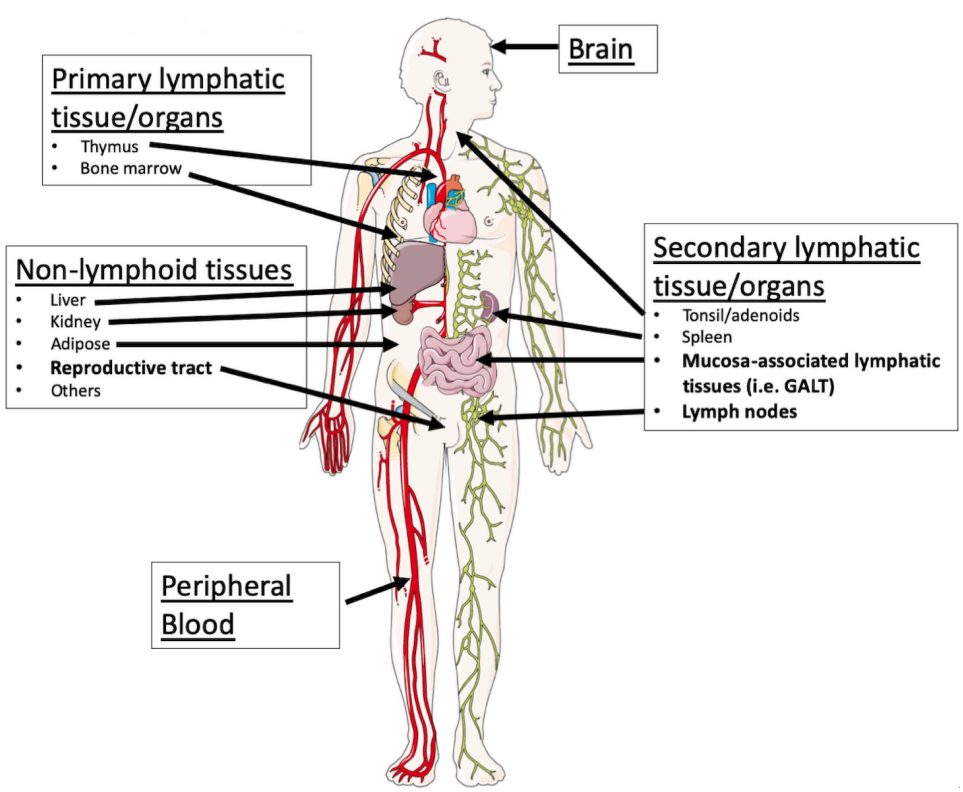

Fig. 6 Anatomical sites of HIV persistence. Sites in bold indicate tissues where replication-competent virus has been recovered in PLWH after prolonged ART. Sites in regular font represent tissues where HIV nucleic acids have been detected in humans or animal models, but recovery of replication-competent virus in humans has not yet been demonstrated. Adapted from Falcinelli et al. 2019 [229]

Studying HIV persistence within tissues remains challenging due to limited sampling opportunities; nonetheless, autopsy and biopsy studies in both humans and non-human primates have provided critical insights [228].

Among anatomical sites, LNs and gut-associated lymphoid tissues (GALT) continue to be primary reservoirs, consistently harboring high frequencies of infected cells despite ART [230]. In particular, the gut has emerged as the dominant reservoir, with in vivo studies in SIV-infected RMs estimating that more than 98% of viral persistence occurs within this compartment [230-232].

Lymphoid tissues further contribute to persistence through the formation of immune-privileged niches: B cell follicles exclude effector $CD8^+$ T cells, thereby creating a microenvironment that fosters reservoir maintenance [233-234].

Beyond these classical sites, human autopsy studies have revealed a strikingly broad distribution of HIV, with proviral DNA detected in at least 28 tissues, including liver,

spleen, brain, and genital tract [235]. Sanctuary sites such as the brain and testes pose additional barriers to eradication, as they are protected by restrictive anatomical barriers that limit ART penetration [236-237].

In parallel, tissue-resident macrophages have been identified as key contributors to reservoir persistence across multiple sites, including seminal vesicles, urethra, adipose tissue, and liver [238-240], with infection also reported in lung and duodenal macrophages of ART-suppressed individuals [241].

The reproductive tract represents another critical reservoir, as both male and female genital tissues harbor infected cells: in men, latent HIV has been observed in reproductive tract macrophages [242], while in women, tissue-resident $CD4^+$ T_M cells in the cervix are particularly enriched in HIV DNA [243].

Collectively those findings showed that the first major obstacle in HIV eradication is the establishment of viral reservoir, which begins so early during acute infection that even immediate ART initiation after exposure cannot fully prevent its seeding and the dramatical widespread distribution throughout the body [244-245]. The second problem is represented by the not static nature of the viral reservoir. Long-lived infected cells, particularly $CD4^+$ T_{SCM} cells, can undergo clonal expansion through homeostatic proliferation, antigen-driven proliferation, and, in some cases, integration-site–linked proliferation, thereby sustaining and even enlarging the pool of latent infection over time [182]. Microfluidic and single-cell sequencing approaches have enabled the isolation of unstimulated $CD4^+$ T cells harboring HIV DNA from the blood and LNs of PLWH on long-term ART. These analyses reveal transcriptomic signatures favoring HIV silencing, cell survival, and proliferation, together with clusters of surface receptors associated with immune checkpoint signaling, enhanced survival, and resistance to cytotoxic killing. However, reliable biomarkers for selectively identifying latently infected cells remain so far elusive, representing another obstacle to viral eradication [182].

Consequently, eradication strategies for HIV universally center on the viral reservoir as their main target.

2. Strategies to eradicate HIV infection

Despite important therapeutic advances in the management of PLWH with the introduction of ART, this strategy is unable to eradicate the virus from the host genome. Furthermore, the presence of reservoirs within anatomical sections rich in $CD4^+$ T_M cells, which has been observed to be the cause of the increase in plasma viremia following drug discontinuation, still represent the main obstacles in the resolutive treatment of AIDS. Due to the partial failure of ART, numerous other therapeutic strategies have

been developed, including (i) Block-and-Lock Approach, (ii) Shock-and-Kill Approach, (iii) Immunological Approach, (iv) Gene therapy, and (v) the Stem Cell Transplantation.

For the purpose of this thesis, only the Shock and Kill approach will be discussed in detail.

2.1 *Shock-and-Kill* strategy

The *Shock-and-Kill* approach was developed using latency-reversing agents (LRAs), which are molecules capable of reactivating (shock) the infected cells from the latency state, increasing viral gene expression.

In 2012, Archin et al. [246] reported a proof-of-concept clinical study in which administration of the histone deacetylase inhibitor (HDAi) vorinostat (VOR) to PLWH on suppressive ART led to a measurable increase in HIV RNA expression in resting $CD4^+$ T cells, thereby demonstrating that latent HIV could be pharmacologically disrupted *in vivo*. This landmark finding laid the foundation for one of the major immunotherapy-based strategies, known as the "Shock-And-Kill" approach (Fig. 7).

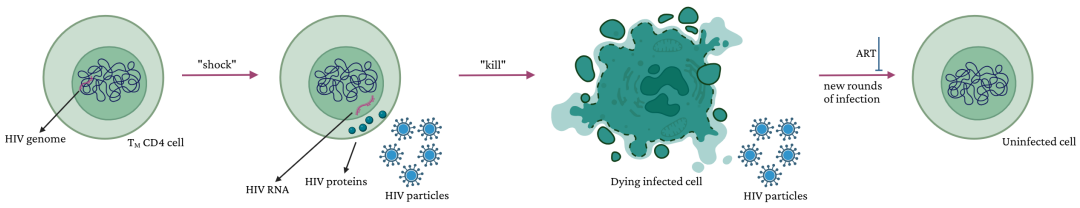

Fig. 7 'Shock-and-Kill' strategy. Latent HIV DNA is reactivated ("shock") by treatment with an LRA to render infected cells susceptible to clearance by viral cytopathic effects or immune-mediated killing ("kill"). Ongoing ART prevents new rounds of infection. Modified from Deeks 2012 [247]

This strategy has become a central paradigm in HIV cure research. It aims to reverse latency using LRAs to induce viral transcription and antigen expression ("shock"), thereby rendering infected cells visible to immune effector mechanisms or susceptible to cytopathic effects, which then eliminate them ("kill") [247-249].

In PLWH, viral reactivation from latency occurs naturally under certain circumstances, and the purpose of LRAs is to mimic this process [250].

HIV reactivation is a stochastic event, but the probability of reactivation strongly depends on the activation state of the host cell: HIV preferentially replicates in activated $CD4^+$ T cells, where stimulation of the T cell receptor (TCR) induces transcription factors such as NF-κB, Activator Protein 1 (AP-1), and Nuclear Factor of Activated T cells (NFAT) that bind to the viral LTRs promoter and drive transcription.

Consistent with this, *ex vivo* stimulation of T_M cells by antigen is an efficient trigger of HIV reactivation, which likely occurs frequently *in vivo*, as recurrent infections (e.g.,

influenza) and chronic co-infections (e.g., CMV) continuously stimulate T_M cells. Notably, a significant portion of the latent reservoir resides in HIV-specific $CD4^+$ T_M cells, and *ex vivo* stimulation with HIV antigens has been shown to reactivate a large fraction of these latently infected cells [250].

A central player in this process is NF-κB signaling, which drives HIV transcription but can be activated through two mechanistically distinct pathways with very different biological outcomes (Fig. 8). The canonical NF-κB (cNF-κB) pathway is rapidly induced by signals such as TCR engagement, Protein Kinase C (PKC) activation, Toll-Like Receptor (TLR) stimulation, or cytokines like TNFα. Activation proceeds via Inhibitor of κB (IκB) kinase beta (IKKβ)-mediated phosphorylation and degradation of IκBα, releasing p50/RelA (p65) dimers that translocate into the nucleus. These dimers potently activate transcription from the HIV LTR but also trigger a broad host transcriptional program, including pro-inflammatory cytokines (IL-2, TNF-α, IL-6), chemokines, and surface activation markers (CD69, CD25). Consequently, cNF-κB–driven latency reversal is effective but tightly linked to global T cell activation and inflammatory responses [251].

In contrast, the non-canonical NF-κB (ncNF-κB) pathway is slower and more tightly regulated, relying on stabilization of NF-κB–inducing kinase (NIK) and IKKα-mediated processing of p100 into p52 to generate RelB/p52 dimers. Unlike the broad p65-driven response, RelB/p52 dimers regulate a narrower transcriptional program focused on lymphoid tissue organization and cell survival. Importantly, they can still bind the HIV LTR and promote viral transcription but without broadly inducing pro-inflammatory cytokines or T cell activation markers [251].

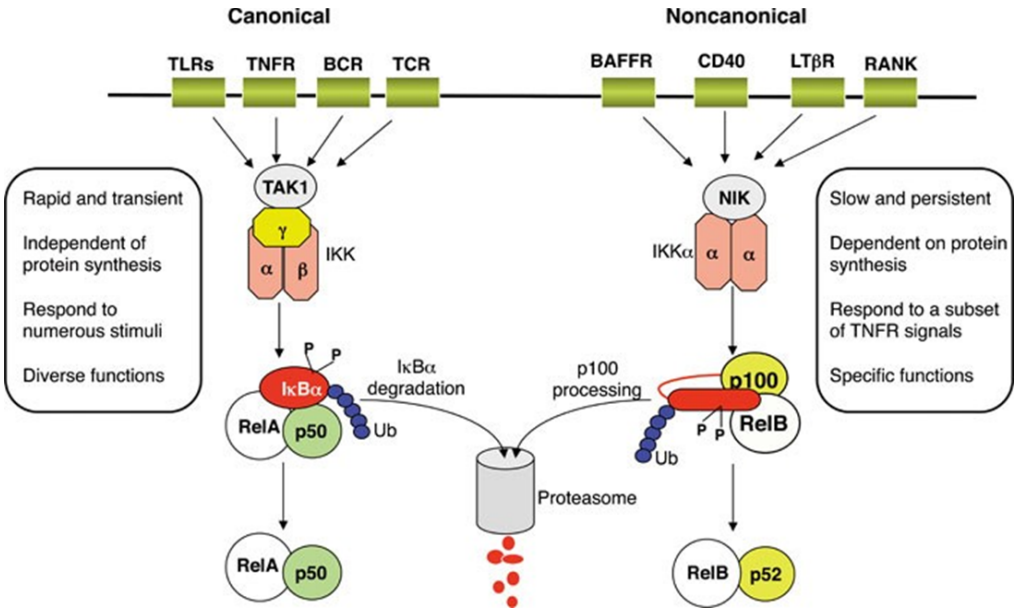

Fig. 8 Canonical and non-canonical NF-κB signaling pathways. The canonical pathway is activated by diverse stimuli, including signals from both innate and adaptive immune receptors. This cascade involves TAK1-

mediated activation of the IKK complex, phosphorylation and degradation of IκBα, and the rapid but transient nuclear translocation of the RelA/p50 NF-κB heterodimer. In contrast, the non-canonical pathway is activated by a restricted subset of TNFR family members and relies on NIK- and IKKα-dependent phosphorylation-induced processing of p100 into p52. This results in the persistent nuclear activation of the RelB/p52 complex, independently of the trimeric IKK complex. Adapted from Sun, 2010 [251].

These mechanistic distinctions highlight why NF-κB–targeting LRAs differ in both potency and risk of systemic effects.

Beyond NF-κB, LRAs engage additional molecular pathways, such as chromatin remodeling, modulation of transcription factors, and T cell signaling, inhibition of immune checkpoints and direct activation of HIV LTR, to reverse HIV latency (Fig. 9). Consequently, based on their mechanism of action to disrupt HIV latency, LRAs are categorized into several distinct classes (Table 3) [250].

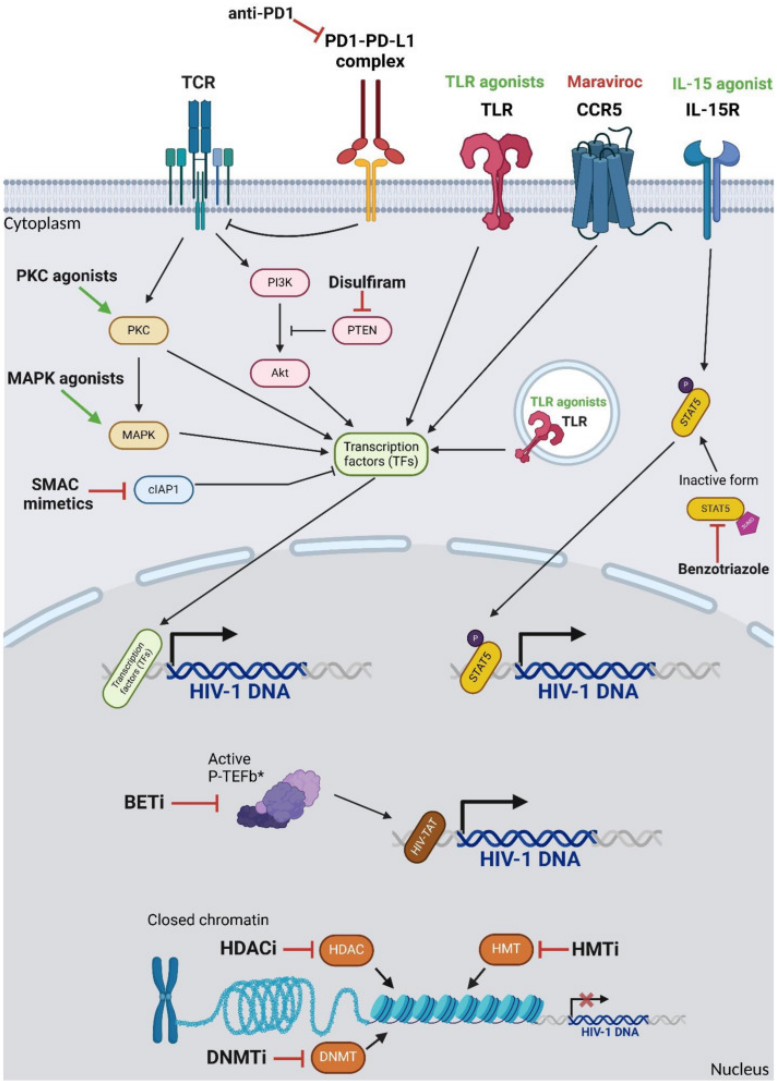

Fig. 9 Overview on the LRAs classes and their mechanisms of action. LRAs aim to disrupt HIV latency by targeting different cellular pathways, including epigenetic regulation, transcriptional activation, and signaling cascades. Adapted from Tioka et al. 2025 [250]

Mode of Action	Compounds	Past and Ongoing Studies		
		In Vitro	*Ex Vivo*	*In Vivo*
PKC AGONISTS				
	Phorbol Esters			
Activation of NF-κB	Phorbol 12-myristate 13-acetate (PMA)	Reactivation of HIV-1 transcription [253]	Reactivation of HIV-1 transcription [253-255]	
	Prostratin	HIV-1 latency reversal [256-257]	HIV-1 latency reversal [256]	
	12-Deoxyphorbol 13-phenylacetate (DPP)	HIV-1 latency reversal [258]	HIV-1 latency reversal [256]	
	Macrocyclic lactones			
	Bryostatin-1 and analogues	Reactivation of HIV-1 gene expression [259-260]	Reactivation of HIV-1 gene expression [261]	Tested in the context of malignancies [262] as well as in a phase I clinical trial on ART-treated PLWH [263]
	Diterpenes			
	Ingenol and derivatives	Reactivation of HIV-1 transcription [264-265]	Reactivation of HIV-1 transcription [264-266]	Tested in non-human primates [267] and PLWH [268]
MAPK AGONISTS				
Activation of MAPK	Procyanidin C1	Reactivation of HIV-1 transcription [269]	Reactivation of HIV-1 transcription [269]	
ACTIVATORS OF AKT PATHWAY				
Activation of NF-κB	Disulfiram	Reactivation of HIV-1 transcription [270]	Reactivation of HIV-1 transcription [270-271]	Phase 1 and 2 clinical studies [272-273]
	Hexamethylene bisacetamide (HMBA)	Reactivation of HIV-1 transcription [274]	Disruption of HIV-1 latency [275]	Phase 2 clinical study in the context of malignancies [276]
	57704	Reactivation of HIV-1 transcription [277]	Reactivation of HIV-1 transcription [277]	
IMMUNE MODULATORY LRAs				
	Toll-Like receptor agonists			
Activation of NF-κB	TLR1/2 (Pam3CSK4)	Reactivation of HIV-1 gene expression [278]	Reactivation of HIV-1 gene expression [279]	
	TLR5 (Flagellin)		Reactivation of HIV-1 gene expression [280]	

	TLR7 (GS-9620)	Reactivation of HIV-1 gene expression [278]	Reactivation of HIV-1 gene expression [281]	Tested in NHP [282] Phase 1 clinical trial [283]
	TLR9 (MGN 1703)		Reactivation of HIV-1 gene expression [284]	Tested in phase 1 and 2 clinical trial [285]
	IL-15 agonists			
Activation of STAT5	IL-15 (ALT-803)	HIV-1 latency reversal [285]	HIV-1 latency reversal [286]	Tested in NHP [286-289] Phase 1 clinical trial [290]
	Immune check-point inhibitors			
Anti-anergic	anti-PD-1		HIV-1 latency reversal [291-292]	Phase 1 clinical trial in adults PLWH [293-296]
	anti-CTLA-4			Phase 1 clinical trial in adults PLWH [293-295]
EPIGENETIC MODIFIERS				
	HDACi			
	Trichostatin A, Trapoxin, Romidepsin, Vorinostat, Entinostat, Valproicacid, Fimepinostat, Chidamide, Panobinostat	Reactivation of HIV-1 transcription [297]	HIV-1 latency reversal [298-299]	Extensively studied in clinical trials [246, 300-302]
	HMTi			
	Chaetocin BIX-01294		Reactivation of HIV-1 gene expression [303-304]	
	Induction of crotonylation			
	No agents published (ACSS2-driven latency reversal)	Reactivation of HIV-1 transcription [305]	HIV-1 latency reversal [305]	
	DNMTi			
	5-aza-cytidine 5-aza-deoxycytidine zebularine	Reactivation of HIV-1 gene expression only in combination with other LRAs [306-308]	Reactivation of HIV-1 gene expression only in combination with other LRAs [306-308]	
SMAC MIMETICS				
Activation of noncanonical NF-κB pathway	SBI-0637142	HIV-1 latency reversal [309]	HIV-1 latency reversal [309]	
	SBI-0953294 (Ciapavir)			Reactivation of HIV-1 gene expression in a humanized mouse model [310]
	AZD5582			Reactivation of HIV-1 gene expression Hu-

				mice and RMs studies [311]
STAT5 sumoylation inhibitors				
Activation of STAT5	1-hydroxybenzotriazol and derivatives	Induction of HIV-1 gene expression [312]	Induction of HIV-1 gene expression	Phase 1 trial [312]
BET inhibitors				
Release of P-TEFb	JQ1 MMQO RVX-208 PFI-1	HIV-1 latency reversal [265, 313-315]	HIV-1 latency reversal [265, 313]	
	I-BET and I-BET151			Reactivation of HIV-1 gene expression in Hu-mice model [316]
CCR5 antagonists				
Activation of NF-κB	MVC HIV-1 latency reversal [317-318]	HIV-1 latency reversal [317-318]	No consistent reactivation pattern [318]	Phase 2 clinical trial [319]
Tat vaccines				
Activation of HIV-1 LTR	Tat-R5M4 protein Reactivation of latently infected cells [320]	Reactivation of latently infected cells [320]	HIV-1 latency reversal [320]	Tested for side effects and immunogenicity in mice [320]

Table 3. Overview of different LRAs. Modified from Tioka et al. 2025 [250]

Given that the primary focus of this thesis is AZD5582, the subsequent discussion will be restricted to this compound and its class of LRAs.

2.2 SMAC mimetics

The regulation of apoptosis is central to understanding the therapeutic potential of second mitochondria-derived activator of caspase (SMAC) mimetics as LRAs.

Apoptosis is a type of programmed cell death, executed through two interconnected pathways: the intrinsic (mitochondrial) and extrinsic (death receptor–mediated) cascades, both of which converge on the activation of cysteine proteases known as caspases [321-322] (Fig. 10).

The intrinsic pathway is triggered by intracellular stressors, including DNA damage, oxidative stress, hypoxia, or oncogene activation, which induce the activation of B-cell lymphoma 2 (BCL-2) homology 3 (BH3)-only proteins (BID, BIM, BAD, BIK, BMF, Noxa, PUMA and HRK). BH3-only proteins can interact with either pro-survival or pro-apoptotic members of the BCL-2 family, thereby influencing whether apoptosis is halted or allowed to proceed [324].

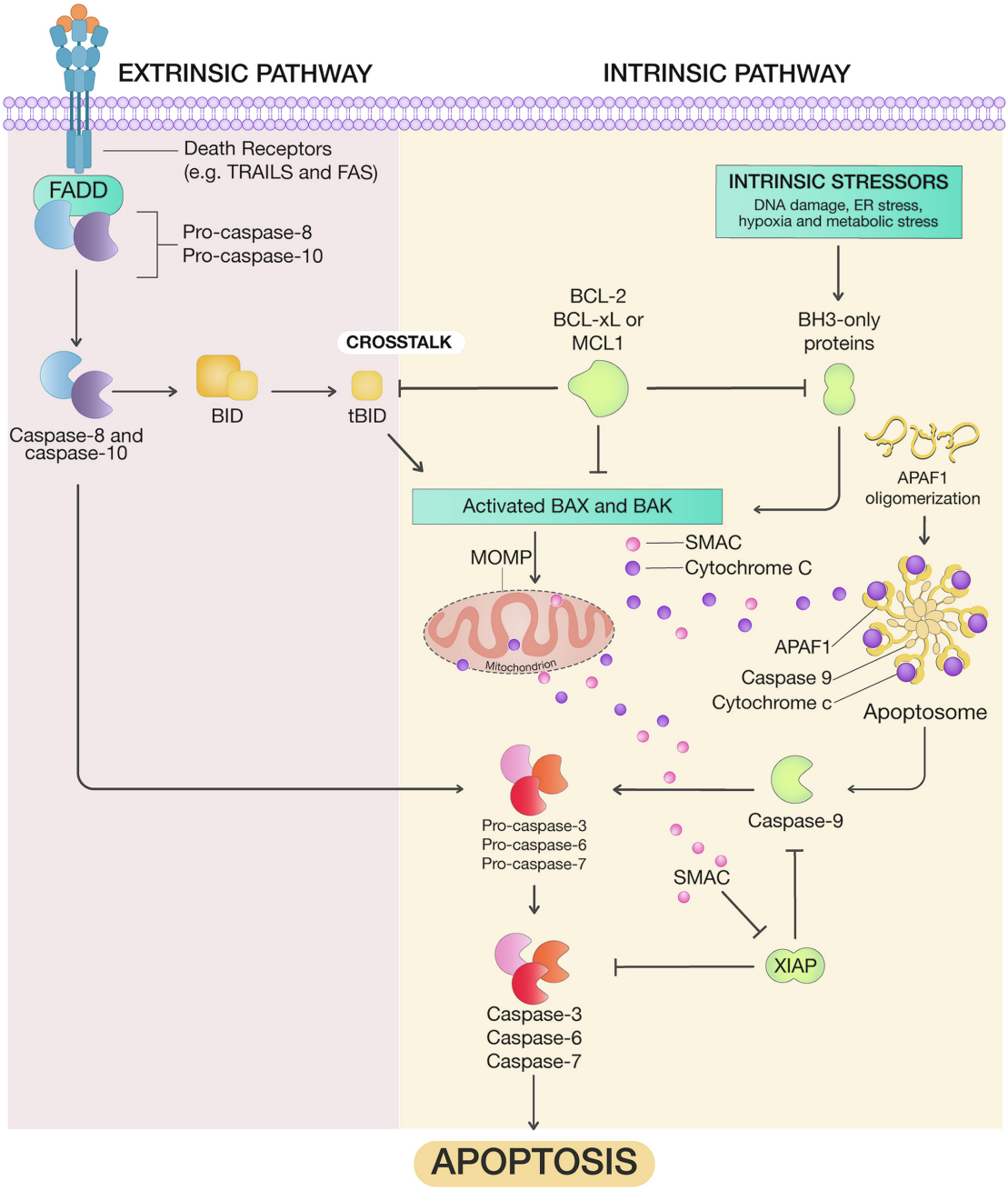

Fig. 10 Intrinsic and extrinsic apoptotic pathways. The intrinsic pathway is triggered by cellular stressors such as DNA damage, which induce mitochondrial outer membrane permeabilization (MOMP). This event promotes the activation of caspase (CASP)-9, which subsequently activates the executioner CASP-3, -6, and -7, leading to apoptosis. The extrinsic pathway begins with the engagement of cell surface death receptors by their ligands, resulting in the activation of CASP-8. Activated CASP-8 then initiates the executioner CASP-3, -6, and -7, and also amplifies the intrinsic pathway through cleavage of the Bcl-2 family protein BID into truncated BID (tBID). Adapted from Balaji et al. 2021 [323].

When pro-survival proteins such as BCL-2, BCL-XL, BCL-w, MCL-1, or BFL-1/A1 dominate, they suppress the apoptotic cascade at that stage. Conversely, activation of the pro-apoptotic factors BCL-2-associated X protein (BAX) or BCL-2 antagonist/killer (BAK) promotes mitochondrial outer membrane permeabilization (MOMP). This is an irreversible event, as it triggers the release of mitochondrial proteins into the cytosol

that initiate caspases activation, alongside progressive acidification of the peri mitochondrial environment [325].

During MOMP, proteins such as cytochrome c (Cyt-c) and the pro-apoptotic factors SMAC/DIABLO and Omi/HtrA2 are released into the cytoplasm. Cyt-c triggers the formation of the apoptosome, a multiprotein complex composed of Cyt-c, apoptotic protease-activating factor 1 (Apaf-1), and procaspase-9 (ProC9). This assembly begins with Cyt-c binding to Apaf-1 monomers, followed by ATP-dependent formation of the heptameric structure and recruitment of ProC9.

Activation of caspase (CASP)-9 requires its interaction with the caspase recruitment domain (CARD) of Apaf-1, and CASP-9 must remain bound to the apoptosome to maintain catalytic activity. CASP-9 then cleaves and activates executioner caspases, including CASP-3 and CASP-7, reorganizing their active sites. Activated executioner caspases further amplify the cascade by processing additional caspases, driving the execution phase of apoptosis [325].

The extrinsic pathway, in contrast, is initiated by the engagement of cell-surface death receptors (such as Fas, TNFR1, or TRAIL receptors) with their ligands (TNF, FasL, TRAIL), leading to assembly of the death-inducing signaling complex (DISC) and activation of CASP-8 [325]. CASP-8 can directly activate executioner caspases (CASP-3, CASP-6, CASP-7) or cleave BID into truncated BID (tBID), which feeds into the intrinsic pathway by activating BAX and BAK to drive MOMP [326].

Inhibitor of apoptosis proteins (IAPs) serve as essential regulators of programmed cell death, acting as brakes on both intrinsic and extrinsic pathways. They share conserved baculovirus IAP repeat (BIR) domains that mediate interactions with caspases and signaling proteins.

X-linked inhibitor of apoptosis protein (XIAP) is the most potent direct inhibitor of apoptosis, binding and suppressing CASP-9 via its BIR3 domain and CASP-3 and -7 through BIR2. In contrast, cellular inhibitors of apoptosis proteins 1 and 2 (cIAP1 and cIAP2) modulate apoptosis indirectly, primarily through ubiquitination of adaptor proteins. By binding TNF receptor-associated factor 2 (TRAF2) via BIR1 and utilizing their RING E3 ligase activity, cIAP1/2 redirect TNF receptor signaling toward cNF-κB activation, while also continuously ubiquitinating NIK to prevent activation of the non-canonical ncNF-κB pathway [325].

Upon mitochondrial release, the 55-amino-acid N-terminal region of SMAC is cleaved, revealing an Ala-Val-Pro-Ile (AVPI) motif that facilitates its binding to IAPs, including XIAP, cIAP1, and cIAP2. SMAC can form dimers and engage both the BIR2 and BIR3 domains of XIAP, thereby disrupting XIAP's inhibition of CASP-9. Additionally, SMAC interacts with the BIR3 domains of cIAP1 and cIAP2, triggering their autoubiquitination and subsequent proteasomal degradation [327]. In the context of HIV infection, cIAP1

suppresses activation of the ncNF-κB pathway, contributing to the repression of HIV LTR–driven transcription.

SMAC mimetics are small molecules exploiting this regulatory mechanism by mimicking the endogenous SMAC/DIABLO proteins, promoting the activation of the ncNF-κB–dependent gene expression, thereby facilitating reactivation of HIV transcription from the latent reservoir (Fig.11).

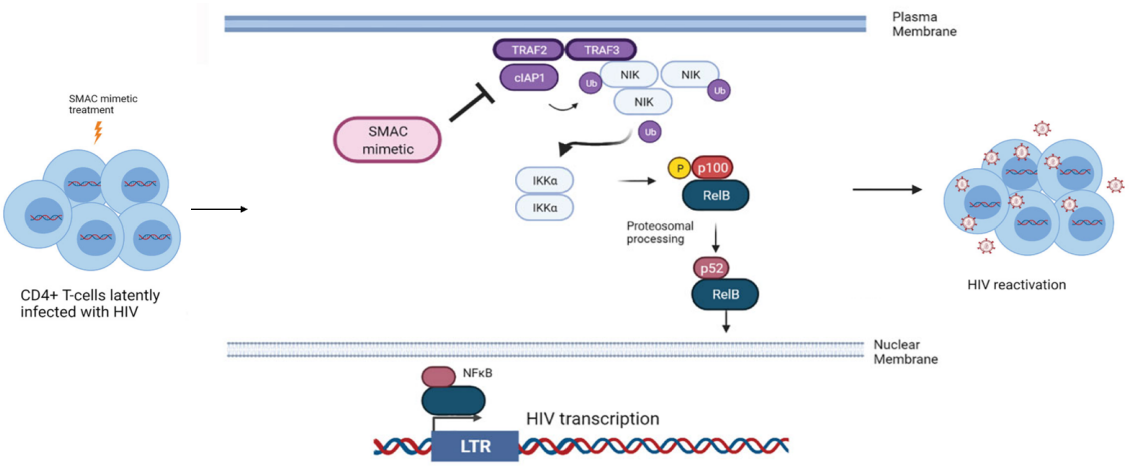

Fig. 11 SMAC mimetics trigger non-canonical NF-κB signaling to reverse HIV latency. By promoting cIAP1 degradation, SMAC mimetics stabilize NIK, which activates IKKα and drives p100 processing into p52. The resulting RelB/p52 NF-κB complex translocates to the nucleus, binds the HIV LTR, and induces viral gene expression, leading to latency reversal. Modified from Molyer et al. 2021 [327]

Moreover, SMAC mimetics not only reactivate latent HIV but also directly sensitize infected cells to apoptosis (Fig 12). HIV proteins themselves profoundly alter apoptotic pathways: for instance, Tat can upregulate anti-apoptotic proteins like BCL-2 and cFLIP, conferring resistance to FasL-mediated apoptosis, but can also increase CASP-8 activation, sensitizing $CD4^+$ T cells to death; Vpr enhances XIAP stability, promotes BCL-2 expression, and suppresses pro-apoptotic proteins such as BAD, but it can also trigger Cyt c release by acting on mitochondrial ion channels. Similarly, gp120 increases XIAP, cIAP1, and cIAP2 expression in macrophages, shielding them from TRAIL-mediated apoptosis, while also inducing apoptosis of $CD4^+$ T cells through CD4 engagement.
HIV hijacks anti-apoptotic pathways, thereby stabilizing reservoirs and creating a therapeutic rationale for IAPs antagonists. In vitro, HIV-producing cells exposed to SMAC mimetics undergo preferential cell death. Thus, SMAC mimetics offer a dual mechanism of action: disrupting latency via ncNF-κB signaling and weakening the survival advantage of reservoir cells by disabling IAP-mediated apoptosis control [250, 327].

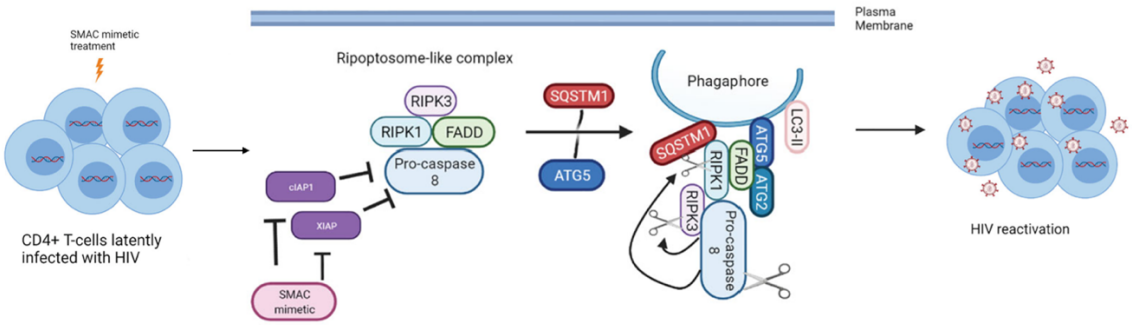

Fig. 12 SMAC mimetics selectively induce apoptosis in HIV-infected cells. By promoting degradation of cIAP1 and XIAP, SMAC mimetics trigger autophagy, which provides a scaffold for the formation of a ripoptosome-like DISC complex (CASP-8, RIPK1, RIPK3, FADD) on unclosed phagophore membranes (involving SQSTM1, ATG5, ATG2, LC3-II). This mechanism results in targeted killing of HIV-infected $CD4^+$ T cells. Adapted from Molyer et al. 2021 [327]

Based on their structural features and selectivity profiles, SMAC mimetics are categorized into two generations (Table 4). First-generation SMAC mimetics are typically monovalent compounds designed to bind to the BIR3 domain of IAPs, leading to the degradation of cIAP1 and cIAP2. However, these agents often have limited selectivity and can induce systemic inflammation due to broad activation of the NF-κB pathway. Second-generation SMAC mimetics are bivalent compounds containing two AVPI-mimicking motifs tethered by a linker, allowing them to simultaneously engage the BIR2 and BIR3 domains of XIAP. This dual engagement enhances potency and selectivity, preferentially targets cIAP1, and leads to more controlled activation of the NF-κB pathway, often with improved tolerability and reduced systemic inflammation compared to first-generation agents.

Another major difference between the two generations is their ability to antagonize XIAP. Monovalent SMAC mimetics potently block XIAP BIR3-mediated inhibition of CASP-9 but are much less effective against XIAP proteins containing both BIR2 and BIR3 domains. In contrast, bivalent SMAC mimetics act as ultra-potent antagonists of XIAP by concurrently binding both BIR2 and BIR3 domains, more efficiently relieving caspase inhibition. Both monovalent and bivalent SMAC mimetics can induce apoptosis in a subset of human cancer cell lines in a TNFα-dependent manner, but bivalent compounds are generally much more potent. A notable advantage of monovalent mimetics is their favorable pharmacokinetic profile, with some designed for excellent oral bioavailability. Monovalent SMAC mimetics have been extensively tested in vitro and vivo in oncology research (e.g., SM-406/AT-406), demonstrating effective antagonism of XIAP BIR3, rapid degradation of cIAP1, and inhibition of cancer cell growth in multiple human cancer lines [328].

Feature	Monovalent SMAC Mimetics (1st Gen)	Bivalent SMAC Mimetics (2nd Gen)
Structure	Single AVPI-mimicking motif	Two AVPI-mimicking motifs tethered by a linker
XIAP Binding	Primarily binds BIR3 domain; less effective against XIAP containing both BIR2 and BIR3	Simultaneously binds BIR2 and BIR3 domains; ultra-potent XIAP antagonism
cIAP Targeting	Induces degradation of cIAP1 and cIAP2	Preferentially targets cIAP1; more controlled degradation
NF-κB Activation	Broad activation; can induce systemic inflammation	More selective activation; reduced systemic inflammation
Apoptosis Induction	TNFα-dependent; effective but less potent than bivalent	TNFα-dependent; highly potent apoptosis induction
Pharmacokinetics	Favorable; some compounds with excellent oral bioavailability	Less favorable pharmacokinetics
Cancer Cell Line Activity	Effective in subset of lines	More potent than corresponding monovalent compounds
Examples	SM-406/AT-406, SBI-0637142	SM-164, ciapavir, AZD5582
HIV Research Use	Activates ncNF-κB via BIRC2 inhibition; enhances HIV replication in vitro	Controlled activation of ncNF-κB; reactivation of HIV gene expression in humanized mice and RMs

Table 4 Key differences between monovalent and bivalent SMAC mimetics.

In HIV research, monovalent SMAC mimetics such as SBI-0637142 preferentially target BIRC2, leading to NIK accumulation and activation of the noncanonical NF-κB pathway, enhancing HIV replication in cell models [309]. Pache et al. Showed that in latently infected J-lat 10.6 cells and in resting $CD4^+$ T cells from PLWH, treatment with SBI-0637142 induced cIAP1 degradation, a dose-dependent increase in HIV transcription, with minimal cytotoxicity. Moreover, SBI-0637142 acted synergistically with the HDACi panobinostat to reactivate HIV in J-lat 10.6, 2D10, and 5A8 cells, as well as in CD4+ T_M cells from ART-treated PLWH [309].

Building on this, the same group developed Ciapavir, a bivalent derivative of SBI-0637142, which showed greater potency than the parent compound in latency reversal in both J-lat 2D10 cells and in humanized BLT (bone marrow–liver–thymus) mice. In these models, Ciapavir elevated HIV gag RNA expression without provoking substantial cytokine release or generalized T-cell activation [329], as a result of a more controlled activation on the ncNF-κB pathway [250].

Similarly, the SMAC mimetic Debio-1143 was found to degrade cIAP1 and activate the ncNF-κB pathway, thereby reversing latency in J-lat 10.6, 2D10, and 5A8 cells, as well as in resting $CD4^+$ T cells from ART-suppressed PLWH. In humanized BLT mice, Debio-1143 treatment induced HIV RNA expression at levels comparable to pharmacological stimulation with PMA and ionomycin [330].

Among the Second-generation SMAC mimetics, AZD5582 has shown superior efficacy in reversing HIV latency *in vitro* compared with other agents [309]. In cells from ART-suppressed PLWH, AZD5582 reactivated replication-competent HIV, inducing far fewer off-target genes than ingenol B [331], limiting pleiotropic transcriptional effects through the selective activation of the ncNF-κB pathway. [311].

The latency-reversing activity of AZD5582 was validated in BLT mice infected with HIV-1JR-CSF and maintained on ART [332-334]. Following a single 3 mg/kg intraperitoneal dose, plasma HIV RNA increased within 48 hours in most treated animals, and resting $CD4^+$ T cells from multiple tissues, including bone marrow, thymic organoid, lymph node, spleen, liver, and lung, showed significantly higher HIV RNA levels than controls. Additional studies in Hu-mice demonstrated that AZD5582 also reactivated HIV transcription in the female reproductive tract and brain, further supporting systemic latency reversal [311].

In RMs infected with SIVmac239 and suppressed on ART, weekly intravenous (IV) AZD5582 infusions (0.1 mg/kg) for 3–10 weeks triggered on-ART viraemia above 60 copies/mL in nearly half of the treated animals, with peaks up to 1,390 copies/ml. Viral sequencing confirmed reactivation from diverse reservoirs, including clonally expanded infected cells. Despite robust induction of SIV RNA, total reservoir size, as measured by cell-associated DNA and quantitative outgrowth assays, remained largely unchanged [311].

Although transient increases in liver enzymes and mild immune activation were observed, AZD5582 was generally well-tolerated across >95% of administered doses. Moreover, SIV-specific T cell responses were preserved, with no major impairment of $CD8^+$ T cell function or systemic inflammatory cytokine induction [311].

Efforts to enhance clearance using combination therapy approaches have so far been unsuccessful. In a SHIV-infected RMs study, AZD5582 was combined with HIVxCD3 Dual-Affinity Re-Targeting (DART) molecules, bispecific compounds designed to simultaneously bind HIV-1 Env on infected cells and CD3 on T cells, thereby redirecting cytotoxic T cells to kill infected targets. Despite adequate serum concentrations, this combination did not increase on-ART viremia, boost cell-associated SHIV RNA, or reduce the viral reservoir, likely due to low pre-ART viral loads, small reservoir size, and the emergence of anti-drug antibodies (ADAs) that limited DART activity [335].

More recently, AZD5582 has been combined with rhesus-derived monoclonal antibodies (RhmAbs) against the SIV Env glycoprotein and with the IL-15 superagonist N-803, a potent stimulator of NK and $CD8^+$ T cell responses on SIVmac239 infected on long-term ART RMs [289]. AZD5582 not only potently reverted latency, inducing on-ART viremia in 78–100% of treated RMs, but also, in combination with RhmAbs, significantly reduced SIV-DNA levels in $CD4^+$ T cells from LNs, spleen, and bone marrow, demonstrating effective impact on the viral reservoir. The addition of N-803 produced similar reductions in spleen and peripheral blood, but not in LNs [289]. Moreover,

AZD5582 combined with RhmAb and N-803 led to increased $CD8^+$ T cell counts and Ki-67 expression in both $CD4^+$ and $CD8^+$ T cells in LNs and enhanced Natural Killer (NK) cell proliferation and effector function (higher expression of granzyme B, perforin) [289].

2.3 Interleukin-15 Agonists

IL-15 is a 14-15kDa pleiotropic cytokine belonging to the common γ-chain family (including IL-2, IL-4, IL-7, IL-9, and IL-21) originally identified as a T cell growth factor. It plays a central role in the development, survival, and activation of several lymphocyte populations, most notably NK, $CD8^+$ T cells and intraepithelial lymphocytes, but also on mast cells, monocytes, macrophages, neutrophils, and eosinophils [336-337]. Although IL-15 shares the IL-2/IL-15βγ receptor complex with IL-2, their biological effects diverge substantially due to differences in cellular sources, receptor usage, and delivery (Fig. 13).

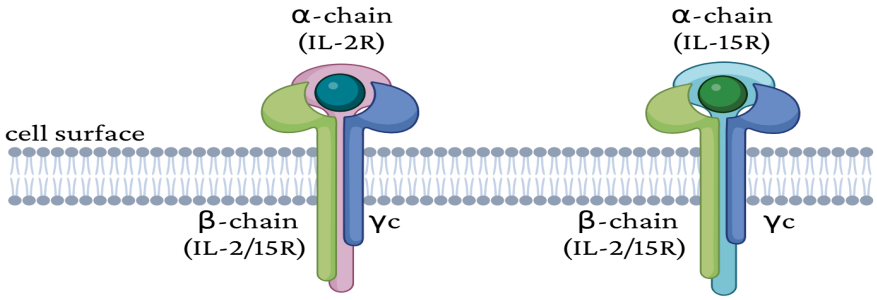

Fig. 13 IL-15 structure. IL-15 and IL-2 share the β-chain (IL-2/15Rβ) and γ-chain (γc) subunits, but each also uses a unique α-chain (IL-15Rα or IL-2Rα) [338].

Unlike IL-2, which is primarily produced by activated lymphocytes, IL-15 is constitutively expressed by stromal and APCs and crucially depends on its high-affinity binding partner, IL-15 receptor α (IL-15Rα), for stability and bioactivity. Whereas IL-2 promotes regulatory T-cell (Treg) expansion and induces activation-induced cell death (AICD), IL-15 bypasses these tolerogenic pathways, instead favoring long-lived effector and memory lymphocyte populations [338].

A defining feature of IL-15 biology is also its synthesis and secretion as a heterodimer with IL-15Rα. Co-expression of IL-15 and IL-15Rα within the same cell stabilizes the cytokine, facilitates its surface presentation, and enables its eventual cleavage and secretion as a soluble, bioactive heterodimer [339-340] (Fig. 14).

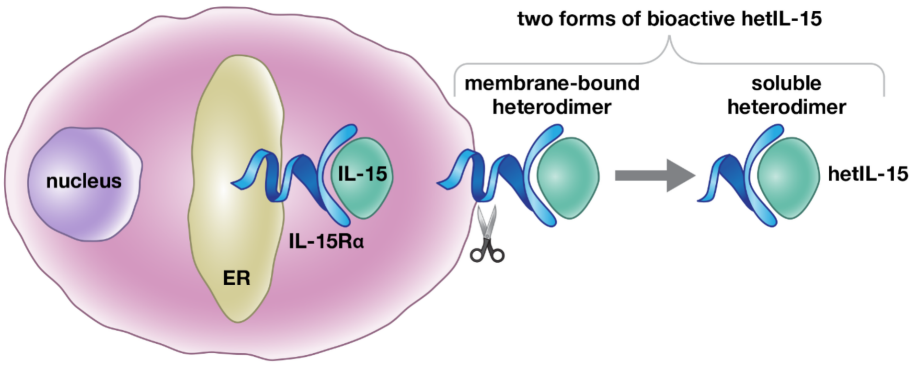

Fig. 14 Schematic overview of hetIL-15 production. IL-15 is secreted as a heterodimer with its receptor subunit IL-15Rα, which must be co-expressed in the same cells. In the Endoplasmic Reticulum (ER), IL-15 tightly associates with IL-15Rα (Kd ≈ 10^{-11} M), and the complex is transported to the surface, where soluble bioactive hetIL-15 is released following proteolytic cleavage (scissors). Adapted from Bergamaschi et al. 2012 [341]

In lymphocytes, IL-15 exerts its effects through a heterotrimeric receptor composed of three subunits: the common γ chain (γc/CD132), the β chain (CD122/IL-2Rβ) shared with IL-2, and the private α chain (IL-15Rα/CD215).

IL-15 signaling can occur via two different modes: *cis-presentation*, where the cytokine engages its receptor on the same cell, and *trans-presentation*, in which IL-15 bound to IL-15Rα on one cell stimulates IL-2Rβ/γc on a neighboring cell (Fig. 15). Soluble IL-15 in both humans and mice has been detected almost exclusively in complex with IL-15Rα, while free single-chain IL-15 is unstable and rapidly degraded [337, 341].

Trans-presentation is considered the predominant mechanism regulating IL-15 activity. IL-15 alone binds with low-to-intermediate affinity to the IL-2Rβ/γc heterodimer but achieves high-affinity binding when engaged by the full heterotrimeric IL-15Rα/IL-2Rβ/γc complex [337]. By preassembling IL-15 with IL-15Rα, the producing cell delivers IL-15 at the plasma membrane of the other cell in a high-affinity binding (Kd ~10^{-11} M) configuration, enhancing its ability to interact with IL-2Rβ/γc [337].

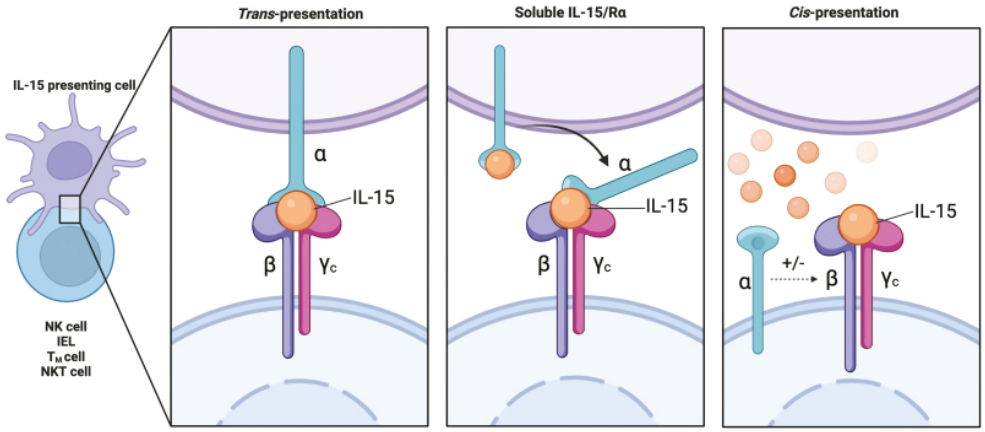

Fig. 15 IL-15 Presentation modes. IL-15 primarily signals through trans-presentation, in which membrane-bound IL-15/IL-15Rα complexes on presenting cells engage IL-2Rβ/γc receptors on neighboring lymphocytes. In an alternative mechanism, soluble IL-15/IL-15Rα complexes, released from presenting cells, can activate

lymphocytes by binding the heterodimeric IL-2Rβ/γc. Additionally, cis-presentation occurs when soluble IL-15 bound to IL-15Rα engages IL-2Rβ/γc receptors on the same cell. Adapted from Skariah et al. 2024 [337]

IL-15 engagement with its receptor complex activates three major intracellular pathways that together coordinate survival, proliferation, and effector functions of lymphocytes.

The most immediate consequence of IL-15 receptor engagement is activation of the Janus kinase (JAK)/signal transducer and activator of transcription (STAT) pathway. IL-15 binding to the IL-2Rβ/γc complex brings together JAK1, associated with IL-2Rβ, and JAK3, associated with γc. These kinases trans-phosphorylate one another and subsequently phosphorylate tyrosine residues in the cytoplasmic tail of IL-2Rβ. These phosphorylated residues serve as docking sites for SH2-domain–containing STAT proteins, mainly STAT5 and STAT3. Once recruited, STATs undergo phosphorylation, dimerize, and translocate into the nucleus, where they activate the transcription of genes that support cell survival, proliferation, and differentiation. In T and NK cells, this includes upregulation of anti-apoptotic proteins (e.g., BCL-2 family members) and cytokines that reinforce immune activation [337-338] (Fig. 16).

IL-15 also activates the MAPK cascade, a pathway critical for cell proliferation and effector function. Phosphorylation of IL-2Rβ at tyrosine 388 enables recruitment of the adaptor protein SHC1, which couples to GRB2 and SOS, initiating the Ras-Raf-MEK-ERK signaling cascade. This leads to the phosphorylation of ERK1/2, transcriptional activation of immediate-early genes such as c-Fos and c-Myc, and subsequent promotion of cell-cycle progression and cytokine production.

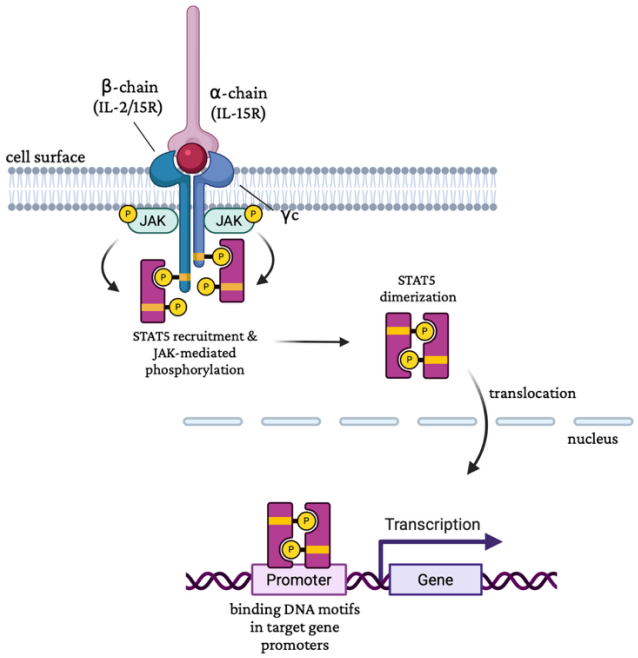

Fig. 16 JAK/STAT signaling downstream of IL-15. IL-15 binding to IL-2Rβ/γc activates JAK1 and JAK3, leading to STAT5/STAT3 phosphorylation, nuclear translocation, and transcription of genes promoting lymphocyte survival and proliferation [337].

Alternative adaptor complexes such as GRB2, GAB2, GARE1 can also propagate MAPK signals, providing versatility in how IL-15 controls immune responses. Through this pathway, IL-15 enhances the clonal expansion of antigen-specific T cells and augments NK cell effector activity [337] (Fig. 17).

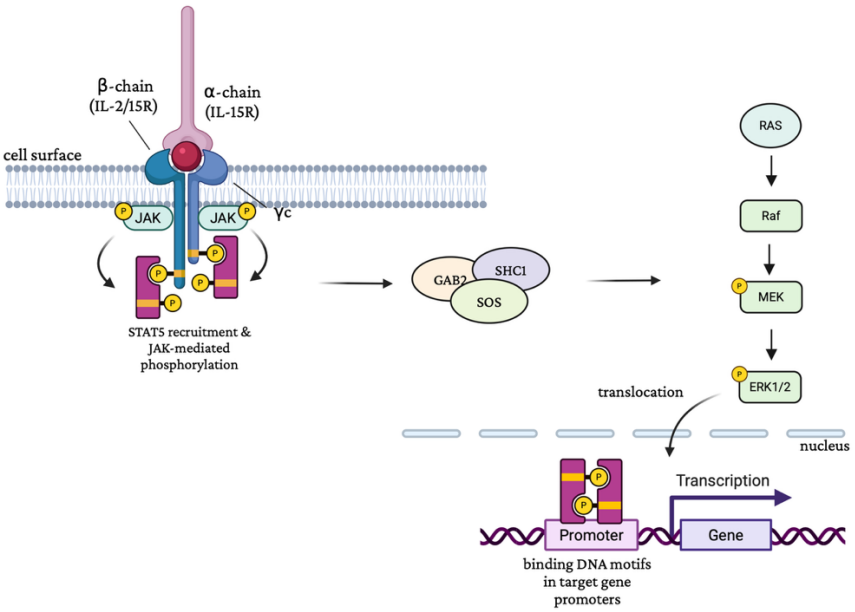

Fig. 17 MAPK signaling downstream of IL-15, Engagement of IL-2Rβ at Tyr388 recruits SHC1 and GRB2, initiating the Ras–Raf–MEK–ERK cascade that drives transcription of immediate-early genes and cell-cycle progression [337].

A third major signaling axis downstream of IL-15 involves PI3K-AKt. Following receptor engagement, PI3K is recruited to the receptor complex, where it phosphorylates PIP2 to generate PIP3 at the inner plasma membrane. PIP3 then recruits AKt and PDK1, enabling phosphorylation and activation of AKT. Activated AKT controls diverse cellular processes: it enhances glucose uptake and metabolism to support bioenergetic needs, promotes the transcription of survival genes, and contributes to cytotoxicity in NK and CD8+ T cells. This pathway also cross-talks with mTOR signaling, further amplifying IL-15's role in sustaining long-term lymphocyte homeostasis and effector function [337] (Fig. 18).

The ability of IL-15 to engage JAK1 and JAK3 and activate STAT5 provides a direct mechanistic link to HIV latency reversal. Upon phosphorylation, STAT5 dimerizes and translocates to the nucleus, where it binds consensus motifs within the HIV LTR and promotes transcriptional initiation. Functionally, IL-15 not only promotes HIV gene expression in latently infected $CD4^+$ T cells ("shock") but also enhances the cytotoxic responses of $CD8^+$ T cells and NK cells required for clearance of reactivated cells ("kill"). Prior to its exploration in HIV cure strategies, several IL-15 agonists were evaluated in cancer clinical trials (Fig. 19).

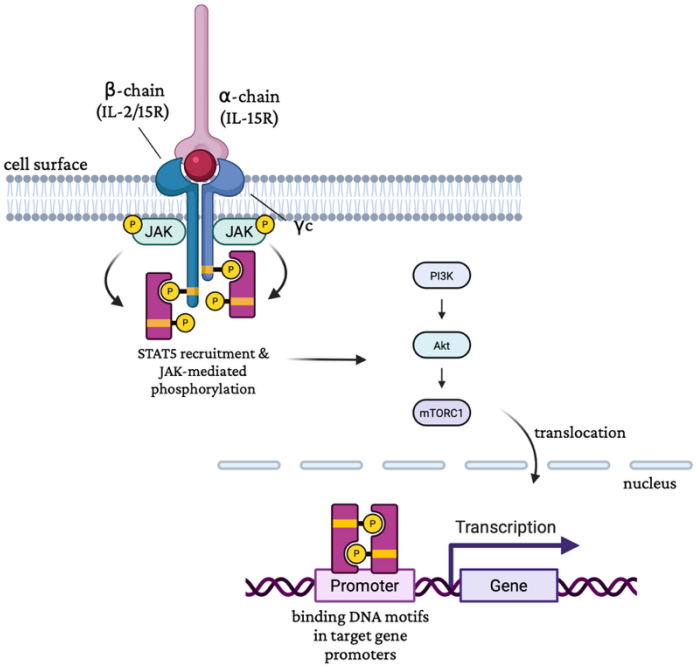

Fig. 18 PI3K-AKT signaling downstream of IL-15. IL-15 receptor engagement activates PI3K, generating PIP3 and enabling AKT activation, which enhances metabolism, survival, and effector functions of T and NK cells [337].

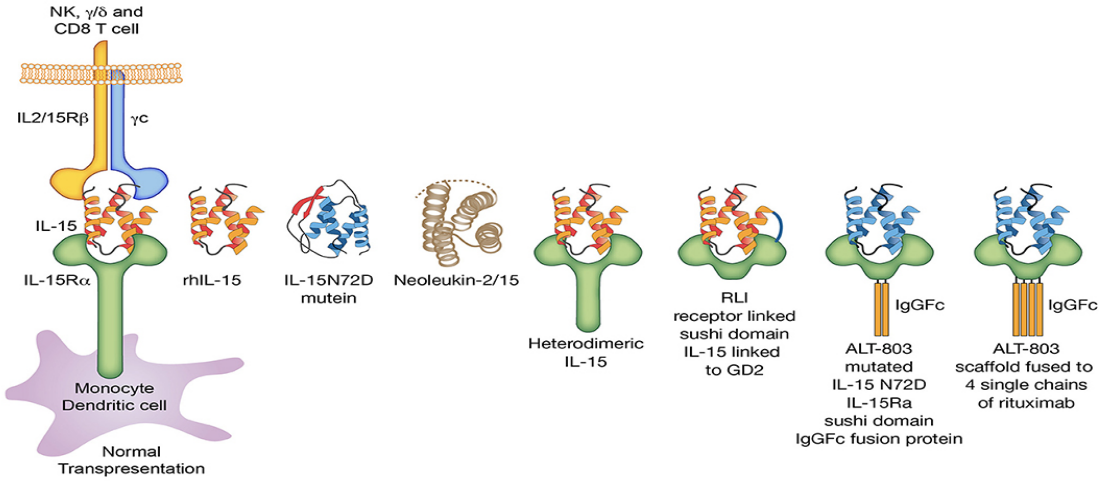

Fig. 19 IL-15 agonists in clinical immunotherapy. IL-15 agonists include recombinant IL-15 (rhIL-15) *E. coli*-produced, the IL-15N72D mutein with enhanced bioactivity, heterodimeric mammalian IL-15 (hetIL-15), and RLI, a fusion protein of IL-15 linked to the cytokine binding (sushi) domain of IL-15Rα. Tumor-targeted variants, including anti-CD20-RLI and anti-GD2-RLI, combine RLI with monoclonal antibodies against CD20 or GD2, respectively. ALT-803 (Altor Pharmaceuticals) incorporates the N72D IL-15 mutant fused to the sushi domain of IL-15Rα and an IgG-Fc fragment to prolong in vivo survival, and its scaffold has been further engineered to include four single chains of the tumor-targeting antibody rituximab. Adapted from Waldmann et al. 2020 [344]

The initial studies employed monomeric *E. coli*–produced IL-15 (rhIL-15) administered as a daily intravenous bolus in patients with metastatic malignancies. This approach induced robust expansion of NK and $CD8^+$ T cells; however, high doses were associated with severe adverse effects, including thrombocytopenia, hypotension, and cytokine release syndrome [342-343].

To reduce toxicity while preserving efficacy, alternative administration routes such as subcutaneous (SQ) injection and continuous intravenous infusion (CIV) were investigated. SQ rhIL-15 produced moderate expansion of NK and $CD8^+$ T cells, whereas a 10-day CIV regimen achieved the highest NK expansion, including a 358-fold increase in $CD56^{bright}$ NK cells, without evidence of NK-cell exhaustion or functional impairment. Despite these immunological effects, objective tumor responses were limited, with stable disease being the most common outcome.

The short *in vivo* half-life of rhIL-15 further motivated the development of engineered IL-15 formulations with enhanced stability and bioactivity [342-343]. Among these, N-803 (formerly ALT-803, Altor Pharmaceuticals) is a next-generation IL-15 agonist specifically designed to extend *in vivo* persistence while maintaining and amplifying bioactivity. It consists of a mutant IL-15 (N72D), in which asparagine replaces aspartic acid at position 72, fused to the cytokine binding (sushi) domain of IL-15Rα and linked to an IgG-Fc fragment. This design prolongs the cytokine's half-life with 25 times the in vivo biological activity of soluble IL-15 thus the name "super agonist" [345].
Clinical administration of N-803 to treat relapse after transplantation, either IV or SQ, has shown the ability to expand NK and $CD8^+$ T-cell populations, with SQ delivery yielding more prolonged serum concentrations. However, dose-limiting adverse effects, including injection-site reactions and systemic inflammation, have constrained maximal dosing [346].

On the HIV research field, several *in vitro* and *ex vivo* studies have explored the potential of N-803 to reverse HIV latency and enhance immune effector functions in cell lines, primary cells, and cells from PLWH.
Building on early observations that IL-15 alone induced only minimal viral replication in chronically infected U1 and ACH2 cell lines and in αCD3/IL-15–stimulated PBMCs from PLWH [347], Jones et al. [286] compared the effect of N-803 with IL-15 in latency reversal. Their work demonstrated that both IL-15 and N-803 increased viral production, with higher p24 levels detected in supernatants from latently infected $CD4^+$ T cells *in vitro* and elevated viral RNA in *ex vivo* $CD4^+$ T cell cultures from ART-suppressed PLWH.
Beyond latency reversal, IL-15 stimulation of PBMCs has long been known to expand and activate HIV-specific $CD8^+$ T cells, enhancing their effector functions [348-349]. Extending these findings, N-803 demonstrated direct enhancement of HIV-specific $CD8^+$ T cell activity. *In vitro*, targeted nanogel delivery of N-803 to an HIV-specific $CD8^+$ T cell clone promoted both proliferation and cytotoxic function. Similarly, *ex vivo* treatment of HIV-specific $CD8^+$ T cells isolated from ART-suppressed PLWH increased their cytotoxic potential, as evidenced by stronger IFN-γ responses in ELISPOT assays [350-352].

In the last years the effects of N-803 have been extensively investigated in nonhuman primate (NHP) models. In ART-naïve, chronically SIV-infected RMs, N-803 administration transiently reduced plasma viremia during the first days post-treatment [352]. This reduction was accompanied by increases in $CD8^+$ T cell and NK cell counts, though no enhancement in cytotoxic activity was detected. Continued therapy led to viral rebound despite ongoing N-803 exposure, suggesting that effector cells had become refractory to cytokine stimulation. Supporting this, surface expression of the IL-15 receptor subunits CD122 and CD132 on central memory $CD8^+$ T and NK cells progressively declined during treatment [353].

An additional observation was that N-803 promoted proliferation, activation, and migration of NK cells and virus-specific $CD8^+$ T cells into B cell follicles in chronically SIV-infected macaques. However, this redistribution did not translate into reduced plasma viral loads, although a decrease in SIV RNA–positive cells within LNs was detected [354].

In a follow-up study by the Sacha group using SHIV-infected, ART-suppressed macaques, N-803 again induced proliferation and follicular homing of NK cells and SHIV-specific $CD8^+$ T cells. Nevertheless, no latency reversal was observed, and there was no reduction in CD4 T cell–associated viral DNA before ART interruption when compared with controls [355].

Afterwards, two studies from the Silvestri group provided evidence that N-803 can reactivate virus *in vivo*, but only when combined with $CD8^+$ T cell depletion. In the first study, SIV-infected RMs on long-term ART received a CD8α-depleting antibody, MT807R1 (which also eliminates NK, NKT, and γδ T cells), either alone or in combination with N-803. In animals receiving the combination, viral reactivation occurred despite ongoing ART, although no measurable change was seen in the size of the latent reservoir after treatment interruption [288]. The second study on SHIV-infected long-term ART suppressed RMs combined N-803 treatment with both CD8α- and CD8β-depleting antibodies, administered sequentially with a six-month interval to allow $CD8^+$ reconstitution between depletions. As in the earlier study, viral reactivation followed CD8α depletion plus N-803 treatment. However, reactivation after CD8β depletion plus N-803 was weaker, possibly due to the animals having spent longer on ART at that time (18 months vs. 12 months). Importantly, CD8β depletion had no impact on reservoir size, and the extent of viral reactivation correlated inversely with the efficiency of $CD8^+$ T cell depletion [287].

More recently, N-803 was tested in combination with SIV Env RhmAbs and the SMAC mimetic AZD5582 in ART-suppressed RMs. On-ART viremia was observed in all animals receiving the triple combination, with four RMs showing detectable virus after N-803 administration but before AZD5582 treatment, suggesting a potential contribution of N-803 to latency reversal. Post-intervention analyses revealed reductions in $CD4^+$ T cell–associated SIV-DNA in blood and spleen in the N-803–treated group, whereas lymph node reductions were more prominent in animals receiving RhmAbs + AZD5582 alone.

"Total body SIV DNA" was used as an approximation of the overall infected cell pool, derived from the sum of SIV DNA levels measured in LNs, peripheral blood, bone marrow, and gastrointestinal tract before and after intervention. Using this metric, despite the limitation of this approach - as it does not account for the relative proportion of CD4+ T cells at each anatomical site – the total body SIV DNA was decreased in both combination groups compared to controls, and virus outgrowth assays confirmed lower replication-competent SIV in LNs in the RhmAb + AZD5582 group [289].

Overall, these findings suggested that N-803 capacity to reverse viral latency *in vivo* remains modest and context dependent.

2.4 hetIL-15

Recognizing both the therapeutic potential and the limitations of N-803, the group led by Dr. George Pavlakis sought to engineer a more physiologic alternative (Table 5). Their work focused on recreating the natural heterodimeric form of IL-15 complexed with IL-15Rα, known as hetIL-15, which more closely mirrors endogenous cytokine biology. By doing so, they aimed to preserve the immune-stimulatory properties of IL-15 while achieving a more controlled pharmacokinetic profile, sustained lymphocyte expansion, and reduced adverse effects.

Feature	hetIL-15	N-803 (ALT-803)
Form	Natural heterodimer IL-15/IL-15Rα	IL-15 superagonist/IL-15Rα-Fc fusion
Receptor engagement	Physiologic engagement of IL-2/IL-15Rβγ on NK & $CD8^+$ T cells	Stronger activation via IL-2/IL-15Rβγ, more potent signaling
Pharmacokinetics (SC)	Long half-life (~12 h), sustained plasma levels, low Cmax	Shorter half-life, higher potency, more pronounced peaks
Immune activation	Gradual, homeostatic expansion of NK & $CD8^+$ T cells	Rapid, strong proliferation and activation of target cells
Toxicity profile	Minimal at step-dose; avoids capillary leak, renal dysfunction, edema	Potential for cytokine-driven toxicities (fever, capillary leak) if not carefully dosed
Dosing flexibility	Highly adaptable; step-dose regimen matches expanding lymphocyte pool	Less flexible; requires precise timing for safety and efficacy
Tissue distribution & expansion	Promotes NK/$CD8^+$ proliferation with controlled tissue redistribution	Strong proliferation but more risk of systemic cytokine effects
Clinical trial readiness	Phase I ongoing (NCT02452268) with SC step-dose showing safety	Tested in HIV latency reversal and oncology trials; effective but higher toxicity risk

Table 5 Comparative properties of hetIL-15 and N-803. The table summarizes key differences between hetIL-15, a natural IL-15/IL-15Rα heterodimer, and N-803, an IL-15 super agonist/IL-15Rα-Fc fusion, in terms of pharmacokinetics, immune activation, toxicity and dosing strategies.

To generate hetIL-15 suitable to be used for *in vivo* studies, initial efforts focused on generating mammalian cell lines capable of secreting the heterodimeric complex. To this end, Pavlakis and colleagues engineered DNA vectors optimized for the expression of human IL-15 together with either the full-length IL-15Rα or its truncated soluble form. These linearized plasmids, purified to remove endotoxin, were introduced into HEK293 cells by calcium phosphate transfection, and stable high-producing clones were selected. Among them, clones 19.7 and 1.5 expressed the full-length IL-15·IL-15Rα complex, while clone 2.66 produced heterodimers of IL-15 with the soluble extracellular IL-15Rα fragment. The engineered cell lines were expanded under serum-free conditions using a hollow fiber bioreactor, which allowed continuous culture and harvest of supernatants for prolonged periods (up to five months) with daily yields monitored through glucose consumption and cytokine quantification by ELISA [336].

Building on this platform, the group next shifted to *in vivo* expression strategies, designing optimized plasmid DNA constructs encoding either hetIL-15 or an Fc-fused variant (hetIL-15-Fc) to improve stability and mimic trans-presentation. Delivery of these constructs into RMs via intramuscular (IM) injection followed by electroporation enabled host cells to produce and secrete hetIL-15 directly, achieving sustained systemic exposure without the need for repeated protein administration [356].

Early studies in RMs comparing IV and SC administration of hetIL-15 demonstrated that SC delivery markedly prolonged plasma half-life (~12 hours versus ~1.5 hours for IV) while reducing peak plasma concentrations, thereby providing more sustained cytokine exposure with reduced risk of acute toxicity. When hetIL-15 was administered repeatedly at fixed SC doses across a two-week cycle, systemic exposure and peak levels progressively declined, reflecting the expansion of target NK and T lymphocytes that effectively consumed circulating cytokine. Low to intermediate doses (≤5 μg/kg) were well tolerated, but high fixed doses (50 μg/kg) caused transient toxicities, including capillary leak, edema, and renal alterations, highlighting the potential toxicity of excess circulating cytokine early in the treatment cycle [357].

To overcome these limitations, Pavlakis and colleagues introduced a step-dose regimen in which SC doses doubled sequentially from 2 to 64 μg/kg over two weeks. This approach maintained stable IL-15 trough levels, sustained robust expansion of NK and $CD8^+$ T cells, and induced comparable lymphocyte redistribution and spleen enlargement to high fixed doses, but with minimal toxicity. Moreover, plasma IL-18, a biomarker of IL-15 activity, rose steadily during step-dosing, confirming ongoing immunostimulatory activity [357].

Building on this optimized approach, Watson et al. evaluated the immunological and virological impact of the same two-week step-dose regimen in both uninfected and chronically SHIV-infected macaques [358]. Consistent with prior pharmacokinetic and

safety data, hetIL-15 was well tolerated, without clinical or biochemical toxicity. Functionally, it drove striking expansion and activation of effector lymphocytes across multiple compartments, including blood, LNs, and mucosal tissues. $CD8^+$ T cells not only expanded and upregulated markers such as Ki-67 and granzyme B but also redistributed into B cell follicles (classically considered immune-privileged sites of viral persistence) where imaging confirmed their accumulation. NK cells and memory $CD4^+$ T cells were also boosted, though to a lesser degree. Importantly, expanded SIV-specific CD8+ T cells retained proliferative and cytolytic function, and their redistribution into follicular zones was associated with reduced cell-associated viral RNA in LNs and lower pVL in some treated animals, despite no change in proviral DNA [358].

These results highlighted that hetIL-15 enhances both the magnitude and the anatomical reach of cytotoxic responses, mobilizing effector $CD8^+$ T cells into reservoir sites and thereby lowering ongoing viral transcription, even in the absence of overt latency reversal [358].

3. Non-Human Primate Models

Animal models have represented and still represent an important tool for research and progress in the field of medicine. In the specific area of HIV, the use of animal models has made possible to clarify numerous aspects related to the infection such as the period of formation of the viral reservoir that has been identified around the first weeks after infection, the observation of the viral rebound upon discontinuation of therapy initiated early post-infection (2 days), the predominant viral reservoir composition in all subsets of $CD4^+$ cells. All this information allows to increase scientific awareness and have a strong basis for trying to develop a prophylactic therapy or new therapeutic molecules. The HIV field is one of the few that uses various NHP species as animal models, in particular macaques which are natural hosts of SIV. Because of their close genetic, anatomical, physiological, and immunological similarities to humans, they are uniquely suited to model complex diseases that cannot be fully replicated in vitro or in other animal species [359].

Research involving NHPs has been central to many medical advances, including the development of treatments for Parkinson's disease and sickle cell anemia, vaccines against polio, measles, Ebola, and COVID-19, and therapies that prevent organ transplant rejection. Their translational relevance stems from the fact that certain studies, limited by ethical, biological, or logistical constraints, cannot be performed in humans, while non-animal models often fail to capture the integrative systemic responses necessary to evaluate disease mechanisms and therapeutic interventions [359].

In recognition of their importance, dedicated primate research infrastructures were established worldwide. In the U.S., the NIH created the National Primate Research

Centers (NPRCs) beginning in the early 1960s. Today, seven NPRCs exist, located at the University of California, Davis, Oregon Health & Science University, the University of Washington, the University of Wisconsin–Madison, Emory University, Tulane University, and the Southwest NPRC at Texas Biomedical Research Institute [360-361]. These centers provide colonies, specialized expertise, and infrastructure for high-quality primate research.

Beyond the U.S., numerous facilities exist globally. In China, more than one hundred institutions and companies maintain primate colonies for research purposes, reflecting the international scale of this enterprise [362]. The oldest U.S. center originated with Robert Yerkes, who in the 1930s established a primate research laboratory that later evolved into the Emory National Primate Research Center [363].

The role of NHPs in HIV research is particularly illustrative of their value. As early as the late 1960s and 1970s, veterinarians observed unusual clusters of infections, lymphomas, and immunodeficiency-like syndromes in captive monkey colonies in the U.S. [364]. When AIDS emerged in humans in 1981 and HIV was identified in the early 1980s, these earlier reports took on new significance. In 1985 SIV was isolated from macaques, establishing it as a natural counterpart of HIV [365]. Around the same period, experimental infection of chimpanzees with HIV at the Yerkes Center confirmed that the virus could cause AIDS in primates, most famously in the chimpanzee Jerom, who developed AIDS following experimental inoculation [366]. Simultaneously, sooty mangabeys and African green monkeys were recognized as natural hosts of SIV, carrying the virus without progressing to AIDS, thus providing an important comparative model for nonpathogenic infection [367]. Molecular investigations later traced the origins of HIV-1 to cross-species transmission of SIV from chimpanzees, while HIV-2 derived from SIV_{smm} in sooty mangabeys, with phylogenetic analyses dating the first human infections to around 1930 in Central Africa [368].

Since then, Old World macaques, particularly rhesus (*Macaca mulatta*) and cynomolgus (*Macaca fascicularis*), have become the cornerstone of experimental HIV/AIDS research (Fig.20). When infected with SIV or SHIV, they recapitulate many features of human HIV infection, including mucosal $CD4^+$ T cell depletion, chronic immune activation, systemic inflammation, and susceptibility to opportunistic infections [363-371].

They have been indispensable in elucidating the rapid seeding of viral reservoirs within days of infection, the distribution of reservoirs across $CD4^+$ T cell subsets, and the near-inevitable viral rebound that follows interruption of ART [370]. These models also reveal interindividual variation in disease progression and viral control linked to host genetics, mirroring findings in human cohorts [369].

Although they share numerous similarities, NHPs fail to fully elucidate HIV-induced infection in humans, this lack is primarily due to financial difficulties in sustaining infections for long period (decades) in animals and secondly due to the differences between HIV-1 and SIV.

	Scientific name	Body lenght	Weight	Life span	Age considered old
 Rhesus macaque	Macaca mulatta	45-64 cm	5-12 Kg	34-40 years	20-25 years old
 Cynomolgus monkeys	Macaca fascicularis	40-65 cm	9 Kg	35 years	20 years old

Fig. 20 Main characteristics of nonhuman primates commonly used in biomedical research. The Rhesus macaque (*Macaca mulatta*) and Cynomolgus macaque (*Macaca fascicularis*) are the most frequently employed species due to their susceptibility to simian immunodeficiency virus (SIV) and resemblance to human disease progression. Adapted from Yost et al. 2023 [359].

Among the most significant differences between the two viruses, there is certainly the envelop, in particular to the Env protein, which prevents the use of animal models (NHP) to test neutralizing antibodies against HIV-1 Env. This difference is due to the pressure induced by the host's antibody responses, which induce evolutions in the genetic sequences coding for the Env protein, and also to the different evolutionary history of HIV-1 versus $SIV_{smm/mac}$, which results in an antigenic difference between the two viruses. The different antigenicity between the two viral species induces a lack of cross-reactivity of the antibodies produced for the gene products of one virus towards the other.

A second relevant difference is linked to the evolution of the sequence of persistent proviruses which show in RMs greater completeness in their structure, together with a lower frequency of deletions or large hypermutations. These inequalities appear to be due to the viral genetic makeup, the features of the host, the progressing state of the disease, and the timeliness of therapeutic treatment. In addition, although the clonal expansion of latent cells appears similar in humans and macaques, the third major inequality between the two species appears to be attributed to the low number of similar viral sequences observed in SIV-infected RMs [369].

Despite these important differences, NHPs remain the only animal systems that faithfully reproduce the systemic and immunological hallmarks of HIV infection. They continue to provide insights into viral replication dynamics, reservoir persistence, and immune control mechanisms, and they serve as an indispensable platform for testing

therapeutic vaccines, broadly neutralizing antibodies (bNAbs), gene-editing strategies, and early ART interventions. Thus, despite ongoing ethical debates and welfare considerations surrounding their use, NHPs remain central to the quest to understand HIV pathogenesis and to develop the interventions needed to control and ultimately cure the infection.

4. Aims and rationale of the study

This study was designed to evaluate whether the SMAC mimetic AZD5582 can be combined with agents that enhance immune-mediated clearance of virus-producing cells, such as hetIL-15, to reduce the seeding and establishment of the latent viral reservoir in SIV-infected, ART-treated RMs. The central hypothesis is that LRAs coupled with immune enhancers may disrupt reservoir formation if applied during the earliest phases of its seeding, before it consolidates into a durable barrier to cure.

AZD5582 functions as a potent LRA by selectively activating the ncNF-κB pathway, inducing transcription of latent HIV or SIV proviruses within infected $CD4^+$ T cells [309, 311]. Administering AZD5582 during acute infection in the context of early ART is hypothesized to interfere with the reservoir while its seeding is more active. By promoting early viral expression, infected cells harboring SIV DNA, may become more susceptible to immune-mediated clearance before they mature into long-lived, treatment-resistant reservoirs. This strategy leverages the principle that timely reactivation of HIV provirus can expose infected cells to cytotoxic effector mechanisms while limiting reservoir expansion.

Complementing this approach, hetIL-15 activates and expands cytotoxic antiviral populations, including $CD8^+$ T and NK cells, while promoting their trafficking to sites of active viral replication [357-358].

The dosing strategy for hetIL-15 in RMs was informed by prior studies demonstrating the benefits of step-dose administration. Bergamaschi and colleagues [357] showed that progressively increasing SQ doses from 2 to 64 μg/kg maintained stable plasma levels, induced robust NK and $CD8^+$ T-cell expansion, and achieved comparable lymphocyte redistribution and tissue responses to high fixed doses, while minimizing toxicity. Watson et al. [358] applied a similar two-week step-dose regimen, demonstrating that repeated SQ hetIL-15 significantly expanded effector lymphocytes across multiple compartments, including LNs, blood, and mucosal tissues, and promoted infiltration of cytotoxic $CD8^+$ T cells into lymph node follicles, a major HIV/SIV reservoir site.

Building on these findings, our study implemented a tailored step-dose schedule, starting at 10 μg/kg, escalating to 20 μg/kg for the second dose and 40 μg/kg for doses three through eight, followed by a de-escalation to 20 μg/kg and finally 10 μg/kg for the last two doses. The initial dose escalation was designed to gradually achieve the desired biological activity while minimizing the likelihood of tolerance that can arise with

repeated uniform dosing. The subsequent de-escalation strategy, while not previously systematically explored, was chosen to maintain the biological activity achieved during mid-treatment, while limiting cytokine-driven toxicities during treatment withdrawal.
Interventions were initiated 14 days after SIV infection, corresponding to the period of most active reservoir seeding, with the aim of preventing or substantially limiting the establishment of long-lived latently infected $CD4^+$ T cells.
What makes this work novel is that targets the earliest stages of reservoir seeding, a critical yet understudied window; it explores the combination of a well-known potent second generation SMAC mimetic with an improved IL-15 agonist in a regimen that has not been tested; it implements a tailored step-dose and de-escalation strategy for hetIL-15, designed to maximize immune clearance while minimizing toxicity. Together, these features make this study a unique contribution to the development of early, combinatorial HIV cure strategies.

5. Results

5.1 Study design and interventions strategies

35 Indian-origin adult RMs were infected with an IV bolus of 10,000 IU of barcoded SIVmac239M [372]. All the animals were negative for the Mamu*B08 and Mamu*B17 MHC class I alleles; the following animals were Mamu*$A01^+$: NB38, RKc20, Ryf20, NC80, RQn18, MK91, RQy19, RRl18, RBg19, MK92 (Table 6). At the time of infection, the average age was 53.8 ± 9.1 months. An antiretroviral regimen consisting of DTG (2.5 mg/kg/day), TDF (5.1 mg/kg/day), and FTC (40 mg/kg/day), was administered daily via single SQ injection from day 14 post infection (p.i.) until the end of the study.

Arm	ID Code	Sex	Mamu A01* genotype	Age at infection (months)	Peak pVL (copies/mL)
hetIL-15 (n=9)	RSf20	F	Negative	41	6700000
	MT18	M	Negative	56	64000000
	MT40	M	Negative	56	31000000
	NB38	F	Positive	53	6200000
	RKc20	M	Positive	46	18000000
	ROo19	F	Negative	55	57000000
	RYf20	M	Positive	46	33000000
	MP11	M	Negative	58	150000000
	NA32	M	Negative	55	7000000
	mean± SD			*51.8 ± 5.9*	*4.14E+07 ± 4.60E+07*
AZD5582 (n=9)	RLq19	F	Negative	56	49000000
	NC80	M	Positive	46	18000000

	RLc20	M	Negative	46	81000000
	RQn18	F	Positive	70	28000000
	RIt19	F	Negative	52	150000000
	MK91	M	Positive	53	22000000
	MN32	M	Negative	58	28000000
	RHz19	M	Negative	47	150000000
	MV42	M	Negative	56	120000000
	mean± SD			*53.8 ± 7.6*	*7.18E+07 ± 5.52E+07*
hetIL-15 + AZD5582 (n=9)	RRq20	M	Negative	43	110000000
	RQy19	M	Positive	47	60000000
	RNd20	M	Negative	46	10000000
	RPr20	M	Negative	43	91000000
	RRl18	F	Positive	70	44000000
	RBg19	F	Positive	58	37000000
	MR27	M	Negative	56	16000000
	RDg18	F	Negative	78	47000000
	RLn18	F	Negative	70	64000000
	mean± SD			*56.8 ± 13.2*	*5.32E+07 ± 3.25E+07*
ART only (n=8)	MK02	M	Negative	53	18000000
	MK92	M	Positive	53	20000000
	ME53	M	Negative	64	35000000
	MN10	M	Negative	52	6500000
	MR79	M	Negative	68	27000000
	RJb21	M	Negative	44	130000000
	RPw20	M	Negative	45	34000000
	RUf21	M	Negative	44	160000000
	mean± SD			52.9 ± 9.0	4.78E+07 ± 5.68E+07

Table 6 RMs' characteristics. Data are expressed as mean ± SD.

The RMs were assigned to four experimental groups (Fig. 21) in a balanced manner considering weight, age, and Mamu*A01 status, to minimize baseline differences between groups that could otherwise confound the study outcomes:

Arm 1 – hetIL-15 monotherapy (n = 9). RMs received 10 weekly SQ injections of hetIL-15 starting three days before ART initiation (day 11 p.i.). The dosing was step-escalating: 10 µg/kg for the first dose, 20 µg/kg for the second, 40 µg/kg from the third to the eighth dose, then de-escalating to 20 µg/kg for the ninth dose and 10 µg/kg for the final dose.

Arm 2 – AZD5582 monotherapy (n = 9). RMs received 10 weekly IV infusions of AZD5582 starting at the time of ART initiation (day 14 p.i.), at a dose of 0.1 mg/kg.

Arm 3 – Combination therapy (n = 9). RMs received both hetIL-15 and AZD5582, administered in parallel according to the schedules described above for Arm 1 and 2.

Arm 4 – Control (n = 8). RMs received ART only and served as untreated controls for the experimental interventions.

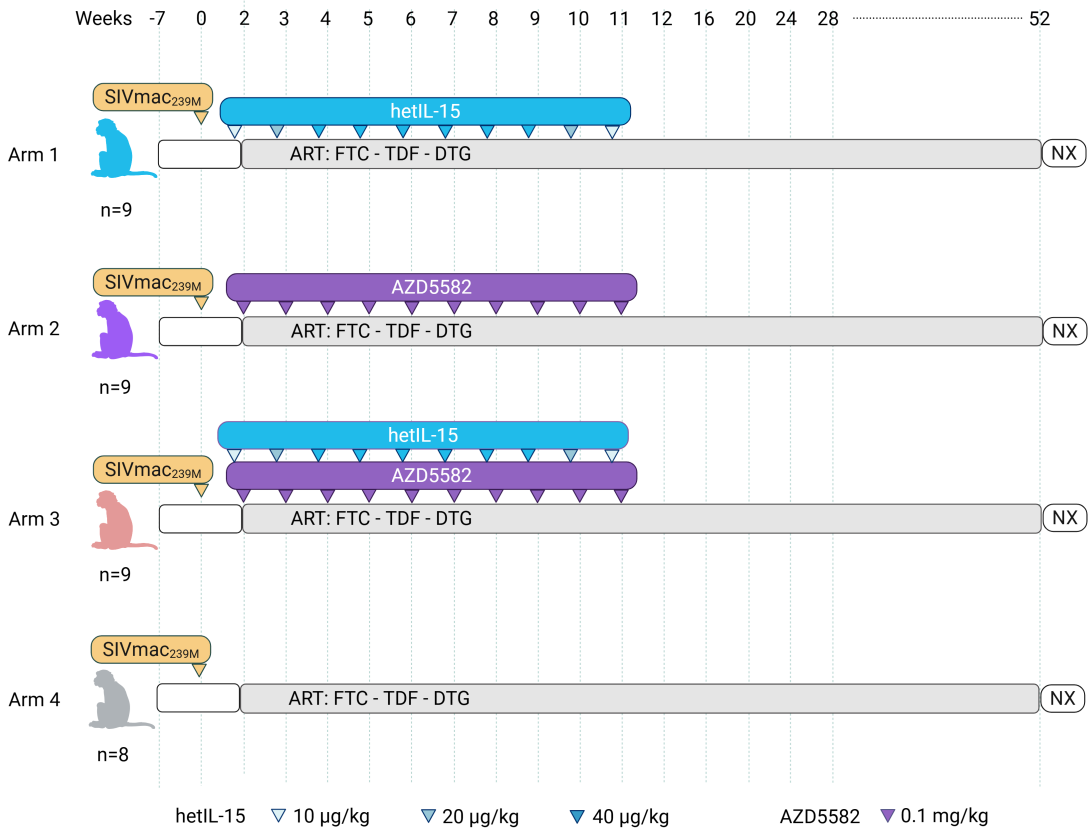

Fig. 21 Study design. Thirty-five Indian-origin RMs were infected IV with 10,000 IU of barcoded SIVmac239M and initiated on ART at day 14 p.i.. Animals were randomized into four experimental groups: Arm 1 (hetIL-15, n=9) received 10 weekly SQ injections of hetIL-15 in a step-dosing regimen; Arm 2 (AZD5582, n=9) received 10 weekly IV infusions of AZD5582; Arm 3 (Combination, n=9) received both hetIL-15 and AZD5582 in parallel; and Arm 4 (Control, n=8) received ART only. ART was continued for the duration of the study, and the animals were necropsied within 12 months of ART initiation.

During the study, one animal in Arm 3 developed severe respiratory distress followed by cardio-circulatory collapse and death after 9 doses of hetIL-15 and 8 doses of AZD5582. Autopsy revealed severe fibrinous pericarditis with extension to the pleura, diaphragm, and serosal surfaces of the abdominal organs. Another animal in Arm 2 was euthanized after the sixth dose of AZD5582 following a severe adverse reaction

characterized similarly by respiratory distress and cardio-circulatory collapse. All remaining animals were necropsied within 12 months of ART initiation. No additional adverse events were reported in association with treatment using either compound.

5.2 Slower decline of viremia after treatment with AZD5582, alone or in combination with hetIL-15

At the time of ART initiation (day 14 p.i.), all RMs exhibited comparable pVL (Fig. 22) and the majority of the animals reached complete virological suppression by week 24 p.i., with pVL below the limit of detection (LOD) of 15 copies per mL of plasma.

During the intervention period, RMs receiving AZD5582, either alone or in combination with hetIL-15, consistently maintained higher SIV-RNA levels compared to ART-only controls and animals treated with hetIL-15 alone (Fig. 22). Specifically, AZD5582-treated animals exhibited significantly higher pVL levels compare to the controls at multiple timepoints: day 21 p.i. (p = 0.0475), day 25 p.i. (p = 0.0470), and day 49 p.i. (p = 0.0287), as well as at a later timepoint, day 196 p.i. (p = 0.0384) (Fig. 23).

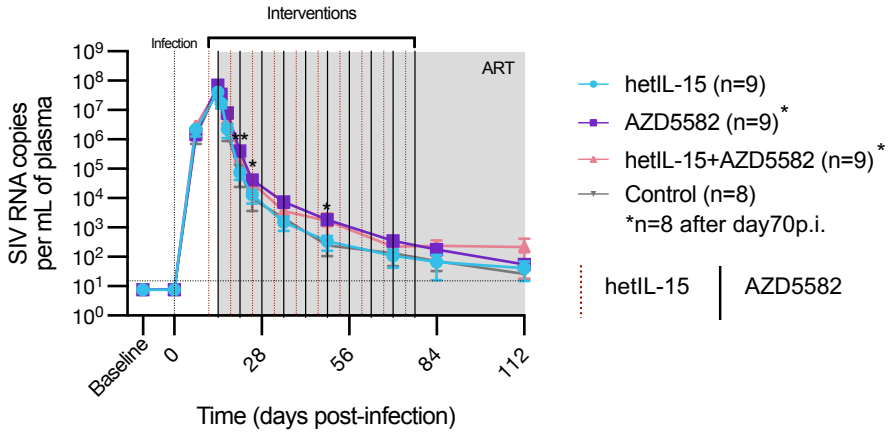

Fig. 22 Plasma SIV RNA levels during the intervention phase. SIV plasma viral load in the first 112 days p.i. in the four experimental groups (n = 35 macaques). Limit of detection is 15 copies of SIV RNA per mL of plasma (horizontal dashed line). AZD5582 doses are indicated by vertical continuous black lines, and hetIL-15 administrations by vertical red dashed lines. The shaded grey area represents ART treatment. After day 70 p.i., due to severe adverse reactions, only 8 animals were in AZD5582 and in AZD5582+hetIL-15 arms. Data are mean ± s.e.m. A two-sided Welch's t-test was used to compare values between the groups. Each intervention arm was compared individually with the ART-only control group. *P < 0.05, **P < 0.01, ***P < 0.001, ****P < 0.0001.

Analysis of the viral load kinetics during the intervention period revealed a trend to a slower pVL decline rate in AZD5582-treated animals compared to ART-only controls at the earliest timepoints (Fig. 24). Specifically, between days 15 and 17 p.i., animals receiving AZD5582 alone displayed a significantly slower rate of viral decline (p = 0.0056), and a similar delay was observed in the combination AZD5582+hetIL-15 group

(p = 0.0279). Notably, the difference in decline rate was transient and disappeared by the following measurements.

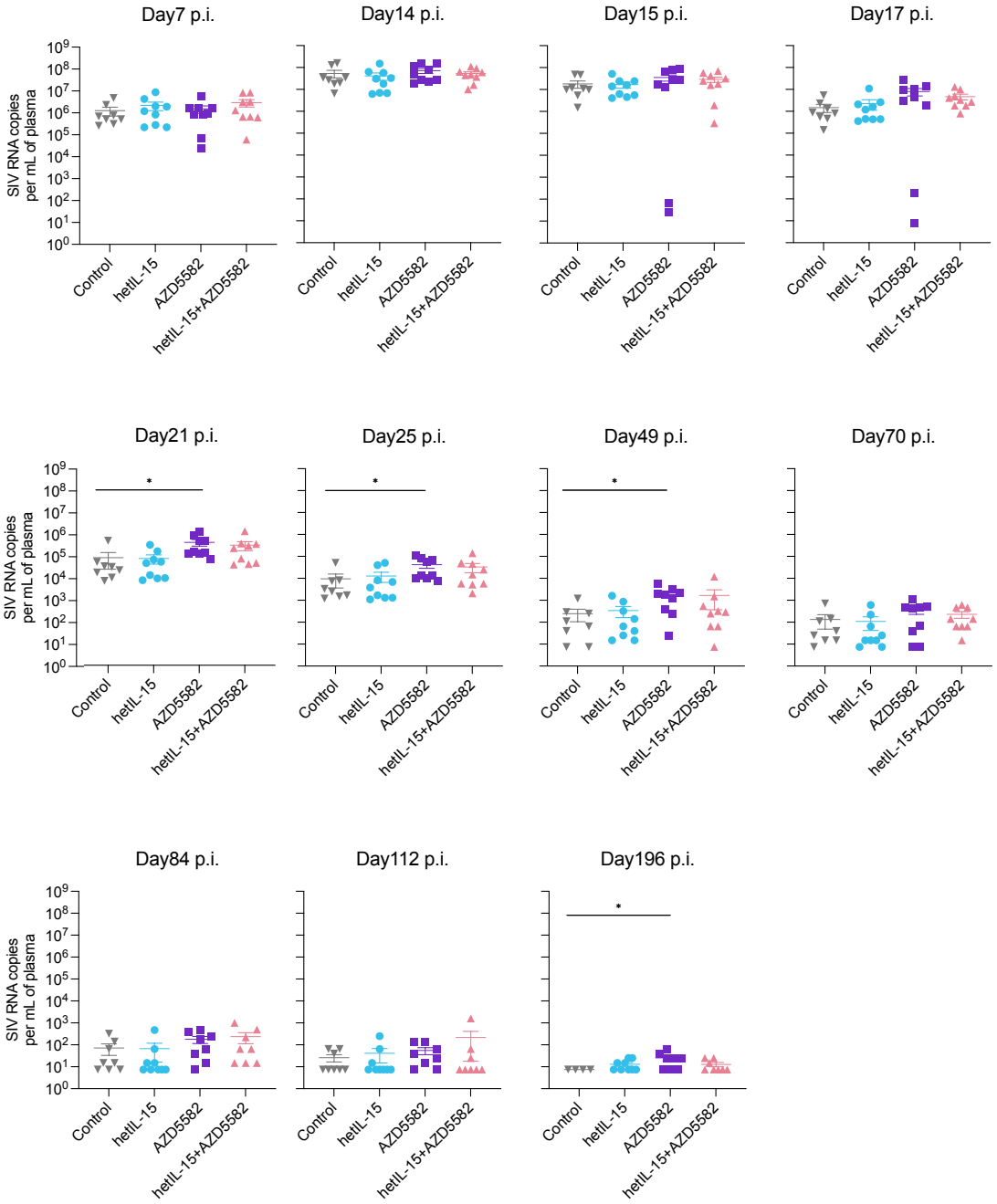

Fig. 23 Comparison of plasma SIV viral load across intervention arms at multiple timepoints. SIV plasma viral load at various timepoints (day 7, 14, 15, 17, 21, 25, 49, 70, 84, 112, 196) in the four experimental groups (n = 35 macaques). After day 70 p.i., due to severe adverse reactions, only 8 animals were in AZD5582 and in AZD5582+hetIL-15 arms. Data are mean ± s.e.m. A two-sided Welch's t-test was used to compare values between the groups. Each intervention arm was compared individually with the ART-only control group. *P < 0.05, **P < 0.01, ***P < 0.001, ****P < 0.0001.

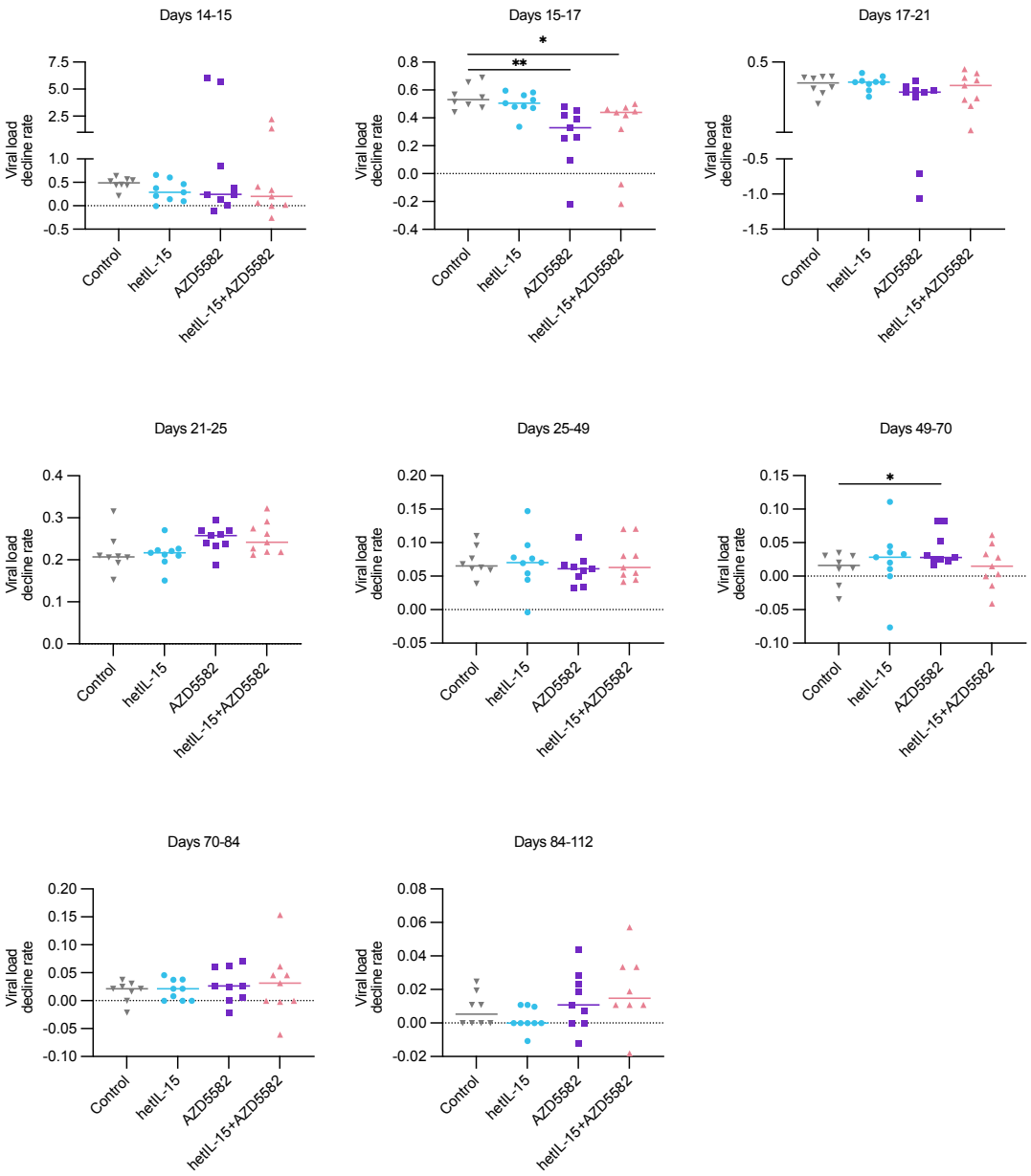

Fig. 24 Plasma viral load decline rates across all experimental groups. SIV plasma viral load decline rate between various timepoints after ART initiation. After day 70 p.i., due to severe adverse reactions, only 8 animals were in AZD5582 and in AZD5582+hetIL-15 arms. Data are mean ± s.e.m. A two-sided Welch's t-test was used to compare values between the groups. Each intervention arm was compared individually with the ART-only control group. *P < 0.05, **P < 0.01, ***P < 0.001, ****P < 0.0001.

5.3 Perturbation of viral reservoir establishment in AZD5582 treated RMs at ART initiation

To assess the impact of AZD5582, hetIL-15, and their combination on SIV reservoir establishment, intact SIV DNA was quantified longitudinally in $CD4^+$ T cells from PBMC and LNs (Figs. 25a, 25b). Overall, animals receiving AZD5582, either alone or in combination with hetIL-15, exhibited lower levels of intact SIV DNA. Specifically, the

frequency of SIV-DNA$^+$ cells in the AZD5582 group was significantly lower than in controls in both PBMC and LNs at day 25 p.i. (PBMC p = 0.0020; LNs p = 0.0291) and day 70 p.i. (PBMC p = 0.0271; LNs p = 0.0056). The combination group showed a significantly lower frequency of SIV-DNA$^+$ cells at day 14 p.i. (p = 0.0145) and day 25 p.i. (p = 0.0009) in PBMC, and at day 25 p.i. (p = 0.0246), day 70 p.i. (p = 0.0032) and 301 p.i. (p = 0.0302) in LN. The hetIL-15 monotherapy group also displayed a significant lower level on SIV-DNA$^+$ cells at day 14 p.i. (p = 0.0163), day 25 p.i. (p = 0.0348), day 70 p.i. (p= 0.0187) in PBMC, and at day 70 p.i. (p = 0.0368) in LN.

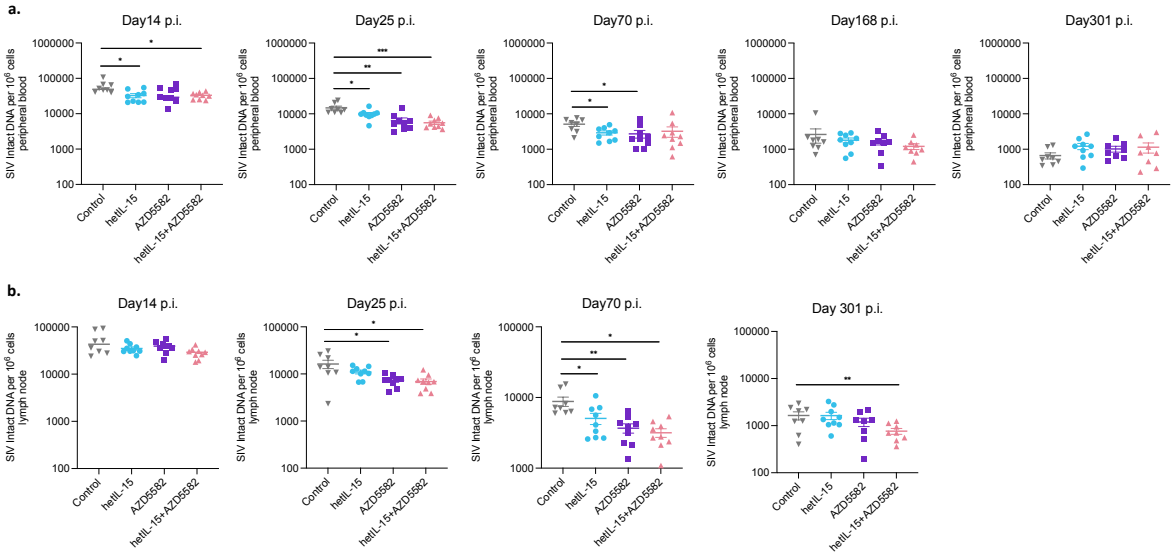

Fig. 25 Impact of AZD5582, hetIL-15, and their combination on SIV reservoir establishment. Levels of intact SIV DNA were quantified longitudinally in CD4$^+$ T cells isolated from peripheral blood (a) and LNs (b). After day 70 p.i., due to severe adverse reactions, only 8 animals were in AZD5582 and in AZD5582+hetIL-15 arms. Data are mean ± s.e.m. The horizontal bar in each group represents the mean. A two-sided Welch's t-test was used to compare values between the groups. Each intervention arm was compared individually with the ART-only control group. *P < 0.05, **P < 0.01, ***P < 0.001, ****P < 0.0001.

Analysis of the decline rate of intact SIV DNA further revealed differences across groups. Between days 168 and 301 p.i., animals treated with AZD5582 alone (p = 0.0366) or in combination with hetIL-15 (p = 0.0415) exhibited significantly lower decline in peripheral blood compared to controls (Fig. 26a). Similarly, between days 70 and 301 p.i., animals receiving hetIL-15 alone showed a significantly lower decline rate in LNs compared to controls (p = 0.0462) (Fig. 26b).

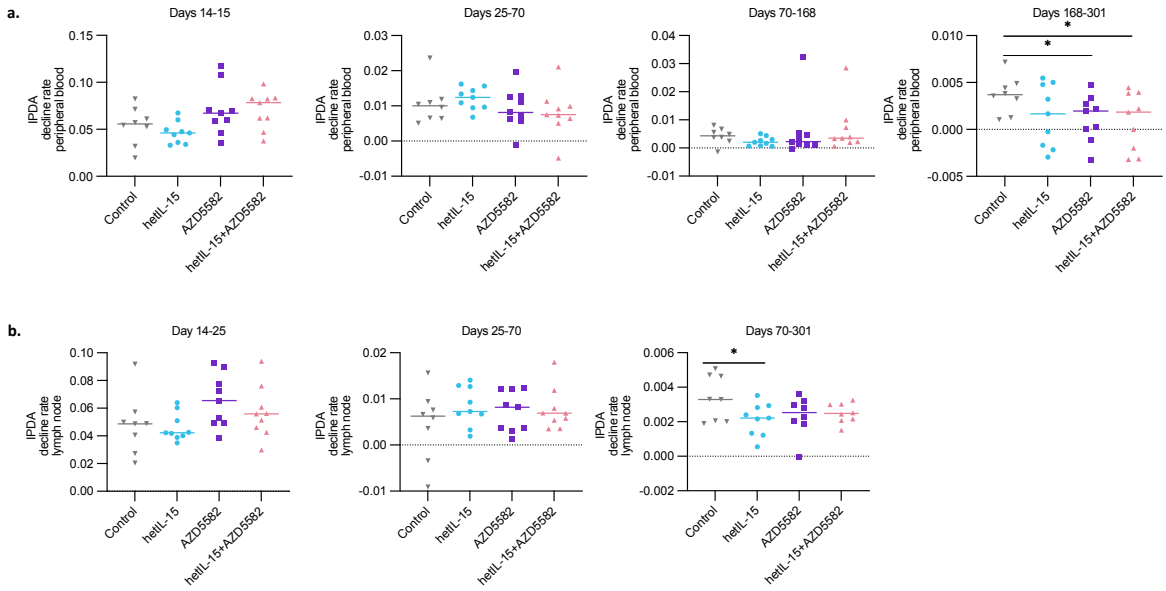

Fig. 26 Decline rate of intact SIV DNA in peripheral blood and LNs. SIV DNA decline rate between various timepoints after ART initiation in peripheral blood (a) and LNs (b). After day 70 p.i., due to severe adverse reactions, only 8 animals were in AZD5582 and in AZD5582+hetIL-15 arms. Data are mean ± s.e.m. The horizontal bar in each group represents the mean. A two-sided Welch's t-test was used to compare values between the groups. Each intervention arm was compared individually with the ART-only control group. *P < 0.05, **P < 0.01, ***P < 0.001, ****P < 0.0001.

5.4 Immunological impact of AZD5582, hetIL-15, and their combination in peripheral blood and LNs

To investigate the immunological effects of AZD5582, hetIL-15, and their combination, we performed longitudinal analyses of peripheral blood and LNs samples using flow cytometry.

In peripheral blood, the frequency of $CD4^+$ T cells was significantly higher in AZD5582-treated animals at day 301 p.i. (p = 0.0271), whereas no differences were observed at earlier timepoints (days 14, 25, and 70 p.i.) (Fig. 27). In LNs, $CD4^+$ T cell frequencies were significantly lower in hetIL-15–treated animals (p = 0.0395), significantly higher in AZD5582-treated animals (p = 0.0182) compared to controls at day 70 p.i. with no differences in the combination group (Fig. 28). The frequencies of $CD4^+$ T_{EM} cells tended to be lower than the control group in all the interventions arms remained comparable across all groups at all timepoints in both compartments, with the only exception in LNs at day 301 p.i. (Figs. 29, 30).

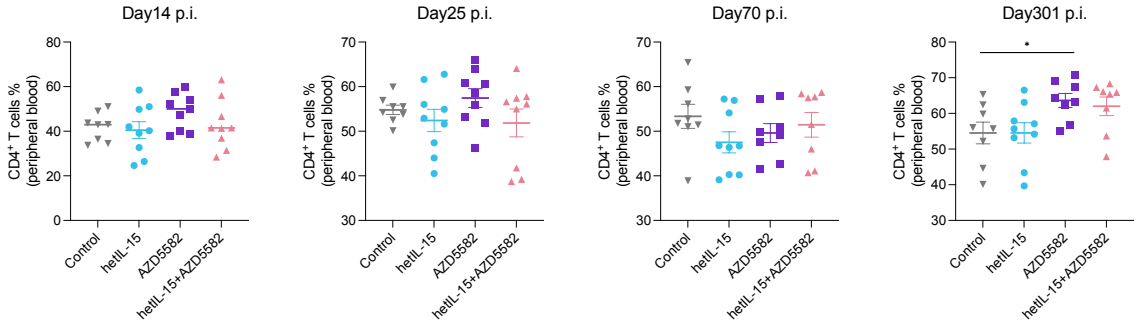

Fig. 27 Frequency of total CD4⁺ T cell in peripheral blood. Flow cytometry analysis of CD4⁺ T cell frequencies in peripheral blood at various timepoints (day 14 p.i., day 25 p.i., day 70 p.i, day 301 p.i.). After day 70 p.i., due to severe adverse reactions, only 8 animals were in AZD5582 and in AZD5582+hetIL-15 arms. Data are mean ± s.e.m. The horizontal bar in each group represents the mean. A two-sided Welch's t-test was used to compare values between the groups. Each intervention arm was compared individually with the ART-only control group. *P < 0.05, **P < 0.01, ***P < 0.001, ****P < 0.0001.

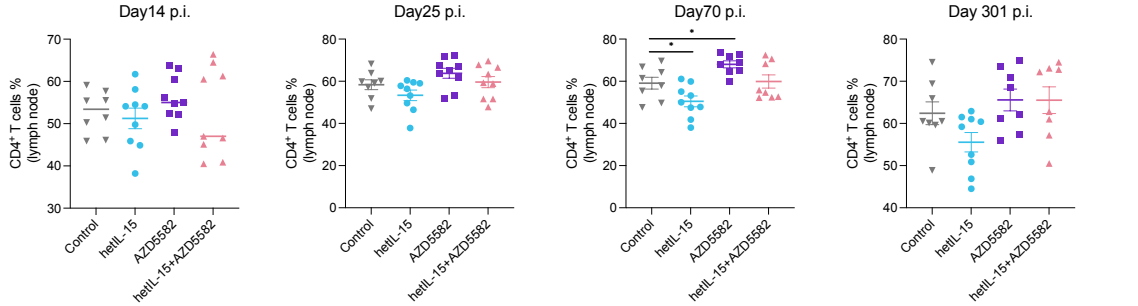

Fig. 28 Frequency of total CD4⁺ T cell frequencies in LNs. Flow cytometry analysis of CD4⁺ T cell frequencies in LNs at various timepoints (day 14 p.i., day 25 p.i., day 70 p.i, day 301 p.i.). After day 70 p.i., due to severe adverse reactions, only 8 animals were in AZD5582 and in AZD5582+hetIL-15 arms. Data are mean ± s.e.m. The horizontal bar in each group represents the mean. A two-sided Welch's t-test was used to compare values between the groups. Each intervention arm was compared individually with the ART-only control group. *P < 0.05, **P < 0.01, ***P < 0.001, ****P < 0.0001.

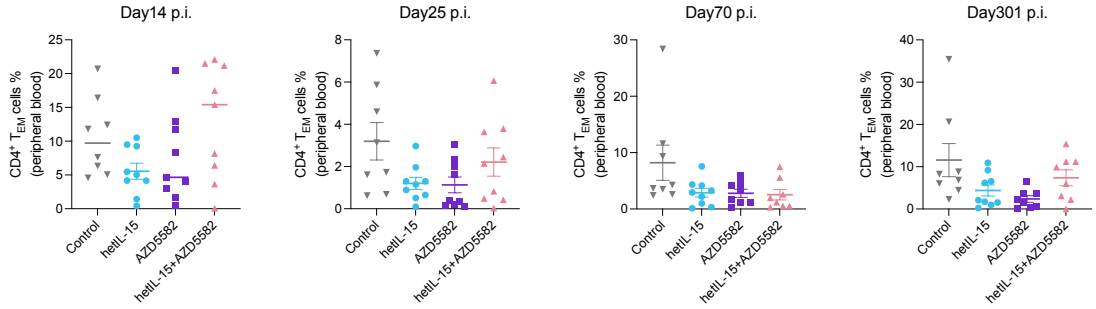

Fig. 29 Frequency of CD4⁺ T_{EM} cells in peripheral blood. Flow cytometry analysis of effector memory CD4⁺ T cell frequencies in peripheral blood at various timepoints (day 14 p.i., day 25 p.i., day 70 p.i, day 301 p.i.). After day 70 p.i., due to severe adverse reactions, only 8 animals were in AZD5582 and in AZD5582+hetIL-15 arms. Data are mean ± s.e.m. The horizontal bar in each group represents the mean. A two-sided Welch's t-test was used to compare values between the groups. Each intervention arm was compared individually with the ART-only control group. No significant differences were observed at any timepoint.

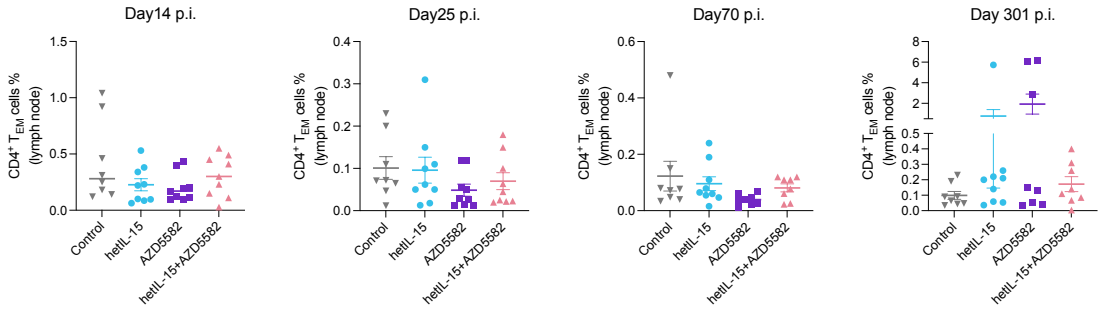

Fig. 30 Frequency of CD4⁺ T_{EM} cells in LNs. Flow cytometry analysis of effector memory CD4⁺ T cell frequencies in LNs at various timepoints (day 14 p.i., day 25 p.i., day 70 p.i, day 301 p.i.). After day 70 p.i., due to severe adverse reactions, only 8 animals were in AZD5582 and in AZD5582+hetIL-15 arms. Data are mean ± s.e.m. The horizontal bar in each group represents the mean. A two-sided Welch's t-test was used to compare values between the groups. Each intervention arm was compared individually with the ART-only control group. No significant differences were observed at any timepoint.

In peripheral blood, the frequency of CD8⁺ T cells tended to be lower in AZD5582 animals compared to the control group at all the timepoints analyzed (with the only exception at day 70 p.i), with a statistically significant difference observed at day 301 p.i. (p = 0.0366). No differences were observed in hetIL-15 and combination arm compared to the controls except a lower, not significant, lower frequency of CD8⁺ T cells in the AZD5582-treated animals at day 301p.i. (Fig. 31).

In LN, the AZD5582 arm showed lower CD8⁺ T cell frequencies at all the timepoints, with a statistically significant difference at day 70 p.i. (p = 0.0234); in contrast, hetIL-15 treated animals showed higher CD8⁺ T cell frequencies at all measured time points, reaching significance at day 70 p.i. (p = 0.0219). The combination group initially displayed higher frequencies than controls (day 14 p.i.), but the levels became comparable at days 25 and 70 p.i., and declined below control levels by day 301 p.i.; however, these differences did not reach statistical significance (Fig. 32).

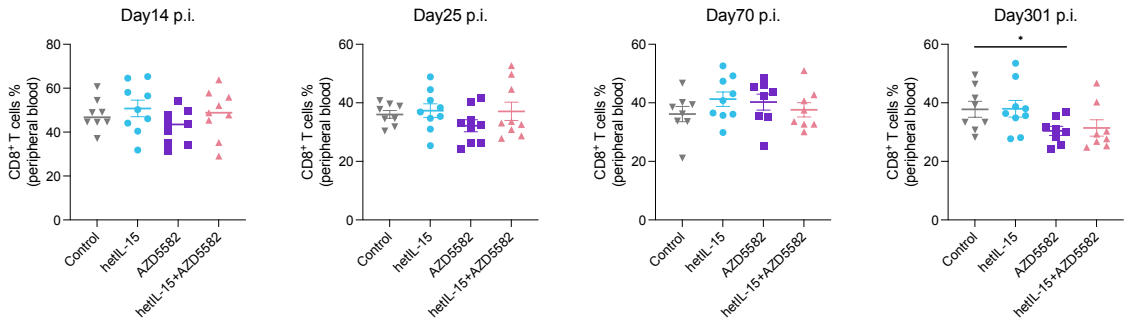

Fig. 31 Frequency of CD8⁺ T cells in peripheral blood. Flow cytometry analysis of CD8⁺ T cell frequencies in peripheral blood at various timepoints (day 14 p.i., day 25 p.i., day 70 p.i, day 301 p.i.). After day 70 p.i., due to severe adverse reactions, only 8 animals were in AZD5582 and in AZD5582+hetIL-15 arms. Data are mean ± s.e.m. The horizontal bar in each group represents the mean. A two-sided Welch's t-test was used to compare values between the groups. Each intervention arm was compared individually with the ART-only control group. *P < 0.05, **P < 0.01, ***P < 0.001, ****P < 0.0001.

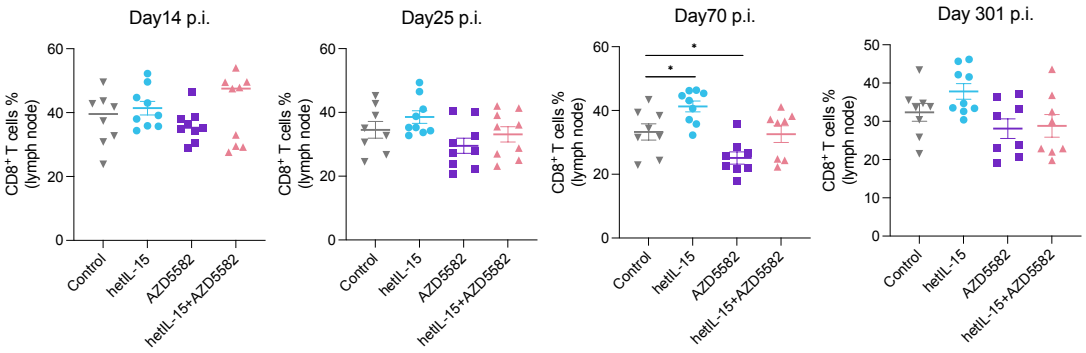

Fig. 32 Frequency of CD8⁺ T cells in LNs. Flow cytometry analysis of CD8⁺ T cell frequencies in LNs at various timepoints (day 14 p.i., day 25 p.i., day 70 p.i, day 301 p.i.). After day 70 p.i., due to severe adverse reactions, only 8 animals were in AZD5582 and in AZD5582+hetIL-15 arms. Data are mean ± s.e.m. The horizontal bar in each group represents the mean. A two-sided Welch's t-test was used to compare values between the groups. Each intervention arm was compared individually with the ART-only control group. *P < 0.05, **P < 0.01, ***P < 0.001, ****P < 0.0001.

CD8⁺ T_{EM} cells frequencies in peripheral blood were decreased in AZD5582-treated animals compared to the control at day 25 p.i. (p = 0.0266) and at day 301 p.i. (p = 0.0027). In the hetIL-15 group, frequencies were consistently lower than controls across all time points, reaching statistical significance only at day 301 p.i. (p = 0.0013). Similarly, in the combination group, lower frequencies were observed at days 25 and 70p.i., with a significant reduction detected at day 301 p.i. (p = 0.0119) (Fig. 33). No significant differences were found in LNs (Fig. 34).

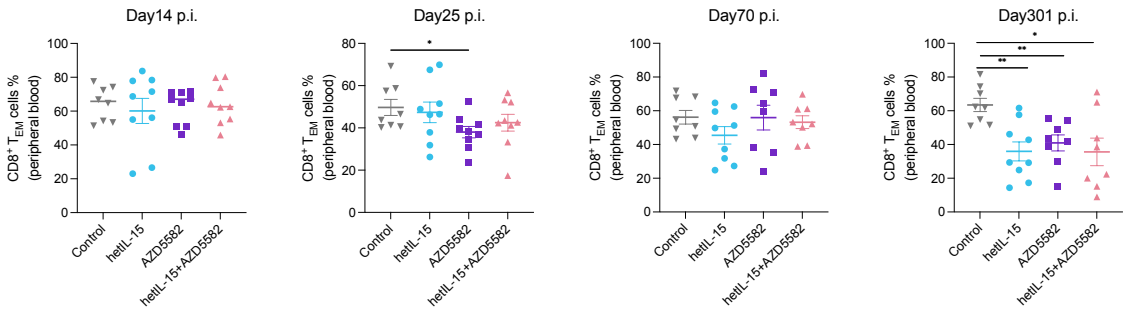

Fig. 33 Frequency of CD8⁺ T_{EM} cells in peripheral blood. Flow cytometry analysis of effector memory CD8⁺ T cell frequencies in peripheral blood at various timepoints (day 14 p.i., day 25 p.i., day 70 p.i, day 301 p.i.). After day 70 p.i., due to severe adverse reactions, only 8 animals were in AZD5582 and in AZD5582+hetIL-15 arms. Data are mean ± s.e.m. The horizontal bar in each group represents the mean. A two-sided Welch's t-test was used to compare values between the groups. Each intervention arm was compared individually with the ART-only control group. *P < 0.05, **P < 0.01, ***P < 0.001, ****P < 0.0001.

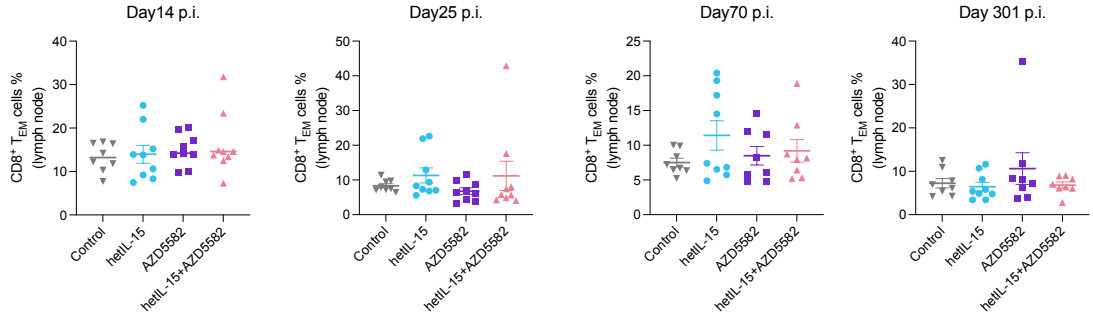

Fig. 34 Frequency of CD8⁺ T_{EM} cells in LNs. Flow cytometry analysis of effector memory CD8⁺ T cell frequencies in LNs at various timepoints (day 14 p.i., day 25 p.i., day 70 p.i, day 301 p.i.). After day 70 p.i., due to severe adverse reactions, only 8 animals were in AZD5582 and in AZD5582+hetIL-15 arms. Data are mean ± s.e.m. The horizontal bar in each group represents the mean. A two-sided Welch's t-test was used to compare values between the groups. Each intervention arm was compared individually with the ART-only control group. No significant differences were observed at any timepoint.

Cell proliferation, as measured by Ki-67 expression, showed consistent trends over time. In peripheral blood, the frequency of Ki-67⁺ CD4⁺ T cells was lower in all the intervention group compared to the control, with a statistically significant differences at day 70 p.i. (hetIL-15 vs control p = 0.0165; AZD5582 vs control p = 0.0336; AZD5582+hetIL-15 vs control p = 0.0384), and day 301 p.i. (hetIL-15 vs control p = 0.0352; AZD5582 vs control p = 0.0426; AZD5582+hetIL-15 vs control p = 0.0389) (Fig. 35). In LN, animals treated with hetIL-15 (arms 1 and 3) showed an increased frequency of Ki-67⁺ CD4⁺ T cells compared to control animals. This difference was lost at subsequent timepoints, with all the intervention groups showing lower Ki-67 expression than controls at day 70 p.i (hetIL-15 vs control p = 0.0019; AZD5582 vs control p = 0.0033; AZD5582+hetIL-15 p = 0.0194) (Fig. 36).

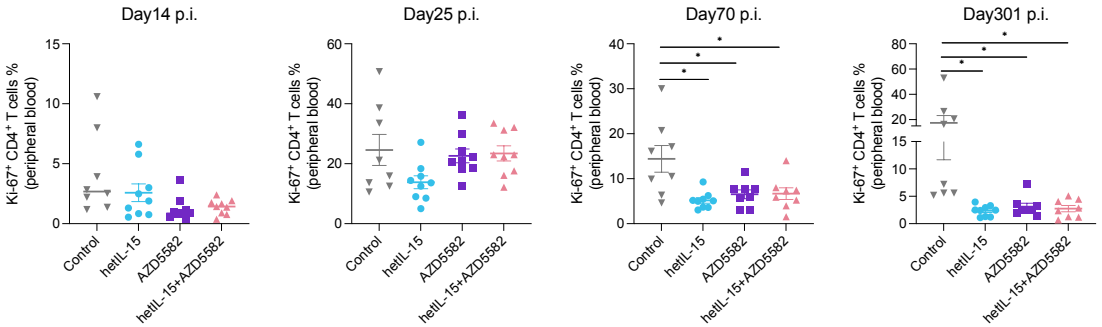

Fig. 35 Ki-67 expression in total CD4⁺ T cells in peripheral blood. Flow cytometry analysis of Ki-67 frequencies in bulk CD4⁺ T cell from peripheral blood at various timepoints (day 14 p.i., day 25 p.i., day 70 p.i, day 301 p.i.). After day 70 p.i., due to severe adverse reactions, only 8 animals were in AZD5582 and in AZD5582+hetIL-15 arms. Data are mean ± s.e.m. The horizontal bar in each group represents the mean. A two-sided Welch's t-test was used to compare values between the groups. Each intervention arm was compared individually with the ART-only control group. *P < 0.05, **P < 0.01, ***P < 0.001, ****P < 0.0001.

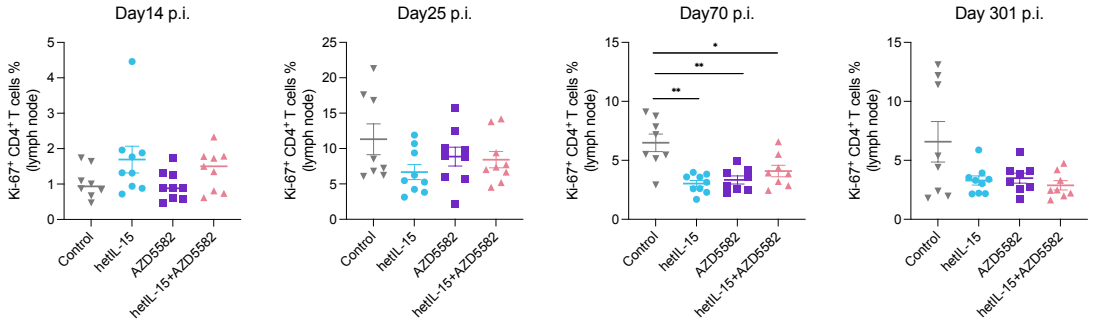

Fig. 36 Ki-67 expression in total CD4⁺ T cells in LNs. Flow cytometry analysis of Ki-67 frequencies in bulk CD4⁺ T cell from lymph node at various timepoints (day 14 p.i., day 25 p.i., day 70 p.i, day 301 p.i.). After day 70 p.i., due to severe adverse reactions, only 8 animals were in AZD5582 and in AZD5582+hetIL-15 arms. Data are mean ± s.e.m. The horizontal bar in each group represents the mean. A two-sided Welch's t-test was used to compare values between the groups. Each intervention arm was compared individually with the ART-only control group. *P < 0.05, **P < 0.01, ***P < 0.001, ****P < 0.0001.

The Ki-67 expression profile of CD8⁺ T cells in peripheral blood mirrored that observed in CD4⁺ T cells and it was consistently lower in all intervention arms compared to the control group across timepoints. A statistically significant difference was observed at day 14 p.i. in the two arms treated with AZD5582 (AZD5582 vs control p = 0.0003; AZD5582+hetIL-15 vs control p = 0.0074). At day 70 p.i., Ki-67 expression in the AZD5582-treated animals (arms 2 and 3) was comparable to the control group, whereas hetIL-15 showed lower levels of Ki-67 expression in CD8⁺ T cells compared to the control (p = 0.0013). At the latest timepoint (day 301 p.i.), all the intervention groups showed a significantly lower frequencies of Ki-67⁺ CD8⁺ T cells compared to the control group (hetIL-15 vs control p = 0.0018); AZD5582 vs control p = 0.0062; AZD5582+hetIL-15 p = 0.0060) (Fig. 37). Interestingly, no differences were observed in LNs at any timepoint (Fig. 38).

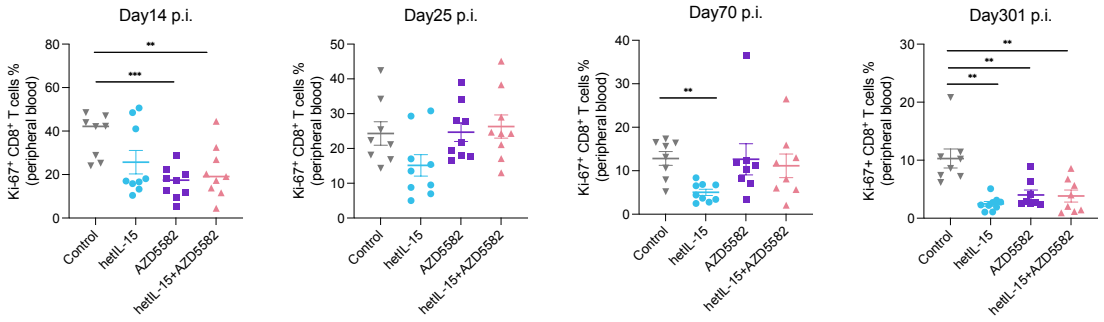

Fig. 37 Ki-67 expression in total CD8⁺ T cells in peripheral blood. Flow cytometry analysis of Ki-67 frequencies in bulk CD8⁺ T cell in peripheral blood at various timepoints (day 14 p.i., day 25 p.i., day 70 p.i, day 301 p.i.). After day 70 p.i., due to severe adverse reactions, only 8 animals were in AZD5582 and in AZD5582+hetIL-15 arms. Data are mean ± s.e.m. The horizontal bar in each group represents the mean. A two-sided Welch's t-test was used to compare values between the groups. Each intervention arm was compared individually with the ART-only control group. *P < 0.05, **P < 0.01, ***P < 0.001, ****P < 0.0001.

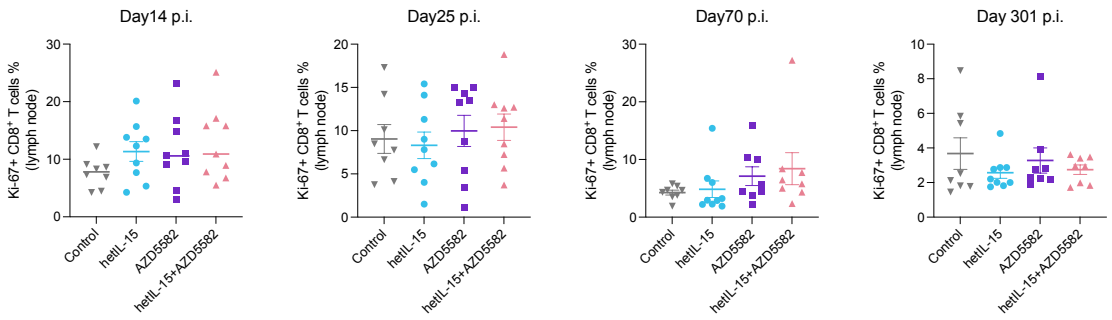

Fig. 38 Ki-67 expression in total CD8⁺ T cells in LNs. Flow cytometry analysis of Ki-67 frequencies in bulk CD8⁺ T cell in peripheral blood at various timepoints (day 14 p.i., day 25 p.i., day 70 p.i, day 301 p.i.). After day 70 p.i., due to severe adverse reactions, only 8 animals were in AZD5582 and in AZD5582+hetIL-15 arms. Data are mean ± s.e.m. The horizontal bar in each group represents the mean. A two-sided Welch's t-test was used to compare values between the groups. Each intervention arm was compared individually with the ART-only control group. No significant differences were observed at any timepoint.

The effector functions of CD8⁺ T cells, assessed by Granzyme B expression, were not impacted by the treatment with AZD5582, alone or in combination with hetIL-15. At day 14 p.i., arm 2 (AZD5582 alone) showed a lower frequency of Granzyme B in peripheral blood compared to the control (p = 0.0377), compared to hetIL-15 (p = 0.0048) and combination groups (p = 0.0430), indicating a baseline difference related to animals variability. By the end of the study (day 301 p.i.), all the intervention arms showed a lower level of Granzyme B compared to the control. This difference was statistically significant for both hetIL-15-treated groups (hetIL-15 vs control p = 0.0048; AZD5582+hetIL-15 vs control p = 0.0430) (Fig. 39). In contrast, in LN, Granzyme B expression was higher in the inteventions arms at all timepoints, with a significant difference at day 25 p.i. for arm1 (p = 0.0433) and at day 70 p.i. for arm 2 (p = 0.0483) compared to controls (Fig. 40).

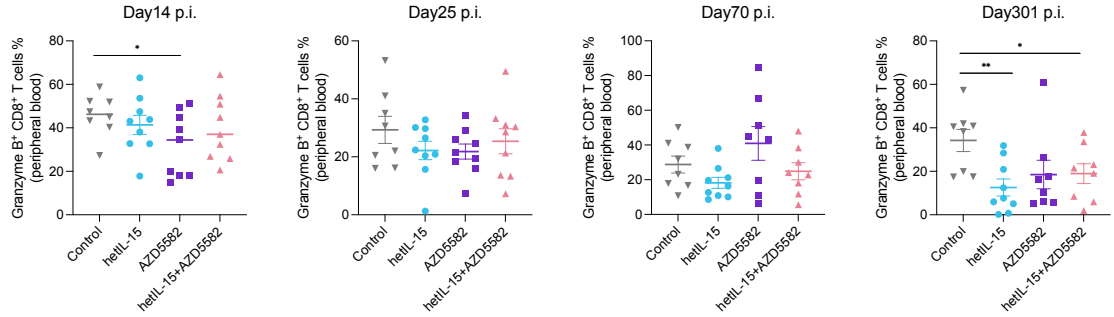

Fig. 39 Granzyme B expression in total CD8⁺ T cells in peripheral blood. Flow cytometry analysis of Granzyme B frequencies in bulk CD8⁺ T cell in peripheral blood at various timepoints (day 14 p.i., day 25 p.i., day 70 p.i, day 301 p.i.). After day 70 p.i., due to severe adverse reactions, only 8 animals were in AZD5582 and in AZD5582+hetIL-15 arms. Data are mean ± s.e.m. The horizontal bar in each group represents the mean. A two-sided Welch's t-test was used to compare values between the groups. Each intervention arm was compared individually with the ART-only control group. *P < 0.05, **P < 0.01, ***P < 0.001, ****P < 0.0001.

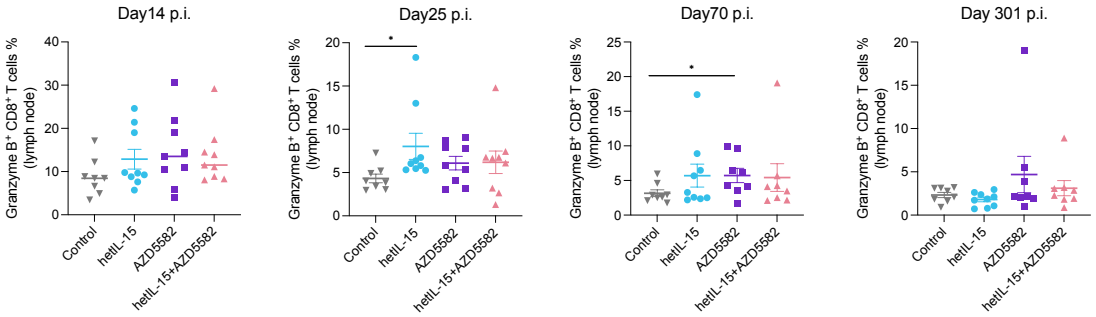

Fig. 40 Granzyme B expression in total CD8⁺ T cells in LNs. Flow cytometry analysis of Granzyme B frequencies in bulk CD8⁺ T cell in LNs at various timepoints (day 14 p.i., day 25 p.i., day 70 p.i, day 301 p.i.). After day 70 p.i., due to severe adverse reactions, only 8 animals were in AZD5582 and in AZD5582+hetIL-15 arms. Data are mean ± s.e.m. The horizontal bar in each group represents the mean. A two-sided Welch's t-test was used to compare values between the groups. Each intervention arm was compared individually with the ART-only control group. *P < 0.05, **P < 0.01, ***P < 0.001, ****P < 0.0001.

NK cell frequencies in peripheral blood were lower in the hetIL-15 group compared to controls at days 25 and 70 p.i., reaching statistical significance only at day 301 p.i. (p = 0.0429). In AZD5582-treated animals, frequencies were generally comparable to controls, except for a nonsignificant reduction at day 25 p.i.. The combination group also displayed lower frequencies than controls across time points, though these differences did not reach statistical significance (Fig. 41).

In LNs at day 14 p.i., NK cell frequencies were higher in all treatment groups compared to controls, with significant higher levels observed in the AZD5582 (p = 0.0417) and combination groups (p = 0.0272). At day 25 p.i., both hetIL-15 and AZD5582 groups maintained higher frequencies than controls, although the differences were not statistically significant. By day 70 p.i., the combination group continued to show slightly higher NK cell frequencies compared to controls, but without significance. At day 301 p.i., all treatment groups exhibited significantly higher NK cell frequencies than controls (hetIL-15 vs control p = 0.0375; AZD5582 vs control p = 0.0004; AZD5582+hetIL-15 vs control p = 0.0016) (Fig. 42).

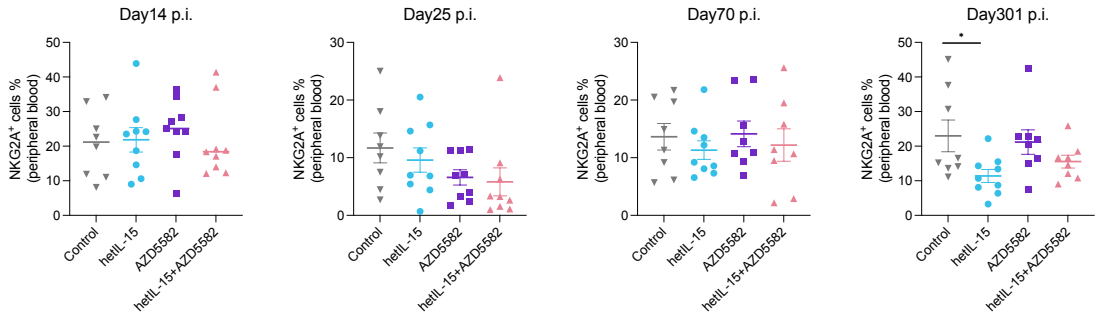

Fig. 41 Frequency of NK cells in peripheral blood. Flow cytometry analysis of NK cell in peripheral blood at various timepoints (day 14 p.i., day 25 p.i., day 70 p.i, day 301 p.i.). After day 70 p.i., due to severe adverse reactions, only 8 animals were in AZD5582 and in AZD5582+hetIL-15 arms. Data are mean ± s.e.m. The horizontal bar in each group represents the mean. A two-sided Welch's t-test was used to compare values

between the groups. Each intervention arm was compared individually with the ART-only control group. *P < 0.05, **P < 0.01, ***P < 0.001, ****P < 0.0001.

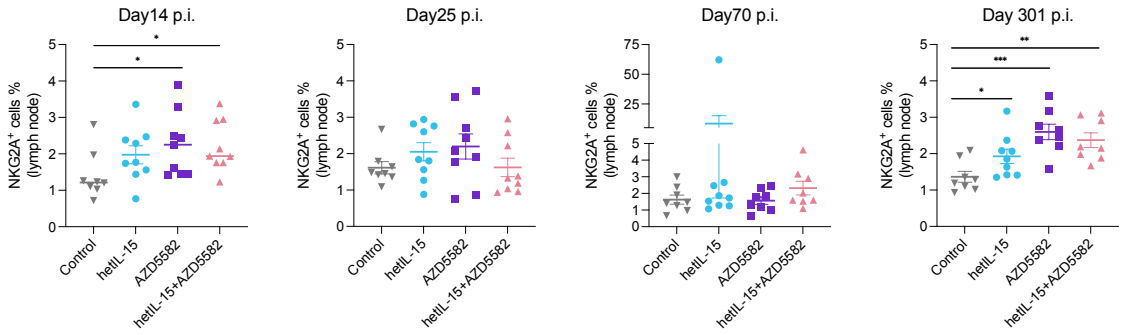

Fig. 42 Frequency of NK cells in LNs. Flow cytometry analysis of NK cell in LNs at various timepoints (day 14 p.i., day 25 p.i., day 70 p.i, day 301 p.i.). After day 70 p.i., due to severe adverse reactions, only 8 animals were in AZD5582 and in AZD5582+hetIL-15 arms. Data are mean ± s.e.m. The horizontal bar in each group represents the mean. A two-sided Welch's t-test was used to compare values between the groups. Each intervention arm was compared individually with the ART-only control group. *P < 0.05, **P < 0.01, ***P < 0.001, ****P < 0.0001.

6. Discussion

The persistence of a long-lived viral reservoir harboring integrated, replication-competent proviruses remains the central obstacle to achieving HIV cure as it can rapidly fuel viral rebound upon ART interruption, making its early disruption a critical goal.

Strategies aimed at preventing or limiting the establishment of the viral reservoir during the earliest stages of infection and ART initiation have emerged as a major focus of recent research. This represents a conceptual shift from the classical "shock and kill" paradigm, in which LRAs were designed to reactivate virus in individuals with chronic infection, thereby exposing infected cells to immune-mediated clearance. While this approach has generated valuable insights, it has repeatedly shown limited success in reducing reservoir size once it is firmly established [287-288].

More recently, however, a new line of investigation has focused on interventions administered during acute or very early infection, with the explicit goal of preventing the formation of a long-lived reservoir rather than attempting to reverse it later. This "latency prevention" strategy is conceptually attractive, as the reservoir is seeded rapidly after infection and becomes extremely stable once ART is initiated.

Within this framework, the study of Statzu et al. [373] is particularly noteworthy. By depleting $CD8^+$ T lymphocytes in ART-treated, SIV-infected RMs at early infection, the authors demonstrated that this intervention did not significantly alter reservoir size or persistence. These finding suggests that $CD8^+$ T cells do not play a critical role in the establishment of the SIV reservoir under ART conditions, highlighting both the

complexity of the mechanisms that stabilize viral persistence and the challenges of identifying effective targets for early intervention. Similarly, our study was designed with a latency-prevention rationale, positioning the intervention phase at the earliest moments of infection and ART initiation (day 14 p.i.).

Another novelty shared by Statzu et al. and our work lies in the repurposing of strategies and compounds traditionally used to reverse latency in chronic infection. Whereas the authors employed $CD8^+$ T cell depletion, we applied the SMAC mimetic AZD5582 alone or in combination with hetIL-15. In both cases, interventions classically associated with latency reversal were tested for their ability to prevent reservoir establishment at ART initiation.

Several studies have been used CD8 depletion and immune enhancers or LRAs in the context of an already well-established reservoir [287-289, 311, 335].

Attempts to enhance immune-mediated clearance through combinations such as CD8 depletion and N-803 in SHIV/SIV models have yielded robust expansion of $CD4^+$, $CD8^+$, and NK cells and potent viral reactivation, yet they failed to reduce the reservoir [287-288]. Similarly, the SMAC mimetic AZD5582 has consistently demonstrated potent latency-reversal activity *in vivo*, whether administered alone [311] or in combination with agents such as HIVxCD3 DART [335], N-803, and RhmAbs [289], including in the context of CD8 depletion [374]. However, significant reductions in reservoir size have only recently been reported [289]. Dashti et al. [289] showed that AZD5582 combined with RhmAbs, with or without N-803, significantly reduced $CD4^+$ T-cell-associated SIV-DNA in LNs, spleen, bone marrow, and peripheral blood, highlighting the potential of combinatorial approaches to enhance clearance of latently infected cells with tissue-specific patterns of efficacy.

Building on these findings, our study adds further nuances to viral dynamics upon early AZD5582 administration on SIV plasma viremia and reservoir.

The higher levels of pVL and the slower decay rate in AZD5582 treated animals was likely a consequence of enhanced viral transcription from recently infected cells whose silencing had not yet been fully established, rather than the results of new rounds of infection under ART. In the early stage of infection, the reservoir is still being seeded, and many infected cells are transcriptionally active so that AZD5582 may transiently prolong the lifespan or increase the productivity of these early-infected cells, leading to detectable plasma SIV-RNA despite concurrent ART.

Moreover, we observed that AZD5582, alone or in combination with hetIL-15, when administered at ART initiation (14 days p.i.), significantly reduced the SIV reservoir in peripheral blood and LN. AZD5582 monotherapy also reduced reservoir size relative to controls at days 25 and 70 p.i., with delayed viral decay consistent with its role in perturbing transcriptional silencing. Importantly, reductions in intact proviral DNA were observed in lymphoid tissues, and these effects persisted beyond the intervention

phase. In the combination arm, reductions remained significant through day 301 p.i., underscoring the central role of lymphoid tissues as critical sites of viral persistence [375-377] and highlighting the value of targeting these compartments for effective reservoir reduction. Unlike N-803, which did not reduce reservoir size when used alone [287-288], in our study hetIL-15 monotherapy given during the early stage of infection consistently decreased SIV-DNA, particularly early in ART initiation (day 14 p.i.) and at later time points in both blood (days 25 and 70 p.i.) and LNs (day 70 p.i.).

However, despite these significant and tissue-specific effects, the overall impact of the interventions was transient. Neither AZD5582 nor hetIL-15 monotherapy were able to maintain sustained lower levels of intact proviral DNA beyond day 70 p.i., as reservoir levels in blood at day 168 p.i. and in both tissues at day 301 p.i. were no longer significantly different from controls (LNs were not sampled at day 168 p.i.). Even in the combination arm, which extended the effect up to day 301p.i. in LN, the intervention did not lead to durable or systemic elimination of the reservoir.

Taken together, these results demonstrate that early administration of AZD5582 and/or hetIL-15 can perturb reservoir seeding and transiently lower its size, but also reveal the formidable capacity of viral persistence mechanisms to stabilize once the intervention ceases. These observations argue strongly for the development of sustained or combinatorial approaches to consolidate and extend the benefits of early latency-prevention strategies.

Interestingly, in contrast to previous studies [288-289, 357-358], we did not observe strong proliferative expansions in $CD4^+$ or $CD8^+$ T cells, and Ki-67 levels were consistently lower in the interventions arms, suggesting that AZD5582 and hetIL-15 did not drive generalized T cell proliferation. Frequencies of $CD4^+$ T_{EM} cells remained unchanged, while $CD8^+$ T_{EM} cell frequencies in peripheral blood were lower than controls in AZD5582-treated animals (day 25 p.i.) and across all arms at day 301 p.i.. Granzyme B expression was transiently increased in hetIL-15–treated LNs (day 25 p.i.) and in AZD5582-treated LNs (day 70p.i.), consistent with prior reports [289]. However, decreased frequencies were observed in blood at early (day 14 p.i.) and late (day 301 p.i.) time points in AZD5582, and in both hetIL-15 and combination arms, respectively.

The dynamics of NK cell responses revealed divergent patterns between peripheral blood and lymphoid tissues. In peripheral blood, NK cell frequencies were reduced in hetIL-15–treated animals compared to controls, reaching significance only at the late time point, while AZD5582 and the combination had minimal impact. In contrast, within LN, all interventions tended to increase NK cell frequencies relative to controls, with significant elevations observed at early (day 14 p.i.) and late (day 301 p.i.) time points. These findings suggest that NK cell responses to hetIL-15 and AZD5582 are highly compartmentalized, with peripheral blood not fully reflecting the tissue-resident NK cell dynamics. The significant enrichment of NK cells in LNs at later stages may indicate a role for these innate effectors in shaping the microenvironment of the viral reservoir.

In line with this, Webb et al. demonstrated that in ART-suppressed, SHIV-infected RMs, N-803 induced activation and mobilization of both NK cells and virus-specific CD8+ T cells from the periphery into lymph node B cell follicles, a sanctuary site for latent virus that typically excludes such effector populations [354].

These results suggest that the reductions in reservoir size were not simply a consequence of generalized immune activation but may reflect targeted enhancement of antiviral effector functions within lymphoid tissues.

Clinically relevant safety concerns were observed in our study as two animals experienced fatal adverse events associated with AZD5582 administration, characterized by respiratory distress, cardiovascular collapse, and, in one case, fibrinous pericarditis identified post-mortem.

Preclinical and clinical experience with first-generation SMAC mimetics (such as birinapant, LCL161, and Debio-1143) has consistently reported cytokine release, endothelial activation, and systemic inflammatory toxicities, often correlated with dose and exposure [378-380]. These agents broadly activate cNF-κB pathways and TNF-α–dependent apoptosis, providing a plausible mechanistic basis for such adverse effects. AZD5582 was developed as a more selective, next-generation bivalent SMAC mimetic, designed to preferentially activate the ncNF-κB pathway, thereby reducing the risk of widespread cytokine release and systemic toxicity [309, 311]. Published studies of AZD5582 in NHP have generally suggested favorable tolerability and minimal overt clinical toxicity, not reporting the occurrence of severe adverse events or fatalities [287-288, 311, 335].

Our findings therefore provide critical additional perspective, underscoring that even a compound designed for improved selectivity is not exempt from context-dependent toxicity. The cardiopulmonary collapse observed in our study may reflect acute hemodynamic instability triggered by cytokine-driven vascular permeability or off-target effects on endothelial or myocardial cells. Similarly, the fibrinous pericarditis identified at necropsy could indicate inflammatory responses extending beyond the intended immune stimulation. These events occurred in the setting of very early ART initiation, a period marked by profound immune activation, dynamic redistribution of lymphocytes, and tissue remodelling, which may have amplified susceptibility to systemic toxicity.

Taken together, these observations underscore that while next-generation SMAC mimetics represent a conceptual advance in latency-reversal strategies, their clinical development must proceed with caution. Selectivity for the ncNF-κB pathway may mitigate, but does not eliminate, the risk of adverse inflammatory events.

These findings underscore the necessity of careful dose optimization, rigorous monitoring, and risk mitigation strategies when translating such interventions to clinical settings. However, the majority of animals tolerated treatment without additional

adverse effects, and no further complications were observed, suggesting that these interventions can still be implemented safely in the context of ART with appropriate precautions.

Overall, our findings support AZD5582 as an effective LRA capable of disrupting intact proviral reservoirs establishment when administered at ART initiation, with lymphoid tissues as the primary sites of activity. The addition of hetIL-15 enhanced these effects, leading to broader and more sustained reductions in reservoir size.

Despite the promising findings, this study has several limitations. First, while peripheral blood and LNs were extensively analyzed, other potential viral reservoirs, such as GALT and the CNS, were not systematically evaluated. Second, the long-term durability of the observed reservoir reductions beyond the study endpoint remains uncertain, and viral rebound dynamics after ART interruption were not assessed. Finally, although AZD5582 and hetIL-15 showed efficacy in this SIV model, differences between SIV and HIV may influence the translational applicability of these results to humans. Future work should explore integration with additional interventions, such as bNAbs or therapeutic vaccines, to achieve more profound and durable clearance of the viral reservoir.

7. Materials and methods

7.1 Ethical statement

All animal experiments were conducted following guidelines established by the Animal Welfare Act and by the NIH's Guide for the Care and Use of Laboratory Animals, 8th edition. All the procedures were approved by the Emory University Institutional Animal Care and Use Committee (IACUC) (Permit number #201700286). Animal care facilities at ENPRC are accredited by the U.S. Department of Agriculture and the Association for Assessment and Accreditation of Laboratory Animal Care International.

7.2 Animals, SIV infection and ART

The study included 35 Indian RMs housed at the ENPRC, Atlanta (GA), consisting of 25 males and 10 females, aged 53.8 ± 9.1 months at the time of enrollment. All of them were negative for the Mamu*B08 and Mamu*B17 MHC class I alleles, and 22.9% of them were positive for Mamu*A01 (NB38, RKc20, RYf20, NC80, RQn18, MK91, RQy19, RRl18, RBg19, MK92) (Table 6).

All animals were infected intravenously with 10,000 IU of barcoded SIVmac239M, containing around 10,000 clonotypes present at approximately equal proportions [372]. Triple combination ART was started on day 14 p.i. and consisted of DTG (2.5 mg/kg/day),

TDF (5.1 mg/kg/day) and FTC (40 mg/kg/day). ART was administered SQ once daily and continued until necropsy.

7.3 HetIL-15 and AZD5582

RMs were stratified into four experimental groups: hetIL-15 (arm1, n = 9), AZD5582 (arm2, n = 9), AZD5582+hetIL15 (arm3, n = 9), ART-only group (arm4; n = 8). hetIL-15 was administered SQ, starting 3 days before ART initiation, once/week for 10 consecutive weeks according to a step-up/step-down dosing schedule: 10μg/kg during the first week, 20μg/kg in the second week, 40μg/kg from weeks three through eight, 20μg/kg in the ninth week, and 10μg/kg in the final week. HetIL-15 was produced and purified by the George Pavlakis laboratory from a cloned cell line derived from human embryonic kidney (HEK293) cells transfected with optimized plasmid DNA encoding IL-15 and IL-15Rα, and cultured in serum-free medium (Lonza) [357]. The compound was kindly provided by Dr. Pavlakis.

AZD5582 monotherapy consisted of weekly IV infusions of 0.1mg/kg for 10 weeks, starting at ART initiation (day 14 p.i.). AZD5582 (Chemietek, Catalog #CT-A5582) was supplied as a powder and reconstituted to 0.4 mg/mL in 10% Captisol (Research Grade, b-Cyclodextrin Sulfobutyl Ethers, Sodium Salt; Cydex, Catalog #RC-0C7-100) the day before administration and stored at 4°C until use. To minimize infusion-related reactions, all animals were pre-treated with 2mg/kg diphenhydramine IV prior to each AZD5582 infusion and AZD5582 was administered in 20-30 minutes.

In the combination arm, the same dosing regimen described above was followed for both compounds, and hetIL-15 was administered 3 days before AZD5582.

7.4 Sample collection and processing

Ethylenediaminetetraacetic acid (EDTA)-anticoagulated blood samples were collected at regular intervals and used for complete blood counts, routine clinical chemistry analyses, and immunophenotyping. Plasma was separated by centrifugation within 1 h of phlebotomy and stored at −80 °C until further analysis.

PBMCs were isolated from whole blood by density gradient centrifugation using Ficoll-Paque (Cytiva, Marlborough, MA Catalog # GE17-1440-02).

LNs biopsies (axillary or inguinal region) were performed longitudinally and at necropsy. For each procedure, the skin overlying the LNs was clipped and surgically prepped. An incision was made, and the LNs was exposed by blunt dissection and excised using clamps, as previously described [373]. Excised LNs were homogenized and filtered through a 70 μm cell strainer to isolate mononuclear cells. Single-cell suspensions were cryopreserved in 10% Dimethyl sulfoxide (DMSO) in Fetal Bovine Serum (FBS).

All samples were processed and analyzed within 24 h of collection.

7.5 Plasma SIV RNA

pVL was monitored longitudinally using a hybrid quantitative real-time PCR (qRT-PCR) assay specific for SIVmac239, as previously described [381]. The assay has a detection limit of 15 copies/mL.

7.6 Intact Proviral DNA Assay (IPDA)

IPDA was conducted on purified $CD4^+$ T-cells by Accelevir Diagnostics using a method analogous to the HIV-1 IPDA [382]. $CD4^+$ T cells were positively selected from frozen cell suspensions using magnetically labeled microbeads, followed by column purification according to the manufacturer's protocol (Miltenyi Biotec). The purified $CD4^+$ cells were resuspended in 200 µL of Dulbecco's Phosphate-Buffered Saline (DPBS) and stored at –80 °C until ready to be used.

7.7 Immunophenotyping by flow cytometry

Multiparametric flow cytometry was performed on PBMCs and LNs derived mononuclear cells using standard protocols [383]. Surface and intracellular staining were carried out using fluorochrome-conjugated anti-human monoclonal antibodies validated for cross-reactivity in RMs in databases maintained by the Nonhuman Primate Reagent Resource (MassBiologics). The full list of antibodies, including fluorochromes, clones, vendors, catalog numbers, and concentrations used per test, is provided in Table 7.

Briefly, cells were first incubated with a Live/Dead viability dye for 5 minutes at room temperature. Chemokine receptor cocktail was then added and incubated at 37 °C for 15 minutes, followed by surface marker staining for 30 minutes at room temperature. Cells were subsequently fixed and permeabilized using the Tonbo Fix/Perm buffer kit (Cat. # SKU TNB-0607-KIT) for 45 minutes at 4 °C. The intracellular staining cocktail was then added for 30 minutes at room temperature. Data acquisition was performed on a FACSymphony A5 Analyzer (BD Bioscience) flow cytometer driven by FACS Diva software (BD Bioscience), maintained by the ENPRC Flow Cytometry Core. Analysis was conducted using FlowJo software (version 10.10 BD Biosciences).

Marker	Fluorochrome	Clone	Company	Catalog #	Amount/ test (µL)
Live/Dead	Fixable Viability Stain 700	—	BD	564997	0.1
CD3	BUV395	SP34-2	BD	564117	2.5
CD4	APC-Cy7	OKT4	Biolegend	317418	2.5
CD8	BUV496	RPA-T8	BD	612942	2.5
CD45	BUV563	D058-1283	BD	741414	5
CCR7	BB700	3D12	BD	566437	5
CD28	BUV737	CD28.2	BD	612815	5
CD95	BV605	DX2	Biolegend	305628	5
Ki-67	BV480	B56	BD	566109	5
Granzyme B	PE-CF594	GB11	Invitrogen	GRB17	5
NKG2a	PE	Z199	Beckman Coulter	A60797	6

Table 7 Antibodies used for multiparametric cytofluorimetric analysis

7.8 Statistical analysis

Data collection and analysis were conducted without blinding to experimental conditions. Statistical analyses were performed with GraphPad Prism 10 software (GraphPad Software, Inc., La Joya, CA, U.S.). Statistical test used to compare the groups was Welch's *t*-test. Data are presented as mean ± SEM. Statistical significance was defined as $p \leq 0.05$.

References

1. Immunocompromised Homosexuals. Lancet. 1981 Dec 12;2(8259):1325-6. PMID: 6118721.
2. Centers for Disease Control (CDC). A cluster of Kaposi's sarcoma and Pneumocystis carinii pneumonia among homosexual male residents of Los Angeles and Orange Counties, California. MMWR Morb Mortal Wkly Rep. 1982 Jun 18;31(23):305-7. PMID: 6811844.
3. Quagliarello V. The Acquired Immunodeficiency Syndrome: current status. Yale J Biol Med. 1982;55(5-6):443-452
4. Mansell PW. Acquired immune deficiency syndrome, leading to opportunistic infections, Kaposi's sarcoma, and other malignancies. Crit Rev Clin Lab Sci. 1984;20(3):191-204. doi:10.3109/10408368409165774
5. Collier AC, Handsfield HH. Acquired immune deficiency syndrome. Urol Clin North Am. 1984;11(1):187-197
6. Broder S, Gallo RC. A pathogenic retrovirus (HTLV-III) linked to AIDS. N Engl J Med. 1984 Nov 15;311(20):1292-7. doi: 10.1056/NEJM198411153112006.
7. Gottlieb MS, Schroff R, Schanker HM, Weisman JD, Fan PT, Wolf RA, Saxon A. Pneumocystis carinii pneumonia and mucosal candidiasis in previously healthy

homosexual men: evidence of a new acquired cellular immunodeficiency. N Engl J Med. 1981 Dec 10;305(24):1425-31. doi: 10.1056/NEJM198112103052401.
8. Zagury D, Bernard J, Leibowitch J, et al. HTLV-III in cells cultured from semen of two patients with AIDS. Science. 1984;226(4673):449-doi:10.1126/science.6208607
9. Sarngadharan MG, DeVico AL, Bruch L, Schüpbach J, Gallo RC. HTLV-III: the etiologic agent of AIDS. Princess Takamatsu Symp. 1984;15:301-30
10. Barré-Sinoussi F., Chermann J., Rey F., Nugeyre MT., Chamaret S., Gruest J., Dauguet C., Axler-Blin C., Vézinet-Brun F., Rouzioux C., Rozenbaum W., Montagnier L. - Isolation of a T-lymphotropic retrovirus from a patient at risk for acquired immune deficiency syndrome (AIDS) – Science 1983 May 20; 220(4599):868-71 - doi: 10.1126/science.6189183.
11. Levi JA. - Pathogenesis of Human Immunodeficiency Virus Infection – Microbiological Review 1993 Mar; 57(1):183-289 – doi: 10.1128/mr.57.1.183-289.1993.
12. Shampo MA., Kyle RA., – Luc Montagnier – Discoverer of the AIDS virus – Mayo Clin Proc. 2002 Jun; 77(6):506 – doi: 10.4065/77.6.506.
13. Gallo RC, Salahuddin SZ, Popovic M, Shearer GM, Kaplan M, Haynes BF, Palker TJ, Redfield R, Oleske J, Safai B, et al. Frequent detection and isolation of cytopathic retroviruses (HTLV-III) from patients with AIDS and at risk for AIDS. Science. 1984 May 4;224(4648):500-3. doi: 10.1126/science.6200936.
14. Greene WC. - A history of AIDS: Looking back to see ahead- Eur J Immunol. 2007 Nov; 37 Suppl 1: S94-102 doi 10.1002/eji.200737441.
15. Tagaya Y., Matsuoka M., Gallo R. - 40 years of the human T-cell leukemia virus: past, present, and future – Version 1- F1000Res. 2019; 8 – doi: 10.12688/f1000research.17479.1
16. Seitz R. – Human Immunodeficiency Virus (HIV) – Transfus Med Hemother 2016 May 43(3): 203-222 – doi: 10.1159/000445852
17. Sharp PM, Hahn BH, Origins of HIV and AIDS pandemic, Cold Spring Harb Perspect Med. 2011; 1:a006841
18. Gao F, Bailes E, Robertson DL, Chen Y, Rodenburg CM, Michael SF, Cumminis LB, Arthur LO, Peeters M, Shaw GM, Sharp PM, Hahn BH, Origin of HIV-1 in the chimpanzee Pan troglodytes troglodytes, Nature, 1999; DOI: 397: 436-441
19. van Heuvel Y, Schatz S, Rosengarten JF, Stitz J. Infectious RNA: Human Immunodeficiency Virus (HIV) Biology, Therapeutic Intervention, and the Quest for a Vaccine. Toxins (Basel). 2022;14(2):138. Published 2022 Feb 14. doi:10.3390/toxins14020138
20. Bell SM., Bedford T. - Modern-day SIV viral diversity generated by extensive recombination and cross-species transmission – Plos Pathogens - Published: July 3,2017 - https://doi.org/10.1371/journal.ppat.1006466.
21. Nyamweya S, Hegedus A, Jaye A, Rowland-Jones S, Flanagan KL, Macallan DC. Comparing HIV-1 and HIV-2 infection: Lessons for viral immunopathogenesis. Rev Med Virol. 2013;23(4):221-240. doi:10.1002/rmv.1739
22. Campbell-Yesufu OT., Gandhi RT. - Update on Human Immunodeficiency Virus (HIV)-2 Infection - Clin Infectious Diseases. 2011 Mar 15; 52(6): 780–787.- doi: 10.1093/cid/ciq248
23. Welz T, Wyen C, Hensel M. Drug Interactions in the Treatment of Malignancy in HIV-Infected Patients. Oncol Res Treat. 2017;40(3):120-127. doi: 10.1159/000458443. Epub 2017 Feb 24

24. Murphy RA, Sunpath H, Kuritzkes DR, Venter F, Gandhi RT. Antiretroviral therapy-associated toxicities in the resource-poor world: the challenge of a limited formulary. J Infect Dis. 2007 Dec 1;196 Suppl 3:S449-56. doi: 10.1086/521112
25. INSIGHT START Study Group; Lundgren JD, Babiker AG, Gordin F, Emery S, Grund B, Sharma S, Avihingsanon A, Cooper DA, Fätkenheuer G, Llibre JM, Molina JM, Munderi P, Schechter M, Wood R, Klingman KL, Collins S, Lane HC, Phillips AN, Neaton JD. Initiation of Antiretroviral Therapy in Early Asymptomatic HIV Infection. N Engl J Med. 2015 Aug 27;373(9):795-807. doi: 10.1056/NEJMoa1506816. Epub 2015 Jul 20
26. Harris E. WHO Documents Rising Resistance to First-Line HIV Drug. JAMA. 2024 Apr 23;331(16):1355. doi: 10.1001/jama.2024.4497
27. Altice F, Evuarherhe O, Shina S, Carter G, Beaubrun AC. Adherence to HIV treatment regimens: systematic literature review and meta-analysis. Patient Prefer Adherence. 2019 Apr 3;13:475-490. doi: 10.2147/PPA.S192735
28. Osmond D, Charlebois E, Lang W, Shiboski S, Moss A. Changes in AIDS survival time in two San Francisco cohorts of homosexual men, 1983 to 1993. JAMA. 1994 Apr 13;271(14):1083-7. Erratum in: JAMA 1996 Nov 13;276(18):1472
29. Brockington A, Scott GR. Trends in survival of HIV infected patients attending the Department of Genito-Urinary Medicine, Royal Infirmary of Edinburgh. Scott Med J. 1997 Aug;42(4):114-5. doi: 10.1177/003693309704200405
30. Lee LM, Karon JM, Selik R, Neal JJ, Fleming PL. Survival after AIDS diagnosis in adolescents and adults during the treatment era, United States, 1984-1997. JAMA. 2001 Mar 14;285(10):1308-15. doi: 10.1001/jama.285.10.1308
31. Trickey A, Sabin CA, Burkholder G, Crane H, d'Arminio Monforte A, Egger M, Gill MJ, Grabar S, Guest JL, Jarrin I, Lampe FC, Obel N, Reyes JM, Stephan C, Sterling TR, Teira R, Touloumi G, Wasmuth JC, Wit F, Wittkop L, Zangerle R, Silverberg MJ, Justice A, Sterne JAC. Life expectancy after 2015 of adults with HIV on long-term antiretroviral therapy in Europe and North America: a collaborative analysis of cohort studies. Lancet HIV. 2023 May;10(5):e295-e307. doi: 10.1016/S2352-3018(23)00028-0. Epub 2023 Mar 20
32. Gueler A, Moser A, Calmy A, Günthard HF, Bernasconi E, Furrer H, Fux CA, Battegay M, Cavassini M, Vernazza P, Zwahlen M, Egger M; Swiss HIV Cohort Study, Swiss National Cohort. Life expectancy in HIV-positive persons in Switzerland: matched comparison with general population. AIDS. 2017 Jan 28;31(3):427-436. doi: 10.1097/QAD.0000000000001335
33. UNAIDS. UNAIDS fact sheet 2025. Geneva: Joint United Nations Programme on HIV/AIDS (UNAIDS); 2025.
34. Deeks SG, Lewin SR, Havlir DV. The end of AIDS: HIV infection as a chronic disease. Lancet. 2013 Nov 2;382(9903):1525-33. doi: 10.1016/S0140-6736(13)61809-7. Epub 2013 Oct 23
35. Cohen MS, Chen YQ, McCauley M, Gamble T, Hosseinipour MC, Kumarasamy N, Hakim JG, Kumwenda J, Grinsztejn B, Pilotto JH, Godbole SV, Mehendale S, Chariyalertsak S, Santos BR, Mayer KH, Hoffman IF, Eshleman SH, Piwowar-Manning E, Wang L, Makhema J, Mills LA, de Bruyn G, Sanne I, Eron J, Gallant J, Havlir D, Swindells S, Ribaudo H, Elharrar V, Burns D, Taha TE, Nielsen-Saines K, Celentano D, Essex M, Fleming TR; HPTN 052 Study Team. Prevention of HIV-1 infection with early antiretroviral therapy. N Engl J Med. 2011 Aug 11;365(6):493-505. doi: 10.1056/NEJMoa1105243. Epub 2011 Jul 18

36. Rodger AJ, Cambiano V, Bruun T, Vernazza P, Collins S, Degen O, Corbelli GM, Estrada V, Geretti AM, Beloukas A, Raben D, Coll P, Antinori A, Nwokolo N, Rieger A, Prins JM, Blaxhult A, Weber R, Van Eeden A, Brockmeyer NH, Clarke A, Del Romero Guerrero J, Raffi F, Bogner JR, Wandeler G, Gerstoft J, Gutiérrez F, Brinkman K, Kitchen M, Ostergaard L, Leon A, Ristola M, Jessen H, Stellbrink HJ, Phillips AN, Lundgren J; PARTNER Study Group. Risk of HIV transmission through condomless sex in serodifferent gay couples with the HIV-positive partner taking suppressive antiretroviral therapy (PARTNER): final results of a multicentre, prospective, observational study. Lancet. 2019 Jun 15;393(10189):2428-2438. doi: 10.1016/S0140-6736(19)30418-0. Epub 2019 May 2
37. UNAIDS. Undetectable = Untransmittable (U=U): Public health and HIV prevention. UNAIDS; 2018.
38. Finzi D, Hermankova M, Pierson T, Carruth LM, Buck C, Chaisson RE, Quinn TC, Chadwick K, Margolick J, Brookmeyer R, Gallant J, Markowitz M, Ho DD, Richman DD, Siliciano RF. Identification of a reservoir for HIV-1 in patients on highly active antiretroviral therapy. Science. 1997 Nov 14;278(5341):1295-300. doi: 10.1126/science.278.5341.1295
39. Siliciano JD, Kajdas J, Finzi D, Quinn TC, Chadwick K, Margolick JB, Kovacs C, Gange SJ, Siliciano RF. Long-term follow-up studies confirm the stability of the latent reservoir for HIV-1 in resting CD4+ T cells. Nat Med. 2003 Jun;9(6):727-8. doi: 10.1038/nm880. Epub 2003 May 18
40. Chun TW, Fauci AS. HIV reservoirs: pathogenesis and obstacles to viral eradication and cure. AIDS. 2012 Jun 19;26(10):1261-8. doi: 10.1097/QAD.0b013e328353f3f1
41. Zhu P, Liu J, Bess J Jr, Chertova E, Lifson JD, Grisé H, Ofek GA, Taylor KA, Roux KH. Distribution and three-dimensional structure of AIDS virus envelope spikes. Nature. 2006 Jun 15;441(7095):847-52. doi: 10.1038/nature04817. Epub 2006 May 24
42. Haseltine W.A. - Molecular Biology of the human immunodeficiency virus type 1- FASEB J. 1991; 5(10):2349-60 – doi: 10.1096/fasebj.5.10.1829694.
43. Merk A., Subramaniam S. - HIV-1 envelope glycoprotein structure - Curr Opin Struct Biol. 2013 Apr; 23(2): 268–276. doi:10.1016/j.sbi.2013.03.007.
44. Frank GA., Narayan K., Bess JW., Del Prete GQ., Wu X., Moran Am., Hartnell LM., Earl LA., Lifson JD. Subramaniam S. - Maturation of the HIV-1 core by a non-diffusional phase transition – Nat Commun 2015 Jan 8; 6:5854 – doi: 10.1038/ncomms6854.
45. Sundquist WI, Kräusslich HG. HIV-1 assembly, budding, and maturation. Cold Spring Harb Perspect Med. 2012 Jul;2(7):a006924. doi: 10.1101/cshperspect.a006924. Erratum in: Cold Spring Harb Perspect Med. 2012 Aug;2(8). doi: 10.1101/cshperspect.a015420
46. Proulx J, Ghaly M, Park IW, Borgmann K. HIV-1-Mediated Acceleration of Oncovirus-Related Non-AIDS-Defining Cancers. Biomedicines. 2022 Mar 25;10(4):768. doi: 10.3390/biomedicines10040768
47. Reitz MS Jr, Gallo RC. Retroviridae: Human immunodeficiency viruses. In: Bennett JE, Dolin R, Blaser MJ, editors. Mandell, Douglas, and Bennett's Principles and Practice of Infectious Diseases. 9th ed. Philadelphia: Elsevier; 2020. p. 2202–2210.
48. Flexner C. HIV-protease inhibitors. N Engl J Med. 1998;338:1281–1292
49. Bukrinsky MI, Sharova N, McDonald TL, et al. Association of integrase, matrix, and reverse transcriptase antigens of human immunodeficiency virus type 1 with viral nucleic acids following acute infection. Proc Natl Acad Sci USA. 1993;90:6125–6129

50. Starcich BR, Hahn BH, Shaw GM, et al. Identification and characterization of conserved and variable regions in the envelope gene of HTLV-III/LAV, the retrovirus of AIDS. Cell. 1986;45:637–648
51. White JM. Membrane fusion. Science. 1992;258:917–924
52. Emerman M, Malim MH. HIV-1 regulatory/accessory genes: keys to unraveling viral and host cell biology. Science. 1998;280:1880–1884
53. Kawakami K, Scheidereit C, Roeder RG. Identification and purification of a human immunoglobulin-enhancer-binding protein (NF-kappa B) that activates transcription from a human immunodeficiency virus type 1 promoter in vitro. Proc Natl Acad Sci USA. 1988;85:4700–4704
54. Jones KA, Peterlin BM. Control of RNA initiation and elongation at the HIV-1 promoter. Annu Rev Biochem. 1994;63:717–743
55. Maddon PJ, McDougal JS, Clapham PR, et al. HIV infection does not require endocytosis of its receptor, CD4. Cell. 1988;54:865–874
56. Gartner S, Markovits P, Markovitz DM, et al. The role of mononuclear phagocytes in HTLV-III/LAV infection. Science. 1986;233:215–219
57. Feng Y, Broder CC, Kennedy PE, et al. HIV-1 entry cofactor: functional cDNA cloning of a seven- transmembrane, G protein-coupled receptor. Science. 1996;272:872–877
58. Alkhatib G, Combadiere C, Broder CC, et al. CC CKR5: a RANTES, MIP-1alpha, MIP-1beta receptor as a fusion cofactor for macrophage-tropic HIV-1. Science. 1996;272:1955–1958
59. Choe H, Farzan M, Sun Y, et al. The beta-chemokine receptors CCR3 and CCR5 facilitate infection by primary HIV-1 isolates. Cell. 1996;85:1135–1148
60. Deng H, Liu R, Ellmeier W, et al. Identification of a major co-receptor for primary isolates of HIV-1. Nature. 1996;381:661–666
61. Dragic T, Litwin V, Allaway GP, et al. HIV-1 entry into CD4+ cells is mediated by the chemokine receptor CC-CKR-5. Nature. 1996;381:667–673
62. O'Brien TR, Goedert JJ. Chemokine receptors and genetic variability: another leap in HIV research. JAMA. 1998;279:317–318
63. Misrahi M, Teglas JP, N'Go N, et al. CCR5 chemokine receptor variant in HIV-1 mother-to-child transmission and disease progression in children. French Pediatric HIV Infection Study Group. JAMA. 1998;279:277–280
64. Wei X, Ghosh SK, Taylor ME, et al. Viral dynamics in human immunodeficiency virus type 1 infection. Nature. 1995;373:117–122
65. Hutter G, Nowak D, Mossner M, et al. Long-term control of HIV by CCR5 Delta32/Delta32 stem-cell transplantation. N Engl J Med. 2009;360:692–698
66. Wyatt R, Sodroski J. The HIV-1 envelope glycoproteins: fusogens, antigens, and immunogens. Science. 1998;280:1884–1888
67. Reitter JN, Means RE, Desrosiers RC. A role for carbohydrates in immune evasion in AIDS. Nat Med. 1998;4:679–684
68. Ward AB, Wilson IA. Insights into the trimeric HIV-1 envelope glycoprotein structure. Trends Biochem Sci. 2015;40:101–107
69. Braaten D, Franke EK, Luban J. Cyclophilin A is required for an early step in the life cycle of human immunodeficiency virus type 1 before the initiation of reverse transcription. J Virol. 1996;70:3551–3560
70. Peliska JA, Benkovic SJ. Mechanism of DNA strand transfer reactions catalyzed by HIV-1 reverse transcriptase. Science. 1992;258:1112–1118

71. Shcherbatova O, Grebennikov D, Sazonov I, Meyerhans A, Bocharov G. Modeling of the HIV-1 Life Cycle in Productively Infected Cells to Predict Novel Therapeutic Targets. Pathogens. 2020; 9(4):255. https://doi.org/10.3390/pathogens9040255
72. Sarafianos SG., Marchand B., Das K., Himmel D., Parniak MA., Hughes SH., Arnold E. - Structure and function of HIV-1 reverse transcriptase: molecular mechanisms of polymerization and inhibition - J Mol Biol. 2009 Jan 23; 385(3): 693–713.- doi: 10.1016/j.jmb.2008.10.071.
73. Laguette N, Sobhian B, Casartelli N, et al. SAMHD1 is the - and myeloid-cell-specific HIV-1 restriction factor counteracted by Vpx. Nature. 2011;474(7353):654-657. doi:10.1038/nature10117
74. Ahn J, Hao C, Yan J, et al. HIV/simian immunodeficiency virus (SIV) accessory virulence factor Vpx loads the host cell restriction factor SAMHD1 onto the E3 ubiquitin ligase complex CRL4DCAF1. J Biol Chem. 2012;287(15):12550-12558. doi:10.1074/jbc.M112.340711. PMID: 22362772
75. Hofmann H, Logue EC, Bloch N, et al. The Vpx lentiviral accessory protein targets SAMHD1 for degradation in the nucleus. J Virol. 2012;86(23):12552-12560. doi:10.1128/JVI.01657-12
76. Fassati A 2006. HIV infection of non-dividing cells: A divisive problem. Retrovirology 3: 74
77. Lee K, Ambrose Z, Martin TD, Oztop I, Mulky A, Julias JG, Vandegraaff N, Baumann JG, Wang R, Yuen W, et al. 2010. Flexible use of nuclear import pathways by HIV-1. Cell Host Microbe 7: 221–233
78. Cara A, Guarnaccia F, Reitz MS, et al. Self-limiting, cell type-dependent replication of an integrase-defective human immunodeficiency virus type 1 in human primary macrophages but not T lymphocytes. Virology. 1995;208:242–248
79. Wiskerchen M, Muesing MA. Human immunodeficiency virus type 1 integrase: effects of mutations on viral ability to integrate, direct viral gene expression from unintegrated viral DNA templates, and sustain viral propagation in primary cells. J Virol. 1995;69:376–386
80. Schroder AR, Shinn P, Chen H, et al. HIV-1 integration in the human genome favors active genes and local hotspots. Cell. 2002;110:521–529
81. Hare S, Gupta SS, Valkov E, Engelman A, Cherepanov P 2010. Retroviral intasome assembly and inhibition of DNA strand transfer. Nature 464: 232–236
82. Maertens GN, Hare S, Cherepanov P 2010. The mechanism of retroviral integration from X-ray structures of its key intermediates. Nature 468: 326–329
83. Engelman A, Mizuuchi K, Craigie R 1991. HIV-1 DNA integration: Mechanism of viral DNA cleavage and DNA strand transfer. Cell 67: 1211–1221
84. Mizuuchi K, Adzuma K 1991. Inversion of the phosphate chirality at the target site of Mu-DNA strand transfer—Evidence for a one-step transesterification mechanism. Cell 66: 129–140
85. Daniel R, Katz RA, Skalka AM 1999. A role for DNA-PK in retroviral DNA integration. Science 284: 644–647
86. Yoder K, Bushman FD 2000. Repair of gaps in retroviral DNA integration intermediates. J Virol 74: 11191–11200
87. Campbell EM, Hope TJ. HIV-1 capsid: the multifaceted key player in HIV-1 infection. Nat Rev Microbiol. 2015 Aug;13(8):471-83. doi: 10.1038/nrmicro3503
88. Lusic M, Siliciano RF. Nuclear landscape of HIV-1 infection and integration. Nat Rev Microbiol. 2017 Feb;15(2):69-82. doi: 10.1038/nrmicro.2016.162. Epub 2016 Dec 12. Erratum in: Nat Rev Microbiol. 2017 Feb 27. doi: 10.1038/nrmicro.2017.22

89. Jordan A, Defechereux P, Verdin E 2001. The site of HIV-1 integration in the human genome determines basal transcriptional activity and response to Tat transactivation. EMBO J 20: 1726–1738
90. Lewinski M, Bisgrove D, Shinn P, Chen H, Verdin E, Berry CC, Ecker JR, Bushman FD 2005. Genome-wide analysis of chromosomal features repressing HIV transcription. J Virol 79: 6610–6619
91. Cherepanov P, Maertens G, Proost P, Devreese B, Van Beeumen J, Engelborghs Y, De Clercq E, Debyser Z 2003. HIV-1 integrase forms stable tetramers and associates with LEDGF/p75 protein in human cells. J Biol Chem 278: 372–381
92. Ciuffi A, Llano M, Poeschla E, Hoffmann C, Leipzig J, Shinn P, Ecker JR, Bushman F 2005. A role for LEDGF/p75 in targeting HIV DNA integration. Nat Med 11: 1287–1289
93. Marshall H, Ronen K, Berry C, Llano M, Sutherland H, Saenz D, Bickmore W, Poeschla E, Bushman F 2007. Role of PSIP1/LEDGF/p75 in lentiviral infectivity and integration targeting. PLoS One 2: e1340 10.1371/journal.pone.0001340
94. Lee MS, Craigie R 1998. Protection of retroviral DNA from autointegration: Involvement of a cellular factor. Proc Natl Acad Sci 95: 1528–1533
95. Varmus H. Retroviruses. Science. 1988 Jun 10;240(4858):1427-35. doi: 10.1126/science.3287617
96. Coffin JM, Hughes SH, Varmus HE 1997. Retroviruses. Cold Spring Harbor Laboratory Press, Cold Spring Harbor, NY:
97. Honda Y, Rogers L, Nakata K, et al. Type I interferon induces inhibitory 16-kD CCAAT/enhancer binding protein (C/EBP)β, repressing the HIV-1 long terminal repeat in macrophages: pulmonary tuberculosis alters C/EBP expression, enhancing HIV-1 replication. J Exp Med. 1998;188(7):1255-1265. doi:10.1084/jem.188.7.1255
98. Kawakami K, Scheidereit C, Roeder RG. Identification and purification of a human immunoglobulin-enhancer-binding protein (NF-κB) that activates transcription from a human immunodeficiency virus type 1 promoter in vitro. Proc Natl Acad Sci U S A. 1988;85:4700–4704
99. Kim SY, Byrn R, Groopman J, et al. Temporal aspects of DNA and RNA synthesis during human immunodeficiency virus infection: evidence for differential gene expression. J Virol. 1989;63:3708–3713
100. ME, Kim SY, Buchbinder A, et al. Kinetics of expression of multiply spliced RNA in early human immunodeficiency virus type 1 infection of lymphocytes and monocytes. Proc Natl Acad Sci U S A. 1992;89:1148
101. Robert-Guroff M, Popovic M, Gartner S, et al. Structure and expression of tat-, rev-, and nef-specific transcripts of human immunodeficiency virus type 1 in infected lymphocytes and macrophages. J Virol. 1990;64:3391–3398
102. Liao Z, Cimakasky LM, Hampton R, et al. Lipid rafts and HIV pathogenesis: host membrane cholesterol is required for infection by HIV type 1. AIDS Res Hum Retroviruses. 2001;17:1009–1019
103. Freed EO. HIV-1 assembly, release and maturation. Nat Rev Microbiol. 2015 Aug;13(8):484-96. doi: 10.1038/nrmicro3490. Epub 2015 Jun 29
104. Douek DC, Picker LJ, Koup RA. T cell dynamics in HIV-1 infection. *Annu Rev Immunol.* 2003;21:265–304
105. Fanales-Belasio E., Raimondo M., Suligoi B., Stefano Buttò S. - HIV virology and pathogenetic mechanisms of infection: a brief overview - Ann Ist Super Sanità 2010 - Vol. 46, No.1: 5-14 - doi: 10.4415/ANN_10_01_02.

106. Santoro MM., Perno CF. - HIV-1 Genetic Variability and Clinical Implications - ISRN Microbiol. 2013; 2013: 481314 – doi: 10.1155/2013/481314.
107. Coffin JM. HIV population dynamics in vivo: implications for genetic variation, pathogenesis, and therapy. Science. 1995;267(5197):483-489. doi:10.1126/science.7824947
108. Ho DD, Neumann AU, Perelson AS, et al. Rapid turnover of plasma virions and CD4 lymphocytes in HIV-1 infection. Nature. 1995;373:123–126
109. Pakker NG, Notermans DW, de Boer RJ, et al. Biphasic kinetics of peripheral blood T cells after triple combination therapy in HIV-1 infection: a composite of redistribution and proliferation. Nat Med. 1998;4:208–214
110. Mohri H, Bonhoeffer S, Monard S, et al. Rapid turnover of T lymphocytes in SIV-infected rhesus macaques. Science. 1998;279:1223–1227
111. Herbein G, Mahlknecht U, Batliwalla F, et al. Apoptosis of CD8+ T cells is mediated by macrophages through interaction of HIV gp120 with chemokine receptor CXCR4. Nature. 1998;395:189–194
112. Zagury D. A naturally unbalanced combat [new; comment]. Nat Med. 1997;3:156–157
113. Gulick RM, Mellors JW, Havlir D, et al. Treatment with indinavir, zidovudine, and lamivudine in adults with human immunodeficiency virus infection and prior antiretroviral therapy. N Engl J Med. 1997;337:734–739
114. Gougeon ML, Garcia S, Heeney J, et al. Programmed cell death in AIDS-related HIV and SIV infections. AIDS Res Hum Retroviruses. 1993;9:553–563
115. Oyaizu N, McCloskey TW, Coronesi M, et al. Accelerated apoptosis in peripheral blood mononuclear cells from human immunodeficiency virus type 1–infected patients and in CD4 cross-linked PBMCs from normal individuals. Blood. 1993;82:3392–3400
116. Zagury D, Bernard J, Leonard R, et al. Long-term cultures of HTLV-III–infected T cells: a model of cytopathology of T-cell depletion in AIDS. Science. 1986;231:850–853.
117. McCutchan FE. Understanding the genetic diversity of HIV-1. AIDS. 2000;14 Suppl 3:S31–S44
118. Keele BF, Van HF, Li Y, et al. Chimpanzee reservoirs of pandemic and nonpandemic HIV-1. Science. 2006;313:523–526
119. Gilbert MT, Rambaut A, Wlasiuk G, et al. The emergence of HIV/AIDS in the Americas and beyond. Proc Natl Acad Sci USA. 2007;104:18566–18570
120. Wolinsky SM, Wike CM, Korber BT, et al. Selective transmission of human immunodeficiency virus type-1 variants from mothers to infants. Science. 1992;255:1134–1137
121. Keele BF, Giorgi EE, Salazar-Gonzalez JF, et al. Identification and characterization of transmitted and early founder virus envelopes in primary HIV-1 infection. Proc Natl Acad Sci USA. 2008;105:7552–7557
122. Simon V., Ho DD., Quarraisha AK. - HIV/AIDS epidemiology, pathogenesis, prevention, and treatment - Lancet. 2006 August 5; 368(9534): 489–504. doi:10.1016/S0140-6736(06)69157
123. Thippeshappa R., Ruan H., Kimata JT. – Breaking Barriers to an AIDS Model with Macaque-Tropic HIV-1 Derivatives - Biology 2012, 1(2), 134-164 – doi: 10.3390/biology1020134
124. Requejo HIZ. - Worldwide molecular epidemiology of HIV - Rev Saúde Pública 2006; 40 (2): 331-45 – doi: 10.1590/s0034-89102006000200023

125. McMichael AJ., Borrow P., Tomaras GD., Goonetilleke N., Haynes BF. – The immune response during acute HIV-1 infection: clues for vaccine development – Nat Rev Immunol. 2010; 10(1): 11-23 – doi: 10.1038/nri2674
126. McBrien JB., Kumar NA., Silvestri G. – Mechanisms of CD8+T cell-mediated suppression of HIV/SIV replication – Eur J Immunol 2018 Jun; 48(6): 898-914 – doi: 10.1002/eji.201747172
127. York A. – Undetectable equals untransmittable 2019 May 13; - Nature review microbiology – volume 17 – doi,org/10.1038/s41564-019-0455-0
128. Justiz Vaillant AA., Naik Roopa – HIV-1 Associated Opportunistic Infections - StatPearls Publishing 2021 Jan – Bookshelf ID: NBK5398787.
129. Altfeld M, Rosenberg ES, Shankarappa R, et al. Cellular immune responses and viral diversity in individuals treated during acute and early HIV-1 infection. J Exp Med. 2001;193:169–180
130. Wilson JD, Ogg GS, Allen RL, et al. Direct visualization of HIV-1-specific cytotoxic T lymphocytes during primary infection. AIDS. 2000;14:225–233
131. Appay V, Papagno L, Spina CA, et al. Dynamics of T cell responses in HIV infection. J Immunol. 2002;168:3660–3666
132. McRae B, Lange JA, Ascher MS, et al. Immune response to HIV p24 core protein during the early phases of human immunodeficiency virus infection. AIDS Res Hum Retroviruses. 1991;7:637–643
133. Cooper DA, Imrie AA, Penny R. Antibody response to human immunodeficiency virus after primary infection. J Infect Dis. 1987;155:1113–1118
134. Healey DS, Maskill WJ, Gust ID. Detection of anti-HIV immunoglobulin M by particle agglutination following acute HIV infection. AIDS. 1989;3:301–304
135. Horsburgh CR Jr, Ou CY, Jason J, et al. Duration of human immunodeficiency virus infection before detection of antibody. Lancet. 1989;2:637–640
136. Loveday C, Tedder RS. Enzyme-linked immunosorbent assays for the measurement of human immunodeficiency virus, type 1 reverse transcriptase antigen and antibodies. J Virol Methods. 1993;41:181–192
137. Constantine NT, van der Groen G, Belsey EM, et al. Sensitivity of HIV-antibody assays determined by seroconversion panels. AIDS. 1994;8:1715–1720
138. Aptima HIV-1 RNA qualitative package insert. 2006 [Gen-Probe, San Diego, CA].
139. U.S. Department of Health and Human Services, AIDS Information; FDA Talking Paper. FDA Approves First Nucleic Acid Test (NAT) System to Screen Whole Blood Donors for Infections With Human Immunodeficiency Virus (HIV and Hepatitis C Virus (HCV). https://aidsinfo.nih.gov/news/593/fda-approves-first-nucleic-acid-test–nat–system-to-screen-whole-blood-donors-for-infections-with-human-immunodeficiency-virus–hiv–and-hepatitis-c-virus–hcv-.
140. Centers for Disease Control and Prevention. Persistent lack of detectable HIV-1 antibody in a person with HIV infection–Utah, 1995. MMWR Morb Mortal Wkly Rep. 1996;45:181–185
141. Sullivan PS, Schable C, Koch W, et al. Persistently negative HIV-1 antibody enzyme immunoassay screening results for patients with HIV-1 infection and AIDS: serologic, clinical, and virologic results. Seronegative AIDS Clinical Study Group. AIDS. 1999;13:89–96
142. Barthel HR, Wallace DJ. False-positive human immunodeficiency virus testing in patients with lupus erythematosus. Semin Arthritis Rheum. 1993;23:1–7
143. Soriano V, Dronda F, Gonzalez-Lopez A, et al. HIV-1 causing AIDS and death in a seronegative individual. Vox Sang. 1994;67:410–411
144. Candotti D, Adu-Sarkodie Y, Davies F, et al. AIDS in an HIV-seronegative Ghanaian woman with intersubtype A/G recombinant HIV-1 infection. J Med Virol. 2000;62:1–8

145. Montagnier L, Brenner C, Chamaret S, et al. Human immunodeficiency virus infection and AIDS in a person with negative serology. J Infect Dis. 1997;175:955–959
146. Apetrei C, Tamalet C, Edlinger C, et al. Delayed HIV-1 seroconversion after antiretroviral therapy. AIDS. 1998;12:1935–1936
147. Chockalingam M, Clarke L, McCormack WM. HIV infection with negative serological tests: development of seropositivity in association with highly active antiretroviral therapy. AIDS Patient Care STDS. 2000;14:305–308
148. De Rossi A, Giaquinto C, Del Mistro A, et al. Onset of HIV-1 antibody production after highly active antiretroviral therapy in a seronegative HIV-1-infected child. AIDS. 2000;14:1284–1286
149. Morris L, Binley JM, Clas BA, et al. HIV-1 antigen-specific and -nonspecific B cell responses are sensitive to combination antiretroviral therapy. J Exp Med. 1998;188:233–245
150. Kenealy W, Reed D, Cybulski R, et al. Analysis of human serum antibodies to human immunodeficiency virus (HIV) using recombinant ENV and GAG antigens. AIDS Res Hum Retroviruses. 1987;3:95–105
151. Dawson GJ, Heller JS, Wood CA, et al. Reliable detection of individuals seropositive for the human immunodeficiency virus (HIV) by competitive immunoassays using Escherichia coli-expressed HIV structural proteins. J Infect Dis. 1988;157:149–155. PMID: 3275722
152. Ragni MV, O'Brien TA, Reed D, et al. Prognostic importance of antibodies to human immunodeficiency virus by recombinant immunoassay and Western blot techniques in HIV antibody-positive hemophiliacs. AIDS Res Hum Retroviruses. 1988;4:223–231
153. Higgins JR, Pedersen NC, Carlson JR. Detection and differentiation by sandwich enzyme-linked immunosorbent assay of human T-cell lymphotropic virus type III/lymphadenopathy-associated virus- and acquired immunodeficiency syndrome-associated retroviruslike clinical isolates. J Clin Microbiol. 1986;24:424–430
154. Beelaert G, Vercauteren G, Fransen K, et al. Comparative evaluation of eight commercial enzyme linked immunosorbent assays and 14 simple assays for detection of antibodies to HIV. J Virol Methods. 2002;105:197–206
155. Hall HI, Song R, Rhodes P, et al. Estimation of HIV incidence in the United States. JAMA. 2008;300:520–529
156. Makuwa M, Souquiere S, Niangui MT, et al. Reliability of rapid diagnostic tests for HIV variant infection. J Virol Methods. 2002;103:183–190
157. Brauer M, De Villiers JC, Mayaphi SH. Evaluation of the Determine fourth generation HIV rapid assay. J Virol Methods. 2013;189:180–183
158. Lyamuya EFAS, Urassa WK, Sufi J, et al. Evaluation of simple rapid HIV assays and development of national rapid HIV test algorithms in Dar es Salaam, Tanzania. BMC Infect Dis. 2009;9:19
159. Klarkowski DBWJ, Lokuge KM, Shanks L, et al. The evaluation of a rapid in situ HIV confirmation test in a programme with a high failure rate of the WHO HIV two-test diagnostic algorithm. PLoS ONE. 2009;4:e4351
160. O'Connell RJ, Merritt TM, Malia JA, et al. Performance of the OraQuick rapid antibody test for diagnosis of human immunodeficiency virus type 1 infection in patients with various levels of exposure to highly active antiretroviral therapy. J Clin Microbiol. 2003;41:2153–2155
161. Centers for Disease Control and Prevention. Progress toward strengthening blood transfusion services—14 countries, 2003-2007. MMWR Morb Mortal Wkly Rep. 2008;57:1273–1277.

162. Facente S, Dowling T, Vittinghoff E, et al. False-positive rate of rapid oral fluid HIV tests increases as kits near expiration date. [Present at the 16th Conference on Retroviruses and Opportunistic Infections. Montreal, Canada] 2009.
163. Gaines H, von Sydow M, Sonnerborg A, et al. Antibody response in primary human immunodeficiency virus infection. Lancet. 1987;1:1249–1253
164. Preiser W, Brink NS, Hayman A, et al. False-negative HIV antibody test results. J Med Virol. 2000;60:43–47
165. McAlpine L, Parry JV, Shanson D, et al. False negative results in enzyme linked immunosorbent assays using synthetic HIV antigens. J Clin Pathol. 1995;48:490–493. PMID: 7629300
166. Wai CT, Tambyah PA. False-positive HIV-1 ELISA in patients with hepatitis B. Am J Med. 2002;112:737
167. Pearlman ES, Ballas SK. False-positive human immunodeficiency virus screening test related to rabies vaccination. Arch Pathol Lab Med. 1994;118:805–806. PMID: 7605412
168. Plotkin SA, Loupi E, Blondeau C. False-positive human immunodeficiency virus screening test related to rabies vaccination. Arch Pathol Lab Med. 1995;119:679
169. Henderson S, Leibnitz G, Turnbull M, et al. False-positive human immunodeficiency virus seroconversion is not common following rabies vaccination. Clin Diagn Lab Immunol. 2002;9:942–943
170. U.S. Food and Drug Administration. (2025, July 3). FDA-approved HIV medicines. https://www.fda.gov/drugs/human-immunodeficiency-virus-hiv/hiv-treatment
171. Flexner C. HIV drug development: the next 25 years. Nat Rev Drug Discov. 2007 Dec;6(12):959-66. doi: 10.1038/nrd2336
172. Arts EJ, Hazuda DJ. HIV-1 antiretroviral drug therapy. Cold Spring Harb Perspect Med. 2012 Apr;2(4):a007161. doi: 10.1101/cshperspect.a007161
173. Engelman A, Cherepanov P. The structural biology of HIV-1: mechanistic and therapeutic insights. Nat Rev Microbiol. 2012 Mar 16;10(4):279-90. doi: 10.1038/nrmicro2747
174. Vogt VM. Retroviral Virions and Genomes. In: Coffin JM, Hughes SH, Varmus HE, editors. Retroviruses. Cold Spring Harbor (NY): Cold Spring Harbor Laboratory Press; 1997
175. Kemnic TR, Gulick PG. HIV Antiretroviral Therapy. 2022 Sep 20. In: StatPearls [Internet]. Treasure Island (FL): StatPearls Publishing; 2025 Jan–. PMID: 30020680.
176. European AIDS Clinical Society. (2025). EACS guidelines: Version 12.0. Retrieved from https://www.eacsociety.org/guidelines
177. Cohen JP, Wang X, Wade RL, Cuervo HD, Dionne DM. 1036. Persistence of Guideline-Recommended Antiretroviral Therapy Regimens among Persons Living with HIV Newly Initiating Treatment in the US. Open Forum Infect Dis. 2020 Dec 31;7(Suppl 1):S548–9. doi: 10.1093/ofid/ofaa439.1222
178. Siliciano RF, Greene WC. HIV latency. Cold Spring Harb Perspect Med. 2011 Sep;1(1):a007096. doi: 10.1101/cshperspect.a007096
179. Chun TW, Moir S, Fauci AS. HIV reservoirs as obstacles and opportunities for an HIV cure. Nat Immunol. 2015;16:584–589. https://doi.org/10.1038/ni.3152
180. Jonathan Z Li, Evgenia Aga, Ronald J Bosch, Mark Pilkinton, Eugène Kroon, Lynsay MacLaren, Michael Keefer, Lawrence Fox, Liz Barr, Edward Acosta, Jintanat Ananworanich, Robert Coombs, John W Mellors, Alan L Landay, Bernard Macatangay, Steven Deeks, Rajesh T Gandhi, Davey M Smith, AIDS Clinical Trials Group A5345 Study Team, Time to Viral Rebound After Interruption of Modern Antiretroviral Therapies,

Clinical Infectious Diseases, Volume 74, Issue 5, 1 March 2022, Pages 865–870, https://doi.org/10.1093/cid/ciab541

181. Castagna A, Muccini C, Galli L, et al. Analytical treatment interruption in chronic HIV-1 infection: time and magnitude of viral rebound in adults with 10 years of undetectable viral load and low HIV-DNA (APACHE study). J Antimicrob Chemother. 2019;74(7):2039–2046. doi: 10.1093/jac/dkz138
182. Harper J, Betts MR, Lichterfeld M, Müller-Trutwin M, Margolis D, Bar KJ, Li JZ, McCune JM, Lewin SR, Kulpa D, Diallo DD, Lederman MM, Paiardini M. Progress Note 2024: Curing HIV; Not in My Lifetime or Just Around the Corner? Pathog Immun. 2024 Mar 1;8(2):115-157. doi: 10.20411/pai.v8i2.665. Erratum in: Pathog Immun. 2024 Mar 12;8(2):179-222. doi: 10.20411/pai.v8i2.696
183. Chen J, Zhou T, Zhang Y, Luo S, Chen H, Chen D, Li C, Li W. The reservoir of latent HIV. Front Cell Infect Microbiol. 2022 Jul 28;12:945956. doi: 10.3389/fcimb.2022.945956
184. García M., López-Fernández L., Mínguez P., Morón-López S., Restrepo C., Navarrete-Muñoz M. A., et al. (2020). Transcriptional signature of resting-memory CD4 T cells differentiates spontaneous from treatment-induced HIV control. J. Mol. Med. (Berl) 98 (8), 1093–1105. doi: 10.1007/s00109-020-01930-x
185. O'Neil T. R., Hu K., Truong N. R., Arshad S., Shacklett B. L., Cunningham A. L., et al. (2021). The role of tissue resident memory CD4 T cells in herpes simplex viral and HIV infection. Viruses 13 (3):359. doi: 10.3390/v13030359
186. Schulze-Gahmen U., Hurley J. H. (2018). Structural mechanism for HIV-1 TAR loop recognition by tat and the super elongation complex. Proc. Natl. Acad. Sci. U.S.A. 115 (51), 12973–12978. doi: 10.1073/pnas.1806438115
187. Donahue D. A., Bastarache S. M., Sloan R. D., Wainberg M. A. (2013). Latent HIV-1 can be reactivated by cellular superinfection in a tat-dependent manner, which can lead to the emergence of multidrug-resistant recombinant viruses. J. Virol. 87 (17), 9620–9632. doi: 10.1128/jvi.01165-13
188. Pinto D. O., DeMarino C., Vo T. T., Cowen M., Kim Y., Pleet M. L., et al. (2020). Low-level ionizing radiation induces selective killing of HIV-1-Infected cells with reversal of cytokine induction using mTOR inhibitors. Viruses 12 (8):885. doi: 10.3390/v12080885
189. Saleh S., Solomon A., Wightman F., et al. (2007). CCR7 ligands CCL19 and CCL21 increase permissiveness of resting memory CD4+ T cells to HIV-1 infection: a novel model of HIV-1 latency. Blood 110 (13), 4161–4164. doi: 10.1182/blood-2007-06-097907
190. Wu Y. (2010). Chemokine control of HIV-1 infection: beyond a binding competition. Retrovirology 7, 86. doi: 10.1186/1742-4690-7-86
191. López-Huertas M. R., Morín M., Madrid-Elena N., Gutiérrez C., Jiménez-Tormo L., Santoyo J., et al. (2019). Selective miRNA modulation fails to activate HIV replication in in vitro latency models. Mol. Ther. Nucleic Acids 17, 323–336. doi: 10.1016/j.omtn.2019.06.006
192. Murray J. M., Zaunders J. J., McBride K. L., Xu Y., Bailey M., Suzuki K., et al. (2014). HIV DNA Subspecies persist in both activated and resting memory CD4+ T cells during antiretroviral therapy. J. Virol. 88 (6), 3516–3526. doi: 10.1128/jvi.03331-13
193. Zerbato J. M., Serrao E., Lenzi G., Kim B., Ambrose Z., Watkins S. C., et al. (2016). Establishment and reversal of HIV-1 latency in naive and central memory CD4+ T cells in vitro. J. Virol. 90 (18), 8059–8073. doi: 10.1128/jvi.00553-16

194. Corneau A., Cosma A., Even S., Katlama C., Le Grand R., Frachet V., et al. (2017). Comprehensive mass cytometry analysis of cell cycle, activation, and coinhibitory receptors expression in CD4 T cells from healthy and HIV-infected individuals. Cytom. B Clin. Cytom. 92 (1), 21–32. doi: 10.1002/cyto.b.21502
195. Terahara K., Iwabuchi R., Hosokawa M., Nishikawa Y., Takeyama H., Takahashi Y., et al. (2019). A CCR5(+) memory subset within HIV-1-infected primary resting CD4(+) T cells is permissive for replication-competent, latently infected viruses in vitro. BMC Res. Notes 12 (1), 242. doi: 10.1186/s13104-019-4281-5
196. Gálvez C., Grau-Expósito J., Urrea V., Clotet B., Falcó V., Buzón M. J., et al. (2021). Atlas of the HIV-1 reservoir in peripheral CD4 T cells of individuals on successful antiretroviral therapy. mBio 12 (6), e0307821. doi: 10.1128/mBio.03078-21
197. Lugli E., Gattinoni L., Roberto A., Mavilio D., Price D. A., Restifo N. P., et al. (2013). Identification, isolation and in vitro expansion of human and nonhuman primate T stem cell memory cells. Nat. Protoc. 8 (1), 33–42. doi: 10.1038/nprot.2012.143
198. Tabler CO, Lucera MB, Haqqani AA, McDonald DJ, Migueles SA, Connors M, Tilton JC. CD4+ memory stem cells are infected by HIV-1 in a manner regulated in part by SAMHD1 expression. J Virol. 2014;88(9):4976–4986. doi: 10.1128/JVI.00324-14
199. Cartwright E. K., Palesch D., Mavigner M., Paiardini M., Chahroudi A., Silvestri G.. (2016). Initiation of antiretroviral therapy restores CD4+ T memory stem cell homeostasis in simian immunodeficiency virus-infected macaques. J. Virol. 90 (15), 6699–6708. doi: 10.1128/jvi.00492-16
200. Venanzi Rullo E, Pinzone MR, Cannon L, Weissman S, Ceccarelli M, Zurakowski R, Nunnari G, O'Doherty U. Persistence of an intact HIV reservoir in phenotypically naive T cells. JCI Insight. 2020 Oct 15;5(20):e133157. doi: 10.1172/jci.insight.133157
201. Gibellini L., Pecorini S., De Biasi S., Bianchini E., Digaetano M., Pinti M., et al. (2017). HIV-DNA Content in different CD4+ T-cell subsets correlates with CD4+ cell : CD8+ cell ratio or length of efficient treatment. Aids 31 (10), 1387–1392. doi: 10.1097/qad.0000000000001510
202. Zerbato J. M., McMahon D. K., Sobolewski M. D., Mellors J. W., Sluis-Cremer N.. (2019). Naive CD4+ T cells harbor a Large inducible reservoir of latent, replication-competent human immunodeficiency virus type 1. Clin. Infect. Dis. 69 (11), 1919–1925. doi: 10.1093/cid/ciz108
203. Campbell G. R., Bruckman R. S., Chu Y. L., Trout R. N., Spector S.A.. (2018). SMAC mimetics induce autophagy-dependent apoptosis of HIV-1-Infected resting memory CD4+ T cells. Cell Host Microbe 24 (5), 689–702.e7. doi: 10.1016/j.chom.2018.09.007
204. Kwon K. J., Timmons A. E., Sengupta S., Simonetti F. R., Zhang H., Hoh R, et al. (2020). Different human resting memory CD4(+) T cell subsets show similar low inducibility of latent HIV-1 proviruses. Sci. Transl. Med. 12 (528), eaax6795. doi: 10.1126/scitranslmed.aax6795
205. Morris J. H., 3rd, Valente S. T. (2020). Block-And-Lock: New horizons for a cure for HIV-1. Viruses 12 (12). doi: 10.3390/v12121443
206. Chun T. W., Davey R. T., Jr., Ostrowski M., Shawn Justement J., Engel D., Mullins J. I., et al. (2000). Relationship between pre-existing viral reservoirs and the re-emergence of plasma viremia after discontinuation of highly active anti-retroviral therapy. Nat. Med. 6 (7), 757–761. doi: 10.1038/77481
207. Burdo T. H. (2019). Editor's commentary for special issue: "The role of macrophages in HIV persistence". J. Neuroimmun. Pharmacol. 14 (1), 2–5. doi: 10.1007/s11481-019-09836-3

208. Kristoff J., Rinaldo C. R., Mailliard R. B. (2019). Role of dendritic cells in exposing latent HIV-1 for the kill. Viruses 12 (1), 32. doi: 10.3390/v12010037
209. Veenhuis R. T., Clements J. E., Gama L. (2019). HIV Eradication strategies: Implications for the central nervous system. Curr. HIV/AIDS Rep. 16 (1), 96–104. doi: 10.1007/s11904-019-00428-7
210. Veenhuis, R.T., Abreu, C.M., Costa, P.A.G. et al. Monocyte-derived macrophages contain persistent latent HIV reservoirs. Nat Microbiol 8, 833–844 (2023). https://doi.org/10.1038/s41564-023-01349-3
211. Ferreira EA, Clements JE, Veenhuis RT. HIV-1 Myeloid Reservoirs - Contributors to Viral Persistence and Pathogenesis. Curr HIV/AIDS Rep. 2024 Apr;21(2):62-74. doi: 10.1007/s11904-024-00692-2. Epub 2024 Feb 27
212. Clain JA, Rabezanahary H, Racine G, Boutrais S, Soundaramourty C, Joly Beauparlant C, Jenabian MA, Droit A, Ancuta P, Zghidi-Abouzid O, Estaquier J. Early ART reduces viral seeding and innate immunity in liver and lungs of SIV-infected macaques. JCI Insight. 2023 Jul 24;8(14):e167856. doi: 10.1172/jci.insight.167856
213. Saini M, Potash MJ. Chronic, highly productive HIV infection in monocytes during supportive culture. Curr HIV Res. 2014;12(5):317-24. doi: 10.2174/1570162x1205141121100659
214. Lee B, Sharron M, Montaner LJ, Weissman D, Doms RW. Quantification of CD4, CCR5, and CXCR4 levels on lymphocyte subsets, dendritic cells, and differentially conditioned monocyte-derived macrophages. Proc Natl Acad Sci U S A. 1999 Apr 27;96(9):5215-20. doi: 10.1073/pnas.96.9.5215
215. Kruize Z, Kootstra NA. The Role of Macrophages in HIV-1 Persistence and Pathogenesis. Front Microbiol. 2019 Dec 5;10:2828. doi: 10.3389/fmicb.2019.02828
216. Abreu C. M., Veenhuis R. T., Avalos C. R., Graham S., Parrilla D. R., Ferreira E. A., et al. (2019. a). Myeloid and CD4 T cells comprise the latent reservoir in antiretroviral therapy-suppressed SIVmac251-infected macaques. mBio 10 (4):e00065-19. doi: 10.1128/mBio.01659-19
217. Abreu C. M., Veenhuis R. T., Avalos C. R., Graham S., Queen S. E., Shirk E. N., et al. (2019. b). Infectious virus persists in CD4(+) T cells and macrophages in antiretroviral therapy-suppressed simian immunodeficiency virus-infected macaques. J. Virol. 93 (15):e00065–19. doi: 10.1128/jvi.00065-19
218. Martín-Moreno A, Muñoz-Fernández MA. Dendritic Cells, the Double Agent in the War Against HIV-1. Front Immunol. 2019 Oct 23;10:2485. doi: 10.3389/fimmu.2019.02485
219. McDonald D., Wu L., Bohks S. M., KewalRamani V. N., Unutmaz D., Hope T. J., et al. (2003). Recruitment of HIV and its receptors to dendritic cell-T cell junctions. Science 300 (5623), 1295–1297. doi: 10.1126/science.1084238
220. Carter C. C., Onafuwa-Nuga A., McNamara L. A., Riddell J., Bixby D., Savona M. R., et al. (2010). HIV-1 infects multipotent progenitor cells causing cell death and establishing latent cellular reservoirs. Nat. Med. 16 (4), 446–451. doi: 10.1038/nm.2109
221. McNamara L. A., Onafuwa-Nuga A., Sebastian N. T., Riddell J., Bixby D., Collins K.L. (2013). CD133+ hematopoietic progenitor cells harbor HIV genomes in a subset of optimally treated people with long-term viral suppression. J. Infect. Dis. 207 (12), 1807–1816. doi: 10.1093/infdis/jit118

222. Li G., Zhao J., Cheng L., Jiang Q., Kan S., Qin E., et al. (2017). HIV-1 infection depletes human CD34+CD38- hematopoietic progenitor cells via pDC-dependent mechanisms. PLoS Pathog. 13 (7), e1006505. doi: 10.1371/journal.ppat.1006505
223. Carter C. C., McNamara L. A., Onafuwa-Nuga A., Shackleton M., Riddell J., Bixby D., et al. (2011). HIV-1 utilizes the CXCR4 chemokine receptor to infect multipotent hematopoietic stem and progenitor cells. Cell Host Microbe 9 (3), 223–234. doi: 10.1016/j.chom.2011.02.005
224. Guttenplan K. A., Liddelow S. A. (2019). Astrocytes and microglia: Models and tools. J. Exp. Med. 216 (1), 71–83. doi: 10.1084/jem.20180200
225. Valdebenito S, Castellano P, Ajasin D, Eugenin EA. Astrocytes are HIV reservoirs in the brain: A cell type with poor HIV infectivity and replication but efficient cell-to-cell viral transfer. J Neurochem. 2021 Jul;158(2):429-443. doi: 10.1111/jnc.15336. Epub 2021 Mar 22
226. Ganesan M., Poluektova L. Y., Kharbanda K. K., Osna N. A. (2018). Liver as a target of human immunodeficiency virus infection. World J. Gastroenterol. 24 (42), 4728–4737. doi: 10.3748/wjg.v24.i42.4728
227. Katuri A., Bryant J. L., Patel D., Patel V., Andhavarapu S., Asemu G., et al. (2019). HIVAN associated tubular pathology with reference to ER stress, mitochondrial changes, and autophagy. Exp. Mol. Pathol. 106, 139–148. doi: 10.1016/j.yexmp.2018.12.009
228. Cohn L. B., Chomont N., Deeks S. G. (2020). The biology of the HIV-1 latent reservoir and implications for cure strategies. Cell Host Microbe 27 (4), 519–530. doi: 10.1016/j.chom.2020.03.014
229. Falcinelli SD, Ceriani C, Margolis DM, Archin NM. New Frontiers in Measuring and Characterizing the HIV Reservoir. Front Microbiol. 2019 Dec 18;10:2878. doi: 10.3389/fmicb.2019.02878
230. Pieren DKJ, Benítez-Martínez A, Genescà M. Targeting HIV persistence in the tissue. Curr Opin HIV AIDS. 2024 Mar 1;19(2):69-78. doi: 10.1097/COH.0000000000000836. Epub 2024 Jan 8
231. Estes J. D., Kityo C., Ssali F., Swainson L., Makamdop K. N., Del Prete G. Q., et al. (2017). Defining total-body AIDS-virus burden with implications for curative strategies. Nat. Med. 23 (11), 1271–1276. doi: 10.1038/nm.4411
232. Ikeogu N, Ajibola O, Zayats R, Murooka TT. Identifying physiological tissue niches that support the HIV reservoir in T cells. mBio. 2023 Oct 31;14(5):e0205323. doi: 10.1128/mbio.02053-23. Epub 2023 Sep 25
233. Connick E., Folkvord J. M., Lind K. T., Rakasz E. G., Miles B., Wilson N. A., et al. (2014). Compartmentalization of simian immunodeficiency virus replication within secondary lymphoid tissues of rhesus macaques is linked to disease stage and inversely related to localization of virus-specific CTL. J. Immunol. 193 (11), 5613–5625. doi: 10.4049/jimmunol.1401161
234. Fukazawa Y., Lum R., Okoye A. A., Park H., Matsuda K., Bae J. Y., et al. (2015). B cell follicle sanctuary permits persistent productive simian immunodeficiency virus infection in elite controllers. Nat. Med. 21 (2), 132–139. doi: 10.1038/nm.3781
235. Chaillon A., Gianella S., Dellicour S., Rawlings S. A., Schlub T. E., De Oliveira M. F., et al. (2020). HIV Persists throughout deep tissues with repopulation from multiple anatomical sources. J. Clin. Invest. 130 (4), 1699–1712. doi: 10.1172/jci134815
236. Fletcher C. V., Staskus K., Wietgrefe S. W., Rothenberger M., Reilly C., Chipman J. G., et al. (2014). Persistent HIV-1 replication is associated with lower antiretroviral

drug concentrations in lymphatic tissues. Proc. Natl. Acad. Sci. U.S.A. 111 (6), 2307–2312. doi: 10.1073/pnas.1318249111

237. Kalada W, Cory TJ. The Importance of Tissue Sanctuaries and Cellular Reservoirs of HIV-1. Curr HIV Res. 2022 Aug 12;20(2):102-110. doi: 10.2174/1570162X20666211227161237

238. Deleage C., Moreau M., Rioux-Leclercq N., Ruffault A., Jégou B., Dejucq-Rainsford N.. (2011). Human immunodeficiency virus infects human seminal vesicles in vitro and in vivo. Am. J. Pathol. 179 (5), 2397–2408. doi: 10.1016/j.ajpath.2011.08.005

239. Ganor Y., Zhou Z., Bodo J., Tudor D., Leibowitch J., Mathez D., et al. (2013). The adult penile urethra is a novel entry site for HIV-1 that preferentially targets resident urethral macrophages. Mucosal Immunol. 6 (4), 776–786. doi: 10.1038/mi.2012.116

240. Damouche A., Lazure T., Avettand-Fènoël V., Huot N., Dejucq-Rainsford N., Satie A. P., et al. (2015). Adipose tissue is a neglected viral reservoir and an inflammatory site during chronic HIV and SIV infection. PloS Pathog. 11 (9), e1005153. doi: 10.1371/journal.ppat.1005153

241. Cribbs S. K., Lennox J., Caliendo A. M., Brown L. A., Guidot D.M.. (2015). Healthy HIV-1-infected individuals on highly active antiretroviral therapy harbor HIV-1 in their alveolar macrophages. AIDS Res. Hum. Retroviruses 31 (1), 64–70. doi: 10.1089/aid.2014.0133

242. Ganor Y., Real F., Sennepin A., Dutertre C. A., Prevedel L., Xu L., et al. (2019). HIV-1 reservoirs in urethral macrophages of patients under suppressive antiretroviral therapy. Nat. Microbiol. 4 (4), 633–644. doi: 10.1038/s41564-018-0335-z

243. Cantero-Pérez J., Grau-Expósito J., Serra-Peinado C., Rosero D. A., Luque-Ballesteros L., Astorga-Gamaza A., et al. (2019). Resident memory T cells are a cellular reservoir for HIV in the cervical mucosa. Nat. Commun. 10 (1), 4739. doi: 10.1038/s41467-019-12732-2

244. Whitney JB, Hill AL, Sanisetty S, Penaloza-MacMaster P, Liu J, Shetty M, Parenteau L, Cabral C, Shields J, Blackmore S, Smith JY, Brinkman AL, Peter LE, Mathew SI, Smith KM, Borducchi EN, Rosenbloom DI, Lewis MG, Hattersley J, Li B, Hesselgesser J, Geleziunas R, Robb ML, Kim JH, Michael NL, Barouch DH. Rapid seeding of the viral reservoir prior to SIV viraemia in rhesus monkeys. Nature. 2014 Aug 7;512(7512):74-7. doi: 10.1038/nature13594. Epub 2014 Jul 20

245. Henrich TJ, Hatano H, Bacon O, Hogan LE, Rutishauser R, Hill A, Kearney MF, Anderson EM, Buchbinder SP, Cohen SE, Abdel-Mohsen M, Pohlmeyer CW, Fromentin R, Hoh R, Liu AY, McCune JM, Spindler J, Metcalf-Pate K, Hobbs KS, Thanh C, Gibson EA, Kuritzkes DR, Siliciano RF, Price RW, Richman DD, Chomont N, Siliciano JD, Mellors JW, Yukl SA, Blankson JN, Liegler T, Deeks SG. HIV-1 persistence following extremely early initiation of antiretroviral therapy (ART) during acute HIV-1 infection: An observational study. PLoS Med. 2017 Nov 7;14(11):e1002417. doi: 10.1371/journal.pmed.1002417

246. Archin NM, Liberty AL, Kashuba AD, Choudhary SK, Kuruc JD, Crooks AM, Parker DC, Anderson EM, Kearney MF, Strain MC, Richman DD, Hudgens MG, Bosch RJ, Coffin JM, Eron JJ, Hazuda DJ, Margolis DM. Administration of vorinostat disrupts HIV-1 latency in patients on antiretroviral therapy. Nature. 2012 Jul 25;487(7408):482-5. doi: 10.1038/nature11286. Erratum in: Nature. 2012 Sep 20;489(7416):460

247. Deeks S. Shock and kill. Nature 487, 439–440 (2012) https://doi.org/10.1038/487439a

248. Margolis DM, Garcia JV, Hazuda DJ, Haynes BF. Latency reversal and viral clearance to cure HIV-1. Science. 2016 Jul 22;353(6297):aaf6517. doi: 10.1126/science.aaf6517
249. Sengupta S, Siliciano RF. Targeting the Latent Reservoir for HIV-1. Immunity. 2018 May 15;48(5):872-895. doi: 10.1016/j.immuni.2018.04.030
250. Tioka L, Diez RC, Sönnerborg A, van de Klundert MAA. Latency Reversing Agents and the Road to an HIV Cure. Pathogens. 2025 Feb 27;14(3):232. doi: 10.3390/pathogens14030232
251. Sun SC. Non-canonical NF-κB signaling pathway. Cell Res. 2011 Jan;21(1):71-85. doi: 10.1038/cr.2010.177. Epub 2010 Dec 21. PMID: 21173796; PMCID: PMC3193406.
252. Manning BD, Cantley LC. AKT/PKB signaling: navigating downstream. Cell. 2007 Jun 29;129(7):1261-74. doi: 10.1016/j.cell.2007.06.009
253. Spina C.A., Anderson J., Archin N.M., Bosque A., Chan J., Famiglietti M., Greene W.C., Kashuba A., Lewin S.R., Margolis D.M., et al. An In-Depth Comparison of Latent HIV-1 Reactivation in Multiple Cell Model Systems and Resting CD4+ T Cells from Aviremic Patients. PLoS Pathog. 2013;9:e1003834. doi: 10.1371/journal.ppat.1003834
254. Bui J.K., Halvas E.K., Fyne E., Sobolewski M.D., Koontz D., Shao W., Luke B., Hong F.F., Kearney M.F., Mellors J.W. Ex Vivo Activation of CD4+ T-Cells from Donors on Suppressive ART Can Lead to Sustained Production of Infectious HIV-1 from a Subset of Infected Cells. PLoS Pathog. 2017;13:e1006230. doi: 10.1371/journal.ppat.1006230
255. Walker-Sperling V.E.K., Cohen V.J., Tarwater P.M., Blankson J.N. Reactivation Kinetics of HIV-1 and Susceptibility of Reactivated Latently Infected CD4+ T Cells to HIV-1-Specific CD8+ T Cells. J. Virol. 2015;89:9631–9638. doi: 10.1128/JVI.01454-15
256. Kulkosky J., Culnan D.M., Roman J., Dornadula G., Schnell M., Boyd M.R., Pomerantz R.J. Prostratin: Activation of Latent HIV-1 Expression Suggests a Potential Inductive Adjuvant Therapy for HAART. Blood. 2001;98:3006–3015. doi: 10.1182/blood.V98.10.3006.
257. Williams S.A., Chen L.-F., Kwon H., Fenard D., Bisgrove D., Verdin E., Greene W.C. Prostratin Antagonizes HIV Latency by Activating NF-KB. J. Biol. Chem. 2004;279:42008–42017. doi: 10.1074/jbc.M402124200
258. Bocklandt S., Blumberg P., Hamer D. Activation of Latent HIV-1 Expression by the Potent Anti-Tumor Promoter 12-Deoxyphorbol 13-Phenylacetate. Antivir. Res. 2003;59:89–98. doi: 10.1016/S0166-3542(03)00034-2
259. Kulkosky J., Sullivan J., Xu Y., Souder E., Hamer D.H., Pomerantz R.J. Expression of Latent HAART-Persistent HIV Type 1 Induced by Novel Cellular Activating Agents. AIDS Res. Hum. Retroviruses. 2004;20:497–505. doi: 10.1089/088922204323087741.
260. Perez M., de Vinuesa A., Sanchez-Duffhues G., Marquez N., Bellido M., Munoz-Fernandez M., Moreno S., Castor T., Calzado M., Munoz E. Bryostatin-1 Synergizes with Histone Deacetylase Inhibitors to Reactivate HIV-1 from Latency. Curr. HIV Res. 2010;8:418–429. doi: 10.2174/157016210793499312
261. Bullen C.K., Laird G.M., Durand C.M., Siliciano J.D., Siliciano R.F. New Ex Vivo Approaches Distinguish Effective and Ineffective Single Agents for Reversing HIV-1 Latency in Vivo. Nat. Med. 2014;20:425–429. doi: 10.1038/nm.3489
262. Kollár P., Rajchard J., Balounová Z., Pazourek J. Marine Natural Products: Bryostatins in Preclinical and Clinical Studies. Pharm. Biol. 2014;52:237–242. doi: 10.3109/13880209.2013.804100
263. Gutiérrez C., Serrano-Villar S., Madrid-Elena N., Pérez-Elías M.J., Martín M.E., Barbas C., Ruipérez J., Muñoz E., Muñoz-Fernández M.A., Castor T., et al. Bryostatin-1

for Latent Virus Reactivation in HIV-Infected Patients on Antiretroviral Therapy. AIDS. 2016;30:1385–1392. doi: 10.1097/QAD.0000000000001064.

264. Jiang G., Mendes E.A., Kaiser P., Wong D.P., Tang Y., Cai I., Fenton A., Melcher G.P., Hildreth J.E.K., Thompson G.R., et al. Synergistic Reactivation of Latent HIV Expression by Ingenol-3-Angelate, PEP005, Targeted NF-KB Signaling in Combination with JQ1 Induced p-TEFb Activation. PLoS Pathog. 2015;11:e1005066. doi: 10.1371/journal.ppat.1005066.

265. Darcis G., Kula A., Bouchat S., Fujinaga K., Corazza F., Ait-Ammar A., Delacourt N., Melard A., Kabeya K., Vanhulle C., et al. An In-Depth Comparison of Latency-Reversing Agent Combinations in Various In Vitro and Ex Vivo HIV-1 Latency Models Identified Bryostatin-1+JQ1 and Ingenol-B+JQ1 to Potently Reactivate Viral Gene Expression. PLoS Pathog. 2015;11:e1005063. doi: 10.1371/journal.ppat.1005063.

266. Pandeló José D., Bartholomeeusen K., da Cunha R.D., Abreu C.M., Glinski J., da Costa T.B.F., Bacchi Rabay A.F.M., Pianowski Filho L.F., Dudycz L.W., Ranga U., et al. Reactivation of Latent HIV-1 by New Semi-Synthetic Ingenol Esters. Virology. 2014;462–463:328–339. doi: 10.1016/j.virol.2014.05.033

267. Gama L., Abreu C.M., Shirk E.N., Price S.L., Li M., Laird G.M., Pate K.A.M., Wietgrefe S.W., O'Connor S.L., Pianowski L., et al. Reactivation of Simian Immunodeficiency Virus Reservoirs in the Brain of Virally Suppressed Macaques. AIDS. 2017;31:5–14. doi: 10.1097/QAD.0000000000001267.

268. Jiang G., Maverakis E., Cheng M.Y., Elsheikh M.M., Deleage C., Méndez-Lagares G., Shimoda M., Yukl S.A., Hartigan-O'Connor D.J., Thompson G.R., et al. Disruption of Latent HIV in Vivo during the Clearance of Actinic Keratosis by Ingenol Mebutate. JCI Insight. 2019;4:e126027. doi: 10.1172/jci.insight.126027

269. Cary D.C., Peterlin B.M. Procyanidin Trimer C1 Reactivates Latent HIV as a Triple Combination Therapy with Kansui and JQ1. PLoS ONE. 2018;13:e0208055. doi: 10.1371/journal.pone.0208055

270. Doyon G., Zerbato J., Mellors J.W., Sluis-Cremer N. Disulfiram Reactivates Latent HIV-1 Expression through Depletion of the Phosphatase and Tensin Homolog. AIDS. 2013;27:F7–F11. doi: 10.1097/QAD.0b013e3283570620

271. Xing S., Bullen C.K., Shroff N.S., Shan L., Yang H.-C., Manucci J.L., Bhat S., Zhang H., Margolick J.B., Quinn T.C., et al. Disulfiram Reactivates Latent HIV-1 in a Bcl-2-Transduced Primary CD4+ T Cell Model without Inducing Global T Cell Activation. J. Virol. 2011;85:6060–6064. doi: 10.1128/JVI.02033-10

272. Spivak A.M., Andrade A., Eisele E., Hoh R., Bacchetti P., Bumpus N.N., Emad F., Buckheit R., McCance-Katz E.F., Lai J., et al. A Pilot Study Assessing the Safety and Latency-Reversing Activity of Disulfiram in HIV-1-Infected Adults on Antiretroviral Therapy. Clin. Infect. Dis. 2014;58:883–890. doi: 10.1093/cid/cit813

273. Elliott J.H., McMahon J.H., Chang C.C., Lee S.A., Hartogensis W., Bumpus N., Savic R., Roney J., Hoh R., Solomon A., et al. Short-Term Administration of Disulfiram for Reversal of Latent HIV Infection: A Phase 2 Dose-Escalation Study. Lancet HIV. 2015;2:e520–e529. doi: 10.1016/S2352-3018(15)00226-X

274. Chen D., Wang H., Aweya J.J., Chen Y., Chen M., Wu X., Chen X., Lu J., Chen R., Liu M. HMBA Enhances Prostratin-Induced Activation of Latent HIV-1 via Suppressing the Expression of Negative Feedback Regulator A20/TNFAIP3 in NF- κ B Signaling. Biomed. Res. Int. 2016;2016:5173205. doi: 10.1155/2016/5173205

275. Choudhary S.K., Archin N.M., Margolis D.M. Hexamethylbisacetamide and Disruption of Human Immunodeficiency Virus Type 1 Latency in CD4+ T Cells. J. Infect. Dis. 2008;197:1162–1170. doi: 10.1086/529525.
276. Andreeff M., Stone R., Michaeli J., Young C.W., Tong W.P., Sogoloff H., Ervin T., Kufe D., Rifkind R.A., Marks P.A. Hexamethylene Bisacetamide in Myelodysplastic Syndrome and Acute Myelogenous Leukemia: A Phase II Clinical Trial with a Differentiation-Inducing Agent. Blood. 1992;80:2604–2609. doi: 10.1182/blood.V80.10.2604.2604
277. Doyon G., Sobolewski M.D., Huber K., McMahon D., Mellors J.W., Sluis-Cremer N. Discovery of a Small Molecule Agonist of Phosphatidylinositol 3-Kinase P110α That Reactivates Latent HIV-1. PLoS ONE. 2014;9:e84964. doi: 10.1371/journal.pone.0084964
278. Macedo A.B., Novis C.L., De Assis C.M., Sorensen E.S., Moszczynski P., Huang S., Ren Y., Spivak A.M., Jones R.B., Planelles V., et al. Dual TLR2 and TLR7 Agonists as HIV Latency-Reversing Agents. JCI Insight. 2018;3:e122673. doi: 10.1172/jci.insight.122673
279. Novis C.L., Archin N.M., Buzon M.J., Verdin E., Round J.L., Lichterfeld M., Margolis D.M., Planelles V., Bosque A. Reactivation of Latent HIV-1 in Central Memory CD4+T Cells through TLR-1/2 Stimulation. Retrovirology. 2013;10:119. doi: 10.1186/1742-4690-10-119
280. Thibault S., Imbeault M., Tardif M.R., Tremblay M.J. TLR5 Stimulation Is Sufficient to Trigger Reactivation of Latent HIV-1 Provirus in T Lymphoid Cells and Activate Virus Gene Expression in Central Memory CD4+ T Cells. Virology. 2009;389:20–25. doi: 10.1016/j.virol.2009.04.019
281. Tsai A., Irrinki A., Kaur J., Cihlar T., Kukolj G., Sloan D.D., Murry J.P. Toll-Like Receptor 7 Agonist GS-9620 Induces HIV Expression and HIV-Specific Immunity in Cells from HIV-Infected Individuals on Suppressive Antiretroviral Therapy. J. Virol. 2017;91:e02166-16. doi: 10.1128/JVI.02166-16.
282. Lim S.-Y., Osuna C.E., Hraber P.T., Hesselgesser J., Gerold J.M., Barnes T.L., Sanisetty S., Seaman M.S., Lewis M.G., Geleziunas R., et al. TLR7 Agonists Induce Transient Viremia and Reduce the Viral Reservoir in SIV-Infected Rhesus Macaques on Antiretroviral Therapy. Sci. Transl. Med. 2018;10:eaao4521. doi: 10.1126/scitranslmed.aao4521
283. Riddler S.A., Para M., Benson C.A., Mills A., Ramgopal M., DeJesus E., Brinson C., Cyktor J., Jacobs J., Koontz D., et al. Vesatolimod, a Toll-like Receptor 7 Agonist, Induces Immune Activation in Virally Suppressed Adults Living With Human Immunodeficiency Virus–1. Clin. Infect. Dis. 2021;72:e815–e824. doi: 10.1093/cid/ciaa1534
284. Offersen R., Nissen S.K., Rasmussen T.A., Østergaard L., Denton P.W., Søgaard O.S., Tolstrup M. A Novel Toll-Like Receptor 9 Agonist, MGN1703, Enhances HIV-1 Transcription and NK Cell-Mediated Inhibition of HIV-1-Infected Autologous CD4+ T Cells. J. Virol. 2016;90:4441–4453. doi: 10.1128/JVI.00222-16
285. Covino D.A., Desimio M.G., Doria M. Impact of IL-15 and Latency Reversing Agent Combinations in the Reactivation and NK Cell-Mediated Suppression of the HIV Reservoir. Sci. Rep. 2022;12:18567. doi: 10.1038/s41598-022-23010-5
286. Jones R.B., Mueller S., O'Connor R., Rimpel K., Sloan D.D., Karel D., Wong H.C., Jeng E.K., Thomas A.S., Whitney J.B., et al. A Subset of Latency-Reversing Agents Expose HIV-Infected Resting CD4+ T-Cells to Recognition by Cytotoxic T-Lymphocytes. PLoS Pathog. 2016;12:e1005545. doi: 10.1371/journal.ppat.1005545

287. McBrien J.B., Wong A.K.H., White E., Carnathan D.G., Lee J.H., Safrit J.T., Vanderford T.H., Paiardini M., Chahroudi A., Silvestri G. Combination of CD8β Depletion and Interleukin-15 Superagonist N-803 Induces Virus Reactivation in Simian-Human Immunodeficiency Virus-Infected, Long-Term ART-Treated Rhesus Macaques. J. Virol. 2020;94:e00755-20. doi: 10.1128/JVI.00755-20

288. McBrien J.B., Mavigner M., Franchitti L., Smith S.A., White E., Tharp G.K., Walum H., Busman-Sahay K., Aguilera-Sandoval C.R., Thayer W.O., et al. Robust and Persistent Reactivation of SIV and HIV by N-803 and Depletion of CD8+ Cells. Nature. 2020;578:154–159. doi: 10.1038/s41586-020-1946-0.

289. Dashti A, Sukkestad S, Horner AM, Neja M, Siddiqi Z, Waller C, Goldy J, Monroe D, Lin A, Schoof N, Singh V, Mavigner M, Lifson JD, Deleage C, Tuyishime M, Falcinelli SD, King HAD, Ke R, Mason RD, Archin NM, Dunham RM, Safrit JT, Jean S, Perelson AS, Margolis DM, Ferrari G, Roederer M, Silvestri G, Chahroudi A. AZD5582 plus SIV-specific antibodies reduce lymph node viral reservoirs in antiretroviral therapy-suppressed macaques. Nat Med. 2023 Oct;29(10):2535-2546. doi: 10.1038/s41591-023-02570-7. Epub 2023 Oct 2

290. Romee R., Cooley S., Berrien-Elliott M.M., Westervelt P., Verneris M.R., Wagner J.E., Weisdorf D.J., Blazar B.R., Ustun C., DeFor T.E., et al. First-in-Human Phase 1 Clinical Study of the IL-15 Superagonist Complex ALT-803 to Treat Relapse after Transplantation. Blood. 2018;131:2515–2527. doi: 10.1182/blood-2017-12-823757

291. Evans V.A., van der Sluis R.M., Solomon A., Dantanarayana A., McNeil C., Garsia R., Palmer S., Fromentin R., Chomont N., Sékaly R.-P., et al. Programmed Cell Death-1 Contributes to the Establishment and Maintenance of HIV-1 Latency. AIDS. 2018;32:1491–1497. doi: 10.1097/QAD.0000000000001849

292. Fromentin R., DaFonseca S., Costiniuk C.T., El-Far M., Procopio F.A., Hecht F.M., Hoh R., Deeks S.G., Hazuda D.J., Lewin S.R., et al. PD-1 Blockade Potentiates HIV Latency Reversal Ex Vivo in CD4+ T Cells from ART-Suppressed Individuals. Nat. Commun. 2019;10:814. doi: 10.1038/s41467-019-08798-7

293. Van der Sluis R.M., Kumar N.A., Pascoe R.D., Zerbato J.M., Evans V.A., Dantanarayana A.I., Anderson J.L., Sékaly R.P., Fromentin R., Chomont N., et al. Combination Immune Checkpoint Blockade to Reverse HIV Latency. J. Immunol. 2020;204:1242–1254. doi: 10.4049/jimmunol.1901191

294. Lau J.S.Y., McMahon J.H., Gubser C., Solomon A., Chiu C.Y.H., Dantanarayana A., Chea S., Tennakoon S., Zerbato J.M., Garlick J., et al. The Impact of Immune Checkpoint Therapy on the Latent Reservoir in HIV-Infected Individuals with Cancer on Antiretroviral Therapy. AIDS. 2021;35:1631–1636. doi: 10.1097/QAD.0000000000002919

295. Rasmussen T.A., Rajdev L., Rhodes A., Dantanarayana A., Tennakoon S., Chea S., Spelman T., Lensing S., Rutishauser R., Bakkour S., et al. Impact of Anti–PD-1 and Anti–CTLA-4 on the Human Immunodeficiency Virus (HIV) Reservoir in People Living With HIV With Cancer on Antiretroviral Therapy: The AIDS Malignancy Consortium 095 Study. Clin. Infect. Dis. 2021;73:e1973–e1981. doi: 10.1093/cid/ciaa1530

296. Gay C.L., Bosch R.J., Ritz J., Hataye J.M., Aga E., Tressler R.L., Mason S.W., Hwang C.K., Grasela D.M., Ray N., et al. Clinical Trial of the Anti-PD-L1 Antibody BMS-936559 in HIV-1 Infected Participants on Suppressive Antiretroviral Therapy. J. Infect. Dis. 2017;215:1725–1733. doi: 10.1093/infdis/jix191

297. Van Lint C., Emiliani S., Ott M., Verdin E. Transcriptional Activation and Chromatin Remodeling of the HIV-1 Promoter in Response to Histone Acetylation. EMBO J. 1996;15:1112–1120. doi: 10.1002/j.1460-2075.1996.tb00449.x
298. Laird G.M., Bullen C.K., Rosenbloom D.I.S., Martin A.R., Hill A.L., Durand C.M., Siliciano J.D., Siliciano R.F. Ex Vivo Analysis Identifies Effective HIV-1 Latency–Reversing Drug Combinations. J. Clin. Investig. 2015;125:1901–1912. doi: 10.1172/JCI80142
299. Zaikos T.D., Painter M.M., Sebastian Kettinger N.T., Terry V.H., Collins K.L. Class 1-Selective Histone Deacetylase (HDAC) Inhibitors Enhance HIV Latency Reversal While Preserving the Activity of HDAC Isoforms Necessary for Maximal HIV Gene Expression. J. Virol. 2018;92:e02110-17. doi: 10.1128/JVI.02110-17
300. Søgaard O.S., Graversen M.E., Leth S., Olesen R., Brinkmann C.R., Nissen S.K., Kjaer A.S., Schleimann M.H., Denton P.W., Hey-Cunningham W.J., et al. The Depsipeptide Romidepsin Reverses HIV-1 Latency In Vivo. PLoS Pathog. 2015;11:e1005142. doi: 10.1371/journal.ppat.1005142
301. Li J., Ma J., Kang W., Wang C., Bai F., Zhao K., Yao N., Liu Q., Dang B., Wang B., et al. The Histone Deacetylase Inhibitor Chidamide Induces Intermittent Viraemia in HIV-infected Patients on Suppressive Antiretroviral Therapy. HIV Med. 2020;21:747–757. doi: 10.1111/hiv.13027
302. Rasmussen T.A., Tolstrup M., Brinkmann C.R., Olesen R., Erikstrup C., Solomon A., Winckelmann A., Palmer S., Dinarello C., Buzon M., et al. Panobinostat, a Histone Deacetylase Inhibitor, for Latent-Virus Reactivation in HIV-Infected Patients on Suppressive Antiretroviral Therapy: A Phase 1/2, Single Group, Clinical Trial. Lancet HIV. 2014;1:e13–e21. doi: 10.1016/S2352-3018(14)70014-1
303. Bouchat S., Gatot J.-S., Kabeya K., Cardona C., Colin L., Herbein G., De Wit S., Clumeck N., Lambotte O., Rouzioux C., et al. Histone Methyltransferase Inhibitors Induce HIV-1 Recovery in Resting CD4+ T Cells from HIV-1-Infected HAART-Treated Patients. AIDS. 2012;26:1473–1482. doi: 10.1097/QAD.0b013e32835535f5
304. Bernhard W., Barreto K., Saunders A., Dahabieh M.S., Johnson P., Sadowski I. The Suv39H1 Methyltransferase Inhibitor Chaetocin Causes Induction of Integrated HIV-1 without Producing a T Cell Response. FEBS Lett. 2011;585:3549–3554. doi: 10.1016/j.febslet.2011.10.018
305. Jiang G., Nguyen D., Archin N.M., Yukl S.A., Méndez-Lagares G., Tang Y., Elsheikh M.M., Thompson G.R., Hartigan-O'Connor D.J., Margolis D.M., et al. HIV Latency Is Reversed by ACSS2-Driven Histone Crotonylation. J. Clin. Investig. 2018;128:1190–1198. doi: 10.1172/JCI98071
306. Bouchat S., Delacourt N., Kula A., Darcis G., Van Driessche B., Corazza F., Gatot J., Melard A., Vanhulle C., Kabeya K., et al. Sequential Treatment with 5-aza-2'-deoxycytidine and Deacetylase Inhibitors Reactivates HIV-1. EMBO Mol. Med. 2016;8:117–138. doi: 10.15252/emmm.201505557
307. Blazkova J., Trejbalova K., Gondois-Rey F., Halfon P., Philibert P., Guiguen A., Verdin E., Olive D., Van Lint C., Hejnar J., et al. CpG Methylation Controls Reactivation of HIV from Latency. PLoS Pathog. 2009;5:e1000554. doi: 10.1371/journal.ppat.1000554
308. Kauder S.E., Bosque A., Lindqvist A., Planelles V., Verdin E. Epigenetic Regulation of HIV-1 Latency by Cytosine Methylation. PLoS Pathog. 2009;5:e1000495. doi: 10.1371/journal.ppat.1000495

309. Pache L., Dutra M.S., Spivak A.M., Marlett J.M., Murry J.P., Hwang Y., Maestre A.M., Manganaro L., Vamos M., Teriete P., et al. BIRC2/CIAP1 Is a Negative Regulator of HIV-1 Transcription and Can Be Targeted by Smac Mimetics to Promote Reversal of Viral Latency. Cell Host Microbe. 2015;18:345–353. doi: 10.1016/j.chom.2015.08.009
310. Pache L., Marsden M.D., Teriete P., Portillo A.J., Heimann D., Kim J.T., Soliman M.S.A., Dimapasoc M., Carmona C., Celeridad M., et al. Pharmacological Activation of Non-Canonical NF-KB Signaling Activates Latent HIV-1 Reservoirs In Vivo. Cell Rep. Med. 2020;1:100037. doi: 10.1016/j.xcrm.2020.100037
311. Nixon C.C., Mavigner M., Sampey G.C., Brooks A.D., Spagnuolo R.A., Irlbeck D.M., Mattingly C., Ho P.T., Schoof N., Cammon C.G., et al. Systemic HIV and SIV Latency Reversal via Non-Canonical NF-KB Signalling in Vivo. Nature. 2020;578:160–165. doi: 10.1038/s41586-020-1951-3
312. Sorensen E.S., Macedo A.B., Resop R.S., Howard J.N., Nell R., Sarabia I., Newman D., Ren Y., Jones R.B., Planelles V., et al. Structure-Activity Relationship Analysis of Benzotriazine Analogues as HIV-1 Latency-Reversing Agents. Antimicrob. Agents Chemother. 2020;64:e00888-20. doi: 10.1128/AAC.00888-20
313. Lu P., Shen Y., Yang H., Wang Y., Jiang Z., Yang X., Zhong Y., Pan H., Xu J., Lu H., et al. BET Inhibitors RVX-208 and PFI-1 Reactivate HIV-1 from Latency. Sci. Rep. 2017;7:16646. doi: 10.1038/s41598-017-16816-1
314. Abner E., Stoszko M., Zeng L., Chen H.-C., Izquierdo-Bouldstridge A., Konuma T., Zorita E., Fanunza E., Zhang Q., Mahmoudi T., et al. A New Quinoline BRD4 Inhibitor Targets a Distinct Latent HIV-1 Reservoir for Reactivation from Other “Shock” Drugs. J. Virol. 2018;92:e02056-17. doi: 10.1128/JVI.02056-17
315. Li Z., Guo J., Wu Y., Zhou Q. The BET Bromodomain Inhibitor JQ1 Activates HIV Latency through Antagonizing Brd4 Inhibition of Tat-Transactivation. Nucleic Acids Res. 2013;41:277–287. doi: 10.1093/nar/gks976
316. Li G., Zhang Z., Reszka-Blanco N., Li F., Chi L., Ma J., Jeffrey J., Cheng L., Su L. Specific Activation In Vivo of HIV-1 by a Bromodomain Inhibitor from Monocytic Cells in Humanized Mice under Antiretroviral Therapy. J. Virol. 2019;93:e00233-19. doi: 10.1128/JVI.00233-19
317. López-Huertas M.R., Jiménez-Tormo L., Madrid-Elena N., Gutiérrez C., Rodríguez-Mora S., Coiras M., Alcamí J., Moreno S. The CCR5-Antagonist Maraviroc Reverses HIV-1 Latency in Vitro Alone or in Combination with the PKC-Agonist Bryostatin-1. Sci. Rep. 2017;7:2385. doi: 10.1038/s41598-017-02634-y
318. Vicenti I., Dragoni F., Monti M., Trombetta C.M., Giannini A., Boccuto A., Saladini F., Rossetti B., De Luca A., Ciabattini A., et al. Maraviroc as a Potential HIV-1 Latency-Reversing Agent in Cell Line Models and Ex Vivo CD4 T Cells. J. General. Virol. 2021;102:jgv001499. doi: 10.1099/jgv.0.001499
319. Gutiérrez C., Díaz L., Vallejo A., Hernández-Novoa B., Abad M., Madrid N., Dahl V., Rubio R., Moreno A.M., Dronda F., et al. Intensification of Antiretroviral Therapy with a CCR5 Antagonist in Patients with Chronic HIV-1 Infection: Effect on T Cells Latently Infected. PLoS ONE. 2011;6:e27864. doi: 10.1371/journal.pone.0027864
320. Geng G., Liu B., Chen C., Wu K., Liu J., Zhang Y., Pan T., Li J., Yin Y., Zhang J., et al. Development of an Attenuated Tat Protein as a Highly-Effective Agent to Specifically Activate HIV-1 Latency. Mol. Ther. 2016;24:1528–1537. doi: 10.1038/mt.2016.117
321. Julien O, Wells JA. Caspases and their substrates. Cell Death Differ. 2017 Aug;24(8):1380-1389. doi: 10.1038/cdd.2017.44. Epub 2017 May 12.

322. Shalini S, Dorstyn L, Dawar S, Kumar S. Old, new and emerging functions of caspases. Cell Death Differ. 2015 Apr;22(4):526-39. doi: 10.1038/cdd.2014.216. Epub 2014 Dec 19
323. Balaji S, Terrero D, Tiwari AK, Ashby CR, Raman D. Alternative approaches to overcome chemoresistance to apoptosis in cancer. In: Donev R, editor. Advances in Protein Chemistry and Structural Biology. Vol. 126. Academic Press; 2021. p. 91–122. doi:10.1016/bs.apcsb.2021.01.005
324. Lomonosova E, Chinnadurai G. BH3-only proteins in apoptosis and beyond: an overview. Oncogene. 2008 Dec;27 Suppl 1(Suppl 1):S2-19. doi: 10.1038/onc.2009.39
325. Cavalcante GC, Schaan AP, Cabral GF, Santana-da-Silva MN, Pinto P, Vidal AF, Ribeiro-Dos-Santos Â. A Cell's Fate: An Overview of the Molecular Biology and Genetics of Apoptosis. Int J Mol Sci. 2019 Aug 24;20(17):4133. doi: 10.3390/ijms20174133
326. Li H, Zhu H, Xu CJ, Yuan J. Cleavage of BID by caspase 8 mediates the mitochondrial damage in the Fas pathway of apoptosis. Cell. 1998 Aug 21;94(4):491-501. doi: 10.1016/s0092-8674(00)81590-1.
327. Molyer B, Kumar A, Angel JB. SMAC Mimetics as Therapeutic Agents in HIV Infection. Front Immunol. 2021 Nov 26;12:780400. doi: 10.3389/fimmu.2021.780400.
328. Cai Q, Sun H, Peng Y, Lu J, Nikolovska-Coleska Z, McEachern D, Liu L, Qiu S, Yang CY, Miller R, Yi H, Zhang T, Sun D, Kang S, Guo M, Leopold L, Yang D, Wang S. A potent and orally active antagonist (SM-406/AT-406) of multiple inhibitor of apoptosis proteins (IAPs) in clinical development for cancer treatment. J Med Chem. 2011 Apr 28;54(8):2714-26. doi: 10.1021/jm101505d. Epub 2011 Mar 28.
329. Marsden MD, Teriete P, Portillo AJ, Heimann D, Kim JT, et al. Pharmacological Activation of Non-Canonical NF-κb Signaling Activates Latent HIV-1 Reservoirs In Vivo. Cell Rep Med (2020) 1(3):100037. doi: 10.1016/j.xcrm.2020.100037
330. Bobardt M, Kuo J, Chatterji U, Chanda S, Little SJ, Wiedemann N, et al. The Inhibitor Apoptosis Protein Antagonist Debio 1143 Is an Attractive HIV-1 Latency Reversal Candidate. PloS One (2019) 14(2):e0211746. doi: 10.1371/journal.pone.0211746
331. Hennessy EJ, Adam A, Aquila BM, Castriotta LM, Cook D, Hattersley M, Hird AW, Huntington C, Kamhi VM, Laing NM, Li D, MacIntyre T, Omer CA, Oza V, Patterson T, Repik G, Rooney MT, Saeh JC, Sha L, Vasbinder MM, Wang H, Whitston D. Discovery of a novel class of dimeric Smac mimetics as potent IAP antagonists resulting in a clinical candidate for the treatment of cancer (AZD5582). J Med Chem. 2013 Dec 27;56(24):9897-919. doi: 10.1021/jm401075x. Epub 2013 Dec 13.
332. Honeycutt JB, Liao B, Nixon CC, Cleary RA, Thayer WO, Birath SL, Swanson MD, Sheridan P, Zakharova O, Prince F, Kuruc J, Gay CL, Evans C, Eron JJ, Wahl A, Garcia JV. T cells establish and maintain CNS viral infection in HIV-infected humanized mice. J Clin Invest. 2018 Jul 2;128(7):2862-2876. doi: 10.1172/JCI98968. Epub 2018 Jun 4
333. Kessing CF, Nixon CC, Li C, Tsai P, Takata H, Mousseau G, Ho PT, Honeycutt JB, Fallahi M, Trautmann L, Garcia JV, Valente ST. In Vivo Suppression of HIV Rebound by Didehydro-Cortistatin A, a "Block-and-Lock" Strategy for HIV-1 Treatment. Cell Rep. 2017 Oct 17;21(3):600-611. doi: 10.1016/j.celrep.2017.09.080
334. Tsai P, Wu G, Baker CE, Thayer WO, Spagnuolo RA, Sanchez R, Barrett S, Howell B, Margolis D, Hazuda DJ, Archin NM, Garcia JV. In vivo analysis of the effect of panobinostat on cell-associated HIV RNA and DNA levels and latent HIV infection. Retrovirology. 2016 May 21;13(1):36. doi: 10.1186/s12977-016-0268-7
335. Dashti A, Waller C, Mavigner M, Schoof N, Bar KJ, Shaw GM, Vanderford TH, Liang S, Lifson JD, Dunham RM, Ferrari G, Tuyishime M, Lam CK, Nordstrom JL, Margolis DM,

Silvestri G, Chahroudi A. SMAC Mimetic Plus Triple-Combination Bispecific HIVxCD3 Retargeting Molecules in SHIV.C.CH505-Infected, Antiretroviral Therapy-Suppressed Rhesus Macaques. J Virol. 2020 Oct 14;94(21):e00793-20. doi: 10.1128/JVI.00793-20.

336. Chertova E, Bergamaschi C, Chertov O, Sowder R, Bear J, Roser JD, Beach RK, Lifson JD, Felber BK, Pavlakis GN. Characterization and favorable in vivo properties of heterodimeric soluble IL-15·IL-15Rα cytokine compared to IL-15 monomer. J Biol Chem. 2013 Jun 21;288(25):18093-103. doi: 10.1074/jbc.M113.461756. Epub 2013 May 6
337. Skariah N, James OJ, Swamy M. Signalling mechanisms driving homeostatic and inflammatory effects of interleukin-15 on tissue lymphocytes. Discov Immunol. 2024 Jan 30;3(1):kyae002. doi: 10.1093/discim/kyae002.
338. Waldmann TA. The biology of interleukin-2 and interleukin-15: implications for cancer therapy and vaccine design. Nat Rev Immunol. 2006 Aug;6(8):595-601. doi: 10.1038/nri1901.
339. Bergamaschi C, Rosati M, Jalah R, Valentin A, Kulkarni V, Alicea C, Zhang GM, Patel V, Felber BK, Pavlakis GN. Intracellular interaction of interleukin-15 with its receptor alpha during production leads to mutual stabilization and increased bioactivity. J Biol Chem. 2008 Feb 15;283(7):4189-99. doi: 10.1074/jbc.M705725200. Epub 2007 Nov 30.
340. Bergamaschi C, Jalah R, Kulkarni V, Rosati M, Zhang GM, Alicea C, Zolotukhin AS, Felber BK, Pavlakis GN. Secretion and biological activity of short signal peptide IL-15 is chaperoned by IL-15 receptor alpha in vivo. J Immunol. 2009 Sep 1;183(5):3064-72. doi: 10.4049/jimmunol.0900693.
341. Bergamaschi C, Bear J, Rosati M, Beach RK, Alicea C, Sowder R, Chertova E, Rosenberg SA, Felber BK, Pavlakis GN. Circulating IL-15 exists as heterodimeric complex with soluble IL-15Rα in human and mouse serum. Blood. 2012 Jul 5;120(1):e1-8. doi: 10.1182/blood-2011-10-384362. Epub 2012 Apr 10
342. Sneller MC, Kopp WC, Engelke KJ, Yovandich JL, Creekmore SP, Waldmann TA, Lane HC. IL-15 administered by continuous infusion to rhesus macaques induces massive expansion of CD8+ T effector memory population in peripheral blood. Blood. 2011 Dec 22;118(26):6845-8. doi: 10.1182/blood-2011-09-377804. Epub 2011 Nov 8
343. Waldmann TA, Lugli E, Roederer M, Perera LP, Smedley JV, Macallister RP, Goldman CK, Bryant BR, Decker JM, Fleisher TA, Lane HC, Sneller MC, Kurlander RJ, Kleiner DE, Pletcher JM, Figg WD, Yovandich JL, Creekmore SP. Safety (toxicity), pharmacokinetics, immunogenicity, and impact on elements of the normal immune system of recombinant human IL-15 in rhesus macaques. Blood. 2011 May 5;117(18):4787-95. doi: 10.1182/blood-2010-10-311456. Epub 2011 Mar 8.
344. Waldmann TA, Dubois S, Miljkovic MD, Conlon KC. IL-15 in the Combination Immunotherapy of Cancer. Front Immunol. 2020 May 19;11:868. doi: 10.3389/fimmu.2020.00868.
345. Howard JN, Bosque A. IL-15 and N-803 for HIV Cure Approaches. Viruses. 2023 Sep 12;15(9):1912. doi: 10.3390/v15091912.
346. Romee R, Cooley S, Berrien-Elliott MM, Westervelt P, Verneris MR, Wagner JE, Weisdorf DJ, Blazar BR, Ustun C, DeFor TE, Vivek S, Peck L, DiPersio JF, Cashen AF, Kyllo R, Musiek A, Schaffer A, Anadkat MJ, Rosman I, Miller D, Egan JO, Jeng EK, Rock A, Wong HC, Fehniger TA, Miller JS. First-in-human phase 1 clinical study of the IL-15 superagonist complex ALT-803 to treat relapse after transplantation. Blood. 2018 Jun 7;131(23):2515-2527. doi: 10.1182/blood-2017-12-823757. Epub 2018 Feb 20.

347. Chehimi J, Marshall JD, Salvucci O, Frank I, Chehimi S, Kawecki S, Bacheller D, Rifat S, Chouaib S. IL-15 enhances immune functions during HIV infection. J Immunol. 1997 Jun 15;158(12):5978-87.
348. Mueller YM, Bojczuk PM, Halstead ES, Kim AH, Witek J, Altman JD, Katsikis PD. IL-15 enhances survival and function of HIV-specific CD8+ T cells. Blood. 2003 Feb 1;101(3):1024-9. doi: 10.1182/blood-2002-07-1957. Epub 2002 Sep 19.
349. Kanai T, Thomas EK, Yasutomi Y, Letvin NL. IL-15 stimulates the expansion of AIDS virus-specific CTL. J Immunol. 1996 Oct 15;157(8):3681-7.
350. Fisher L, Zinter M, Stanfield-Oakley S, Carpp LN, Edwards RW, Denny T, Moodie Z, Laher F, Bekker LG, McElrath MJ, Gilbert PB, Corey L, Tomaras G, Pollara J, Ferrari G. Vaccine-Induced Antibodies Mediate Higher Antibody-Dependent Cellular Cytotoxicity After Interleukin-15 Pretreatment of Natural Killer Effector Cells. Front Immunol. 2019 Nov 27;10:2741. doi: 10.3389/fimmu.2019.02741.
351. Garrido C, Abad-Fernandez M, Tuyishime M, Pollara JJ, Ferrari G, Soriano-Sarabia N, Margolis DM. Interleukin-15-Stimulated Natural Killer Cells Clear HIV-1-Infected Cells following Latency Reversal Ex Vivo. J Virol. 2018 May 29;92(12):e00235-18. doi: 10.1128/JVI.00235-18. Erratum in: J Virol. 2020 May 18;94(11):e00223-20. doi: 10.1128/JVI.00223-20
352. Seay K, Church C, Zheng JH, Deneroff K, Ochsenbauer C, Kappes JC, Liu B, Jeng EK, Wong HC, Goldstein H. In Vivo Activation of Human NK Cells by Treatment with an Interleukin-15 Superagonist Potently Inhibits Acute In Vivo HIV-1 Infection in Humanized Mice. J Virol. 2015 Jun;89(12):6264-74. doi: 10.1128/JVI.00563-15. Epub 2015 Apr 1.
353. Ellis-Connell AL, Balgeman AJ, Zarbock KR, Barry G, Weiler A, Egan JO, Jeng EK, Friedrich T, Miller JS, Haase AT, Schacker TW, Wong HC, Rakasz E, O'Connor SL. ALT-803 Transiently Reduces Simian Immunodeficiency Virus Replication in the Absence of Antiretroviral Treatment. J Virol. 2018 Jan 17;92(3):e01748-17. doi: 10.1128/JVI.01748-17.
354. Webb GM, Li S, Mwakalundwa G, Folkvord JM, Greene JM, Reed JS, Stanton JJ, Legasse AW, Hobbs T, Martin LD, Park BS, Whitney JB, Jeng EK, Wong HC, Nixon DF, Jones RB, Connick E, Skinner PJ, Sacha JB. The human IL-15 superagonist ALT-803 directs SIV-specific CD8+ T cells into B-cell follicles. Blood Adv. 2018 Jan 23;2(2):76-84. doi: 10.1182/bloodadvances.2017012971.
355. Webb GM, Molden J, Busman-Sahay K, Abdulhaqq S, Wu HL, Weber WC, Bateman KB, Reed JS, Northrup M, Maier N, Tanaka S, Gao L, Davey B, Carpenter BL, Axthelm MK, Stanton JJ, Smedley J, Greene JM, Safrit JT, Estes JD, Skinner PJ, Sacha JB. The human IL-15 superagonist N-803 promotes migration of virus-specific CD8+ T and NK cells to B cell follicles but does not reverse latency in ART-suppressed, SHIV-infected macaques. PLoS Pathog. 2020 Mar 12;16(3):e1008339. doi: 10.1371/journal.ppat.1008339.
356. Bergamaschi C, Kulkarni V, Rosati M, Alicea C, Jalah R, Chen S, Bear J, Sardesai NY, Valentin A, Felber BK, Pavlakis GN. Intramuscular delivery of heterodimeric IL-15 DNA in macaques produces systemic levels of bioactive cytokine inducing proliferation of NK and T cells. Gene Ther. 2015;22(1):76-86. doi:10.1038/gt.2014.84
357. Bergamaschi C, Watson DC, Valentin A, Bear J, Peer CJ, Figg WD Sr, Felber BK, Pavlakis GN. Optimized administration of hetIL-15 expands lymphocytes and minimizes toxicity in rhesus macaques. Cytokine. 2018 Aug;108:213-224. doi: 10.1016/j.cyto.2018.01.011. Epub 2018 May 7.

358. Watson DC, Moysi E, Valentin A, Bergamaschi C, Devasundaram S, Fortis SP, et al. Treatment with native heterodimeric IL-15 increases cytotoxic lymphocytes and reduces SHIV RNA in lymph nodes. PLoS Pathog. 2018;14(2):e1006902. doi:10.1371/journal.ppat.1006902
359. National Academies of Sciences, Engineering, and Medicine; Division on Earth and Life Studies; Health and Medicine Division; Institute for Laboratory Animal Research; Board on Health Sciences Policy; Committee on the State of the Science and Future Needs for Nonhuman Primate Model Systems. Nonhuman Primate Models in Biomedical Research: State of the Science and Future Needs. Yost OC, Downey A, Ramos KS, editors. Washington (DC): National Academies Press (US); 2023 May 4.
360. National Primate Research Centers. https://cnprc.ucdavis.edu/national-primate-research-centers
361. National Primate Research Center Consortium. https://www.nprcresearch.org
362. Wang X, et al. 2020. Nonhuman primates in China for biomedical research: demand, supply, and challenges. Zool Res 41(2): 220–231
363. History of the Emory National Primate Research Center. Emory University https://www.enprc.emory.edu/about/index.html
364. Letvin NL. Animal models for AIDS. Immunol Today. 1990 Sep;11(9):322-6. doi: 10.1016/0167-5699(90)90127-u.
365. Daniel MD, Letvin NL, King NW, Kannagi M, Sehgal PK, Hunt RD, Kanki PJ, Essex M, Desrosiers RC. Isolation of T-cell tropic HTLV-III-like retrovirus from macaques. Science. 1985 Jun 7;228(4704):1201-4. doi: 10.1126/science.3159089.
366. Alter HJ, Eichberg JW, Masur H, Saxinger WC, Gallo R, Macher AM, Lane HC, Fauci AS. Transmission of HTLV-III infection from human plasma to chimpanzees: an animal model for AIDS. Science. 1984 Nov 2;226(4674):549-52. doi: 10.1126/science.6093251.
367. Silvestri G, Sodora DL, Koup RA, Paiardini M, O'Neil SP, McClure HM, Staprans SI, Feinberg MB. Nonpathogenic SIV infection of sooty mangabeys is characterized by limited bystander immunopathology despite chronic high-level viremia. Immunity. 2003 Mar;18(3):441-52. doi: 10.1016/s1074-7613(03)00060-8.
368. Sharp PM, Hahn BH. Origins of HIV and the AIDS pandemic. Cold Spring Harb Perspect Med. 2011 Sep;1(1):a006841. doi: 10.1101/cshperspect.a006841.
369. Van Rompay KK. The use of nonhuman primate models of HIV infection for the evaluation of antiviral strategies. AIDS Res Hum Retroviruses. 2012 Jan;28(1):16-35. doi: 10.1089/aid.2011.0234. Epub 2011 Oct 19.
370. Terrade G, Huot N, Petitdemange C, Lazzerini M, Orta Resendiz A, Jacquelin B, Müller-Trutwin M. Interests of the Non-Human Primate Models for HIV Cure Research. Vaccines (Basel). 2021 Aug 27;9(9):958. doi: 10.3390/vaccines9090958.
371. Del Prete GQ, Lifson JD. Nonhuman Primate Models for Studies of AIDS Virus Persistence During Suppressive Combination Antiretroviral Therapy. Curr Top Microbiol Immunol. 2018;417:69-109. doi: 10.1007/82_2017_73.
372. Fennessey CM, Pinkevych M, Immonen TT, Reynaldi A, Venturi V, Nadella P, et al. Genetically barcoded SIV facilitates enumeration of rebound variants and estimation of reactivation rates in nonhuman primates following interruption of suppressive antiretroviral therapy. PLoS Pathog. 2017;13(5):e1006359. doi:10.1371/journal.ppat.1006359
373. Statzu M, Jin W, Fray EJ, Wong AKH, Kumar MR, Ferrer E, Docken SS, Pinkevych M, McBrien JB, Fennessey CM, Keele BF, Liang S, Harper JL, Mutascio S, Franchitti L, Wang H, Cicetti D, Bosinger SE, Carnathan DG, Vanderford TH, Margolis DM, Garcia-Martinez

JV, Chahroudi A, Paiardini M, Siliciano J, Davenport MP, Kulpa DA, Siliciano RS, Silvestri G. $CD8^+$ lymphocytes do not impact SIV reservoir establishment under ART. Nat Microbiol. 2023;8:299–308. doi:10.1038/s41564-022-01311-9

374. Mavigner M, Liao LE, Brooks AD, Ke R, Mattingly C, Schoof N, McBrien J, Carnathan D, Liang S, Vanderford TH, Paiardini M, Kulpa D, Lifson JD, Dunham RM, Easley KA, Margolis DM, Perelson AS, Silvestri G, Chahroudi A. CD8 lymphocyte depletion enhances the latency reversal activity of the SMAC mimetic AZD5582 in ART-suppressed SIV-infected rhesus macaques. J Virol. 2021 Mar 25;95(8):e01429-20. doi: 10.1128/JVI.01429-20. Epub 2021 Feb 10.
375. Cossarini F, Aberg JA, Chen BK, Mehandru S. Viral Persistence in the Gut-Associated Lymphoid Tissue and Barriers to HIV Cure. AIDS Res Hum Retroviruses. 2023 Dec 13;40(1):54–65. doi: 10.1089/AID.2022.0180. Epub ahead of print.
376. McManus WR, Bale MJ, Spindler J, Wiegand A, Musick A, Patro SC, Sobolewski MD, Musick VK, Anderson EM, Cyktor JC, Halvas EK, Shao W, Wells D, Wu X, Keele BF, Milush JM, Hoh R, Mellors JW, Hughes SH, Deeks SG, Coffin JM, Kearney MF. HIV-1 in lymph nodes is maintained by cellular proliferation during antiretroviral therapy. J Clin Invest. 2019 Jul 30;129(11):4629-4642. doi: 10.1172/JCI126714.
377. Cadena AM, Ventura JD, Abbink P, Borducchi EN, Tuyishime H, Mercado NB, Walker-Sperling V, Siamatu M, Liu PT, Chandrashekar A, Nkolola JP, McMahan K, Kordana N, Hamza V, Bondzie EA, Fray E, Kumar M, Fischinger S, Shin SA, Lewis MG, Siliciano RF, Alter G, Barouch DH. Persistence of viral RNA in lymph nodes in ART-suppressed SIV/SHIV-infected Rhesus Macaques. Nat Commun. 2021 Mar 5;12(1):1474. doi: 10.1038/s41467-021-21724-0.
378. Fulda S. Promises and Challenges of Smac Mimetics as Cancer Therapeutics. Clin Cancer Res. 2015 Nov 15;21(22):5030-6. doi: 10.1158/1078-0432.CCR-15-0365.
379. Bai L, Smith DC, Wang S. Small-molecule SMAC mimetics as new cancer therapeutics. Pharmacol Ther. 2014 Oct;144(1):82-95. doi: 10.1016/j.pharmthera.2014.05.007. Epub 2014 May 16.
380. West, A., Martin, B., Andrews, D. et al. The SMAC mimetic, LCL-161, reduces survival in aggressive MYC-driven lymphoma while promoting susceptibility to endotoxic shock. Oncogenesis 5, e216 (2016). https://doi.org/10.1038/oncsis.2016.26
381. Li H. et al. Envelope residue 375 substitutions in simian-human immunodeficiency viruses enhance CD4 binding and replication in rhesus macaques. Proc Natl Acad Sci U S A 113, E3413–3422 (2016). 10.1073/pnas.1606636113
382. Bender A. M. et al. The Landscape of Persistent Viral Genomes in ART-Treated SIV, SHIV, and HIV-2 Infections. Cell Host Microbe 26, 73–85 e74 (2019). 10.1016/j.chom.2019.06.005
383. Harper J, Ribeiro SP, Chan CN, Aid M, Deleage C, Micci L, Pino M, Cervasi B, Raghunathan G, Rimmer E, Ayanoglu G, Wu G, Shenvi N, Barnard RJ, Del Prete GQ, Busman-Sahay K, Silvestri G, Kulpa DA, Bosinger SE, Easley KA, Howell BJ, Gorman D, Hazuda DJ, Estes JD, Sekaly RP, Paiardini M. Interleukin-10 contributes to reservoir establishment and persistence in SIV-infected macaques treated with antiretroviral therapy. J Clin Invest. 2022 Apr 15;132(8):e155251. doi: 10.1172/JCI155251.

Acknowledgments

This is my first time writing acknowledgments for a thesis, and I have a long list of people to thank. My gratitude extends not only to those who directly contributed to this work, but also to those who supported my growth and encouraged me to begin and persevere through this journey.

First and foremost, I thank my supervisor, **Emmanuele Venanzi Rullo**, whose guidance taught me to handle even the most delicate or unexpected circumstances with calm, initiative, and diplomacy. I am equally grateful to my co-supervisor, **Guido Silvestri**, for his incomparable expertise and our occasional conversations on human history, reminding me that science is only one chapter of life's vast book. To my mentor, **Mirko Paiardini,** I owe deepest gratitude for his guidance, wisdom, and unwavering support, which shaped both my work and my scientific journey. I will forever thank my Italian professor **Giuseppe Nunnari**, whose yes-or-no question during a conference break in Riccione led me to Atlanta for HIV research, opening a door that changed my life.

I am grateful to my lab colleagues in Atlanta, who became more than just coworkers. **Maura Statzu**, my endlessly patient lab tutor, for guiding me from pipette handling to project navigation, surviving my countless "help!" texts, one-minute complainings, and the editing of this work without losing faith in me. **Leonardo Sorrentino, Charlott Morel, Yohannes Abraham, Hannah Flores, Julien Clain, James Auger, Laurence Raymond Marchand, Tomas Raul Wiche Salinas, Kevin Nguen, Sandeep Kaushik, Justin Harper, Cristina Ceriani, Jeffrey Morgan, Barbara Cervasi**, for filling the lab with laughter, encouragement, deep conversations, and camaraderie that made every challenge easier to face.

Beyond the U.S., I thank my oldest friend **Chiara 'Claire' Alaimo**, who can sense when something is wrong from across continents and always knows the right thing to say. **Francesco Manti, Roberto Berté, Paolo Custurone, Pietro Basile**, and my *Infectivologirls* **Mariagiovanna Coco, Livia Marletta, Flavia D'Andrea, Chiara Gullotta,** and **Daniela Maranto** for their friendship, laughter, and connection to home.

Finally, I owe infinite gratitude to my family. To **my mother**, for her morning "ready-with-me" calls and uniquely effective way of pushing me beyond limits. To **my father**, for his gentle reminders about the wonders of medical life in Italy. To **my brother Giorgio**, for our endless reflections on life and society and the certainty that he always has my back.

To all who contributed to this work, even if not mentioned by name, I hope you feel my gratitude. I could not have done this without each of you, in ways big and small. Thank you for the support, wisdom, and memories that made this PhD journey my own Wonderland.